GUIDELINES ON

THE USE OF ACCIDENTAL LIMIT STATES FOR THE DESIGN OF OFFSHORE STRUCTURES

Revision 1. July 2015

Prepared by Committee V.1

J. Czujko, *Norway (Chair)*
G.S. Kim, *Korea*
S.J. Pahos, *UK*
D. Pearson, *Canada*
K. Tabri, *Estonia*

GUIDELINES ON

THE USE OF ACCIDENTAL LIMIT STATES FOR THE DESIGN OF OFFSHORE STRUCTURES

Table of Contents

CHAPTER ONE

INTRODUCTION

Accidents are the aggregate of numerous circumstances leading to an initiating event, often the first step in a sequence of actions that follow with detrimental consequences to human life, assets and the environment. The definition of what constitutes an "accident" is very broad and often the term "event", "accidental action" or simply "action" is used in the same context. Actions are the actual realization of a hazard that has been identified during the design phase.

Typical accidental actions addressed in these Guidelines are:

- Gas Explosion
- Fire/Thermal Effects
- Ship Collision
- Dropped Objects
- Extreme Environmental Loads

The application of Accidental Limit State (ALS) in the design allows for an introspective look in the response of assets when exposed to accidental actions. The series of International Standards applicable to accidental limit states on offshore structures constitute a common ground that describe how hazards, associated with specific probabilities of occurrence, are treated and designed for (ISO19900 Series). These Guidelines apply partial action factors based on the LRFD design methodology as found in API-2A-LRFD (1993).

ALS methodology can highlight key parameters that affect specific output (deformation, pressure, temperature) that can be used as a measure of structural safety and robustness. Ultimately, risk reduction through uncertainties management is possible.

1.1 Objectives

The present Guidelines are intended for the use of ALS in the design of offshore structures to ensure sufficient structural safety for hazards associated with platform's operation. Its primary function is to act as a roadmap for engineers interested in risk mitigation and structural assessment from accidental loads. The principles and terminology being used are common for fixed, ship-shaped (FSO/FPSO), or unmanned floating facilities. The application of ALS in design requires certain actions to be defined by engineers or stake holders.

The intention of these Guidelines is to provide the following:

a. Guidance on how to perform numerical analysis that can be used in studying risk levels, risk mitigation, decision-making and ultimately developing acceptance criteria.
b. Guidance on application prescriptive and probabilistic methods in the assessment of accidental actions and definition of actions to be used in design process.
c. Describe how a structure under the effect of accidental actions should respond.
d. Recommend how numerical analysis should be carried out.
e. Discuss and hopefully encourage further discussion in the field of applying ALS in the design of offshore structures.

Finally, this work hopes to act as a reference document useful for engineers and practitioners involved in the application of ALS in design.

1.2 Assumptions and limitations in the application of ALS

Numerous limitations, as in every design methodology exist in ALS. Central restrictions are presented herein:

a. Closed form solutions, as in serviceability limit state for example, are not always possible as action effects are time and space varying actions. It is therefore not straightforward to establish universally applicable structural design criteria.
b. Application of ALS in the design requires significant investment on software and experienced engineers/analysts.
c. Acceptance criteria need to be in place so that conclusions can be drawn after the analysis has taken place. This requires a risk assessment.
d. Results from numerical analysis are sensitive to the applied boundary conditions and mesh size. Often a number of analyses is necessary before making any decisions.
e. Finally, the definition of "accident" is not precise. It would be erroneous to credit a specific definition to this term.

1.3 Abbreviations and definitions

1.3.1 Following abbreviations and definitions are used in these Guidelines

Abbreviations:

ALARP	As Low As Reasonably Practical
CFD	Computational Fluid Dynamics
DAL	Dimensioning Accidental Loads
DOP	Dropped Object Protection
FEES	Fire, explosion and escape strategy according to ISO-13702 (2015)
F&G	Fire and Gas
FW	Fire Water
FR	Functional Requirements (of the Contract)
HAZID	Hazard Identification Study
HC	Hydrocarbon
HSE	Health, Safety & Environment
LEL	Lower Explosion Limit
LNG	Liquefied Natural Gas
LPG	Liquefied Petroleum Gas
NFPA	National Fire Protection Association
PSA (PTIL)	Petroleum Safety Authority Norway
PFP	Passive Fire Protection
QRA	Quantitative Risk Analysis
TRA	Total Risk Analysis
TRR	Tubing Replacement Rig
TR	Temporary Refuge
UEL	Upper Explosion Limit

Definitions:

Action:	External load applied to the structure (direct action) or an imposed deformation or acceleration (indirect action). Action is the outcome of a hazard.
Accidental Action:	Load originated from identified hazards during the design phase; it is the out-come of QRA.
Action Effect:	Effect of action(s) on the structure or its components.
Design Accidental Load:	Chosen accidental load that is to be used as the basis for design.
	NOTE 1 The applied/chosen design accidental load may sometimes be the same as the dimensioning accidental load (DAL), but it may also be more conservative based on other input and considerations such as ALARP. Hence, the design accidental load may be more severe than the DAL.

	NOTE 2 The design accidental load should as a minimum be capable of resisting the dimensioning accidental load (DAL).
Dimensioning Accidental Event (DAE):	Accidental events that serve as the basis for layout, dimensioning and use of installations and the activity at large.
Dimensioning Accidental Load (DAL):	Most severe accidental load that the function or system shall be able to withstand during a required period of time, in order to meet the defined risk acceptance criteria.
	NOTE 1 DAL is normally defined based on DAE.
	NOTE 2 The dimensioning accidental load (DAL) are typically generated as a part of a risk assessment, while the design accidental load may be based on additional assessments and considerations.
	NOTE 3 The dimensioning accidental load (DAL) are typically established as the load that occurs with an annual probability of 1×10-4.
Explosion load:	Time dependent pressure or drag forces generated by violent combustion of a flammable atmosphere.
Drag load:	Drag force is caused by expanding hydrocarbon gas and air after explosion impinging upon an object. The drag force is a function of the fluid velocity and density along with the object's reference area and drag coefficient. The drag coefficient may further be a function of the Reynolds number. Reynolds number depends on the fluid density, viscosity, and velocity as well as the object's characteristic length. Smaller objects like piping which are inside an exploding gas cloud will be subjected to drag force.
Failure Strain:	Strain level at which the material is no longer providing any stiffness.
Fire load:	Heat flux, normally defined in kW/m2 for a specified duration.
Frequency:	The number of measurements or (expected) observations having a certain value, or characteristic, during a certain observation period (e.g. expected annual frequency is a number of expected observations during one year observation period).
Hazard:	Potential for human injury, damage to the environment, damage to property, or a combination of these.
Hydrocarbon gas explosion:	A process where combustion of a premixed gas cloud, i.e. fuel-air or fuel-oxidiser, is causing rapid increase of pressure. Gas explosions can occur inside process equipment or pipes, in buildings or offshore modules, in open process areas or in unconfined areas.
Integrity:	The ability of a structure to perform its required function effectively and efficiently over a defined time period, while protecting health, safety and the environment.
Jet fire:	Ignited release of pressurized, flammable gas and fluids.
Limit State:	State beyond which the structure no longer fulfils the relevant assessment criteria.
Pool fire:	Combustion of flammable or combustible fluids spilled and retained on a surface.
Probability:	The relative frequency with which an event occurs, or is likely to occur

1.4 How to use these guidelines

These Guidelines are intened as a reference document that contains current practices for the application of ALS in the design of offshore structures. The present Guidelines are separate to the reports of the ISSC Specialist Committee on Accidental Limit States (Czujko et al., 2015) in an attempt to provide a succinct reference for interested professionals and engineers involved in the design of fixed and floating offshore structures.

Section 1 describes the inherent limitations in numerical analyses when studying structural response for ALS. The necessary assumptions made for each of the addressed hazards is also given.

Section 2 discusses the general principles of ALS design.

Section 3 presents the nature of probabilistic and deterministic models employed for determining actions. A reference to target safety levels based on the anticipated variation in the load, resistance and the probabilities that loads act simultaneously is also made.

Section 4 describes the assessment of action effects as a corollary of the previously identified actions. The details of structural models is described, the appropriate material models and type of assessment, per studied hazard.

Section 5 is presenting in detail the hazard of gas explosions from the probabilistic and deterministic point of view. Reference is made to CFD modelling, leak and ignition models, the prevailing environmental conditions and the explosion actions. Specific topics in the application of ALS are summarized with the definition of acceptance criteria, application of explosion actions with details of non-linear dynamic analysis that engineers need to be aware of.

Section 6 is written in a similar fashion as Section 5 where guidance for the design against fire and thermal effects is given together with some design considerations.

Section 7 discusses the nature of probabilistic models for ship collisions, the defined actions from this hazard, assessment of collision effects and relevant design considerations.

Section 8 describes the hazard of dropped objects. Actions, action effects and their assessment is covered with the relevant design considerations.

Section 9 is addressing environmentally driven actions like wind and wave. Due to the uncertainty surrounding most hazardous actions these loads need to be approached probabilistically. The definition of design actions, assessment of action effects from wind and wave and some design considerations are also given.

The Appendix in these Guidelines provide useful data for the application of the presented methodologies. Pertinent terminology is also given in the form of nomenclature to accustom the reader to specific terms and definitions.

The methods and practices presented in the Guidelines cover typical ALS encountered in modern designs. It is the intention that the present document remains a live document with the intention to revise it in the near future as technological advancements take place and further knowledge in the field is gained.

CHAPTER TWO

GENERAL PRINCIPLES OF ALS DESIGN

2.1 Principles of ALS design

These Guidelines apply the limit state (or LRFD) format where the requirements for partial action and partial resistance factors are used for the determination of design actions and action effects.

In LRFD each structural member, or the whole structure, is to be checked for strength using the internal forces (action effects) resulting from the design actions F_d. The generic format of LRFD is given in Eq. 2.1 where the design action F_d is due to the three actions with their corresponding partial resistance factors. The design action(s) for a particular design situation comprise one or more combinations of factored actions, i.e.:

$$F_d = \gamma_G G + \gamma_Q Q + \gamma_T T \tag{2.1}$$

where

- G is permanent action(s) imposed either by the weight of the structure in air, or when submerged during the transient situation being considered.
- Q is variable action(s) imposed by the weight of any temporary equipment or other objects during the transient situation being considered.
- T is represents action(s) from the transient situation being considered (environmental actions, suitable dynamic effects, fabrication tolerances, hydrodynamic actions, lifting actions).

$\gamma_G, \gamma_Q, \gamma_T$ are the partial resistance (or safety) factors for weight, temporary and transient actions respectively.

Although for strength analysis the partial resistance factors take values higher than unity, in ALS design all partial action and resistance factors may be set to 1.0 for both fixed and mobile offshore units (ISO-19902, 2007; ISO-19905-1, 2012; DNV-OS-A101, 2014). Eq. 2.1 does not include any environmental actions as in the context of ALS environmental actions are often disregarded.

Accidental situations attributed to abnormal (extreme) environmental actions with frequency of occurrence of 10^{-4} (10,000 year action) are discussed in Chapter 9.

The main principle of ALS design methodology is to ensure that a structure can tolerate specified action effects through specific performance levels of accidental actions. Accidental actions are the product of selected actions with low probability of exceedance usually identified in QRA. In doing so, the approach is to define a tolerable level of damage following exposure to an accidental action. Ideally the application of ALS design methodology aims at the uninterrupted function of the facility without impairment or impediment to main functions (mainly production, processing, storage, offloading) following an accident.

In case where damage from certain actions can potentially threaten human life, the design is to provide sufficient integrity for a given time to allow personnel to safely abandon the facility. Safe abandonment following an accident should study the integrity of main safety functions that are to remain intact for a given time.

The application of ALS design procedure is portrayed in Figure 2.1 where each identified hazard is treated separately with specific measures of structural response used in the evaluation of structural integrity. The application of ALS is using advanced numerical methods with a combination of theoretical and probabilistic models. Structural integrity in the context of ALS design can be ensured onlocal or global level as per regulatory requirements. Application of risk control options can be decided in cases where structural performance does not conform with acceptable safety levels.

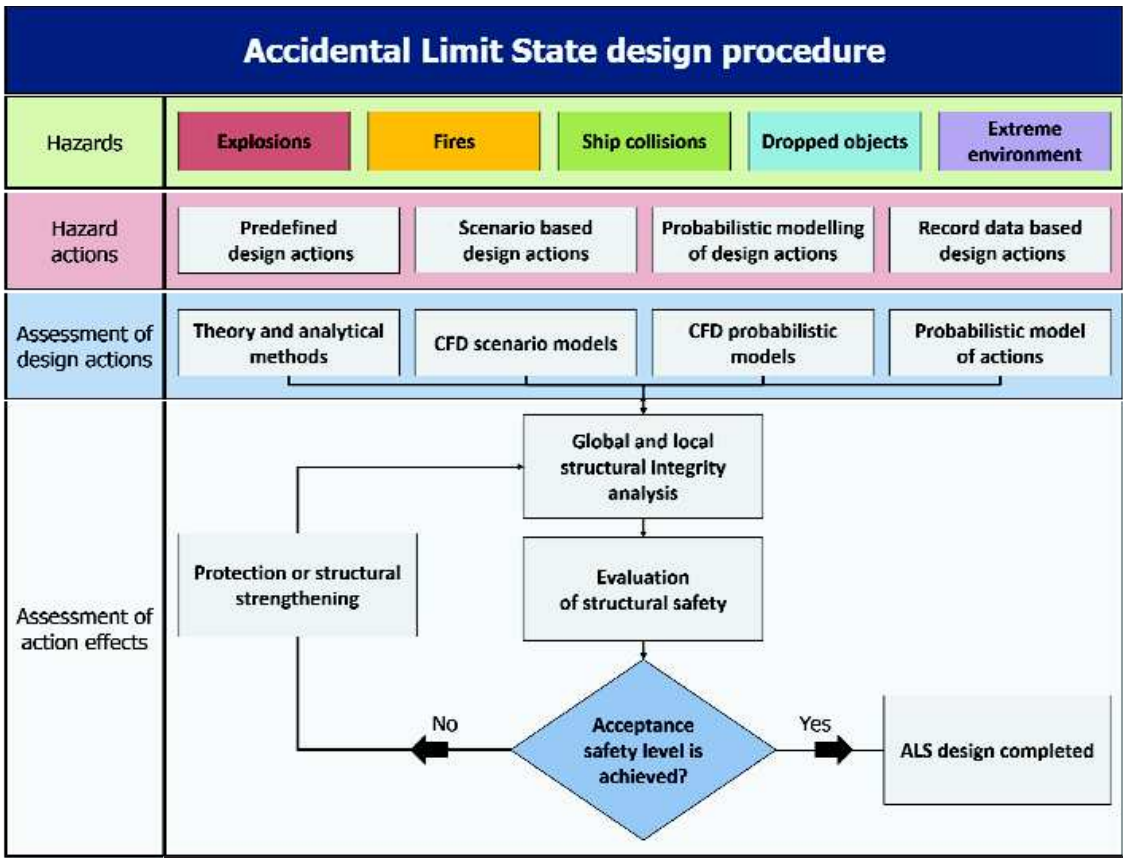

Figure 2.1: Accidental limit state design procedure.

The design procedure on a hazard-by-hazard basis is discussed in the following pragraphs where Figure 2.1 is adapted accordingly

2.2 Assumptions in the Application of ALS

The application of ALS in design is hazard-specific and although it is currently not a regulatory prerequisite, design for identified hazards is a requirement. Application of ALS in the design is an indication that tasks like hazard identification, risk management and safety margins have been considered. In short, ALS is a structured methodology to design for hazards. As in every study several assumptions are necessary that not only reduce desing time but also allow engineers to capture complex phenomena with engineering principles.

Some of the fundamental assumptions in the application of ALS, on a hazard by hazard basis, are given herein:

2.2.1 Gas Explosions[1]

a. Often the variation of overpressure is assumed to be triangular, or rectangular.
b. Material hardening is assumed to follow certain models.

[1]The use of fire/explosion risk studies and use of CFD modelling is the exact assessment of explosion/fire actions.

c. For simple models elastic-perfectly plastic material behaviour is assumed.
d. Inherent assumptions in the finite element models used when meshing on including membrane effects.
e. Assumptions in the enforced failure criteria (based on plastic strain, strain rate effects, time step etcetera)

2.2.2 Fires[2]

a. For simple fire models the elevated temperature is assumed to follow a predefined curve versus time.
b. For local heat up it is assumed that each point is exposed to a pre-determined thermal action (e.g. thermal flux) with the same intensity for a given duration.
c. The integrity of secondary members is often assumed to be maintained during the investigated fire scenario or the members are removed form the assessment models.
d. The convection heat transfer coefficient is conveniently assumed to be identical over the cross section of the exposed member(s).
e. The radiation emissivity coefficient is conveniently assumed to remain constant regardless of temperature changes.
f. Conservatively no shutdown equipment is activated during a leak of combustible agents.

2.2.3 Ship Collisions

a. The employed failure criterion needs to be seen in conjunction with the assumptions made in the safety evaluations.
b. Where no laboratory tests are available, safe and conservative assumptions for ductility limits are often adopted in the analysis. See DNV-RP-C208 (2013) where ductile stress-strain curves, until necking, are given.
c. The applied boundary conditions in the numerical model (FEM) are often an idealization based on conservative assumptions. The extent of the model should be such that no plastic deformations occur in the vicinity of the boundary conditions.
d. In ship impact analyses it is often convenient to treat one body as rigid. However, in some scenarios, this might lead to non-conservative results. A typical example is a simultaneous collision with ship bow and forecastle. A rigid forecastle would concentrate excessive deformations to the upper edge of the struck ship side, leaving less energy to the contact zone with ship bow, which is more critical region in terms of consequences.
e. In ship impact analyses, for beam-, stern end-, and stern corner, against jacket braces all energy is often assumed to be dissipated by the brace.
f. The contact area in boat impact analysis is often an assumption.
g. Often in numerical analysis with beam-only models, failure is assumed as soon as the axial force in a member reaches the axial capacity of the connection. In shell models, or in beam-shell models, failure is typically deformation governed.
h. Often in numerical analysis with beam-only models the employed software is assuming specific collapse mechanisms at the impacted members. In shell, or in beam-shell models, the collapse mechanism is a kinematically admissible model of least energy where no specific collapse mechanism is prescribed.
i. In beam-only models member buckling is assumed to take place when the lateral deformation takes a specific value. In shell, or in beam-shell models, the collapse mechanism is a kinematically admissible model of least energy where no specific collapse mechanism is prescribed.
j. If local buckling does not take place, fracture is assumed to occur when the tensile strain due to combined effects exceeds a critical value.

[2]The use of fire/explosion risk studies and use of CFD modelling is the exact assessment of explosion/fire actions.

2.2.4 Dropped Objects

a. The velocity of dropped objects after impact with the water is assuming that the hydrodynamic resistance is of drag type.
b. As in boat collision, often the striking body is assumed to be rigid so that all energy is to be dissipated by the struck body. Assumptions where both bodies are deformable to a certain degree are also made.
c. The striking body impacts the struck body at a specific angle. Various impact angles can be studied.
d. The trajectory of the striking body after impact is normally neglected, but it may be of crucial safety importance in real situations.
e. Material hardening is assumed to follow certain models.

The above assumptions facilitate the assessment of action effects and rationalize setup of numerical models in a convenient way so that widely accepted formulations are used throughout the industry. More details on setting up numerical models, commonly used material models and acceptance criteria are given in Chapter 4.

2.3 Robustness

The concept of robustness is closely related to accidental actions, consequences of human error, and failure of equipment. In ISO-19900 (2013) these situations are denoted “hazardous circumstances” or “hazards”. Robustness is also important in the event of serious but unidentified fatigue damage.

In ISO-19902 (2007) robustness is achieved by considering accidental limit states that represent the structural effects of hazards. Ideally all such hazards should be identified and quantified by means of rational analyses. However, in many cases it is possible, based on experience and engineering judgment, to identify and reasonably quantify the most important accidental limit states. They will often be those from ship impact, dropped objects, fires and explosions.

A proposal to assign a quantitative measure to the definition of robustness was made by Czujko and Paik (2014) with the concept of robustness index.

Robustness Index, R_I, is defined as (Czujko and Paik, 2014):

$$R_I = 1 - (P_D / P_{DL}) \tag{2.2}$$

where

P_D is frequency of exceedance of damage under accidental action

P_{DL} is frequency of exceedance of design loads (typically 1×10^{-4}).

CHAPTER THREE

PROBABILISTIC AND DETERMINISTIC MODELS OF ACTIONS

3.1 Models of actions for ALS design

A large number of actions needs to be studied particularly when a probabilistic procedure is required. A numerical model should benefit from any symmetry planes, where applicable, with sensible simplifications, while the application of actions should not alter the load path. Advanced numerical analysis is recommended practice in studying ALS with coupled physics where CFD and FE models interact.

The number of simplifications when setting up models for ALS design must be carefully considered particularly when coupled models (fluid-structure interaction) are implemented. Coupled solutions have been shown to yield more representative structural response in structures exposed to explosive actions (Paik et al., 2014), unlike decoupled solutions which can grossly overestimate or underestimate structural response at times.

3.2 Safety levels in ALS design

Safety levels in LRFD-based codes are calibrated by structural reliability analysis associated with acceptable societal and individual risk levels. Risk levels are determined by probabilistic density functions of basic variables that determine annual failure probabilities.

The use of structural codes in ALS design implies certain safety levels where accidental actions are taking characteristic values corresponding to an annual exceedance probability of 10^{-4} per installation ((NORSOK-N-003, 2007), (ISO-19902, 2007), (ISO-19906, 2010)).

The probability of failure associated with an accidental action A can be estimated as:

$$P_F = 2p(F \mid A) \cdot p(A) \tag{3.1}$$

where

$p(F|A)$ is the conditional probability of failure given A

$p(A)$ is the probability of the accidental action

$p(F|A)$ is normally determined using either reliability analysis or by Monte Carlo simulation, while p(A) is determined by QRA.

Acceptable probabilities of failure have been developed by the Nordic Committee on Building Regulations (NKB, 1978) where failure types and consequences of failure are classified in three levels as shown in Table 3.1.

Table 3.1: Acceptable annual failure probabilities (NKB, 1978).

Failure Type		Consequences of Failure		
		Less serious	Serious	Very Serious
I	Ductile failure with reserve strength resulting from strain hardening.	$P_f = 10^{-3}$	$P_f = 10^{-4}$	$P_f = 10^{-5}$
II	Ductile failure with no reserve hardening.	$P_f = 10^{-4}$	$P_f = 10^{-5}$	$P_f = 10^{-6}$
III	Brittle failure and instability.	$P_f = 10^{-5}$	$P_f = 10^{-6}$	$P_f = 10^{-7}$

Probabilistic models are further discussed in Paragraph 3.4.

3.3 Deterministic Models

Deterministic models simplify reality with the assumption that actions are known at all points in a structure over time. Conversely to common perception that accidental actions vary over time, deterministic design is employed through the application of industry standards and rules where prescribed design action effects and design resistance are dictated. Action characteristics are modelled with coefficients, factors of safety and material factors calibrated over the years to produce a safe design and implicitly account for uncertainties.

The basic prerequisites needed to develop a deterministic model according to these Guidelines are the following ones:

- Information/output from risk assessment or QRA where the most detrimental action effects are expected.
- Code of practice where load factors, resistance factors and load combinations are dictated.
- Metocean data from the site.
- A 3-D geometry model of the studied compartment or module.

Specific strength and functionality requirements are to be met depending on the studied action. Example requirements can be of the following types:

- Global structural collapse.
- Rupture or excessive deformation.
- Damage to secondary members (piping, processing equipment) likely to escalate hazardous events (fire, flooding, smoke propagation etc.).
- Unacceptably high temperatures in the escape tunnel/bridge.
- Unacceptable damage to temporary refuge.

3.4 Probabilistic Models

Probabilistic models have the benefit of returning frequency of load exceedance or, more precisely, frequency of exceedance of load parameters, with the aid of exceedance curves. With such models, one can establish safety levels and choose a design load with a specific annual frequency that meets the defined risk acceptance criteria.

Prior to introducing specific details of probabilistic models some fundamental definitions need to be introduced first.

– Probability density function *f(x)*, whose integral equals to 1.0

$$\int_{-\infty}^{+\infty} f(x)dx = 1 \tag{3.2}$$

- Cumulative probability function F(x), which returns the probability of X being less than x. It is monotonically increasing and takes values between 0 (at the left end) and 1 (at the right end).

$$F(x) = P(X < x) = \int_{-\infty}^{x} f(\xi) d\xi \tag{3.3}$$

- Survival function R(x), which returns the probability of X being larger than x. It is monotonically decreasing and takes values between 1 (at the left end) and 0 (at the right end).

$$R(x) = P(X > x) = 1 - F(x) \tag{3.4}$$

If the accidental event described by variable X is assumed to have some specific frequency of occurrence φ[3] then it can be described by a frequency distribution. Frequency distribution is a product of the total frequency of occurrence φ and some probability distribution with the following properties:

- Frequency density function f(x), whose equals to φ (the dimension of φ is time^{-1})

$$\int_{-\infty}^{+\infty} f(x) dx = \varphi \tag{3.5}$$

- Cumulative frequency function F(x), which returns the frequency of X being less than x. It is monotonically increasing and takes values from 0 (at the left end) to φ (at the right end).

$$F(x) = \varphi \cdot P(X < x) = \int_{-\infty}^{x} f(\xi) d\xi \tag{3.6}$$

- Frequency of exceedance function R(x), which returns the frequency of X being greater than x. It is monotonically decreasing and takes values from φ (on the left end) to 0 (on the right end).

$$R(x) = \varphi \cdot P(X > x) = \varphi - F(x) \tag{3.7}$$

As aforementioned probabilistic modelling gives control over safety level where one can choose a design load corresponding to a specific return period and comply with specific requirements.

- Frequency of exceedance of variables x_1, x_2,…, x_n is defined as follows:

$$FOE(x_1, x_1, .., x_n) = F(1 - CDF(x_1, x_1, .., x_n)) \tag{3.8}$$

where, F is the total frequency of occurrence of an accident (collision, fire, blast…) described by variables x_1, x_2,…, x_n, and CDF is the cumulative distribution functions of these variables.

Frequency of exceedance (Eq. 3.8) can be used to identify for example:

- Dimensioning Accidental Load (volume of gas cloud following dispersion, fire design loads etc.).
- Damage level (plasticity, temperature, displacement etc.) corresponding to a specific exceedance frequency.

3.4.1 Generation of Exceedance Curves

Several formulations for the creation of exceedance curves (or hazard curves) can be found in the literature. Exceedance curves are usually plotted on a graph with the load parameter (overpressure, impact energy…) plotted on a linear scale on abscissa, and annual exceedance frequency plotted on a log scale on ordinate. A typical exceedance curve of overpressure is shown in Figure 3.1.

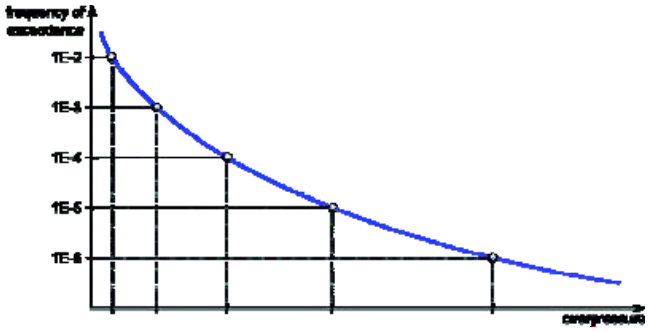

Figure 3.1: Example exceedance curve for blast overpressure.

An exceedance curve will always decrease monotonically. The Log-Normal distribution has been used in the past to create exceedance curves for thin walled structures subjected to hydrocarbon explosion loads (Czujko and Paik, 2014). The sensitivity of any distribution function to its parameters should be studied and appropriate conservatism should be applied when making decisions.

Some of the most popular expressions for the generation of exceedance curves are briefly presented herein.

- UKOOA (2003)
- Is a method of medium complexity for the purpose of identification of the design explosion events corresponding to the Serviceability Limit Blast and Ductility Limit Blast
- An approach tailored to detailed analysis of platforms in operation or in the project phases where the necessary information on all design elements influencing the risk picture is available. Many of the guidelines in this approach might be useful for developing exceedance curves for FPSOs.
- Pressure/Impulse Exceedance curve (Czujko, 2001; NORSOK-Z-013, 2010)
- These are two approaches adapted to blast loaded panels where pressure-impulse curves are created instead of pressure/annual exceedance frequency.

The basic prerequisites needed to develop a probabilistic model according to these Guidelines are the following ones:

- Information/output from risk assessment or QRA (ignition source, fire model, bow/stern collision, typical weight lifted mass).
- Metocean statistics from the site
- A 3-D geometry model of the studied compartment or module.
- Specific properties that affect action effects (gas composition, type of fire, ship mass, mass of lifted hardware).
- Location(s) of particular interest to register analysis output (pressure, temperature, deformation etc.).
- Risk acceptance criteria.

Specific requirements for the development of probabilistic models are given separately in each of the following chapters where hazards are discussed.

CHAPTER FOUR

ASSESSMENT OF ACTION EFFECTS

Analysis is often carried out with CFD and FE methods due to the limitations of theoretical models to predict highly nonlinear responses. The following paragraphs describe the most salient points that engineers should be aware of for the assessment of accidental actions. A thorough discussion is given in Czujko et al. (2015).

4.1 Structural models

Numerical models are set up with the intention of determining action effects and get an estimate of the complicated processes that take place with geometric and material nonlinearities. It is essential to have an understanding of the material properties and ensure that the underlying assumptions are not affecting the structural response unrealistically.

Structural models for the determination of action effects should be set up with a benchmarked finite element analysis programme with dynamic, nonlinear and heat transfer capabilities. Where Computational Fluid Dynamics programmes are used, they should be capable of capturing deflagration and detonation physics with the appropriate turbulence models.

Deterministic models are popular as they can reduce analysis time and provide closed-form solutions to complicate phenomena like blast propagation, hydrodynamics, and damping among other. On the other hand, non-linear effects like yield progression to plasticity, strain rate effects, strain hardening and large deflections can rarely be captured with closed-form solutions.

Table 4.1 very briefly gives the degree of required detail in modelling actions with relevant reference work where the details of each model, per hazard, is studied. The degree of computational effort can vary, as not all actions require the same degree of modelling effort. Nevertheless, common for all structural evaluations is the need to capture non-linear effects like plasticity, thermal softening, shell thinning etc.

Table 4.1: Description of Models for ALS Design.

Accidental Action	Degree of Modelling Effort
Gas Explosion (Paik et al., 2014)	Pressure and drag force from CFD simulations are mapped onto the structural (FE) model to get a dynamic nonlinear response. The exposed structure may consist of beam and shell elements.
Fire (Paik et al., 2013)	Thermal effects from CFD simulations are mapped onto the structural (FE) model. The exposed structure may consist of beam and shell elements.
Ship Collision (LR, 2014a)	Ship-to-Fixed Structure: Beam model where striking body may, or may not, be modelled. Ship-to-Ship Collision: Beam/shell model where both striking and struck bodies are modelled.
Dropped Objects (DNV-OS-C101, 2014)	Beam/shell model where the striking body may, or may not, be modelled.

The degree of detail in numerical models depends on the action being studied. Every studied limit state should be in compliance with the results from risk analyses that have been carried out as a prerequisite to the analysis. The structural response can differ on the basis of structural details included in a model as complicated responses, like web tripping or flange curling, can only be captured with shell elements. Likewise, structural response under fire often neglects any plating contribution and only includes the primary (and in some cases secondary) beams. Understanding the anticipated collapse mechanism(s) and the effects of added, or ignored, structural elements on the output of concern is essential. Table 4.2 gives the modelling requirements per accidental action recreated from the work of Czujko et al. (2015).

Table 4.2: Modelling Requirements per Accidental Action (Czujko et al., 2015).

Accidental Action	Degree of Structural Detail
Gas Explosion	Plated structure (or combination of shell/beam) with flushed members, stools and structural foundations.
Fire	Plated structure or beam-only structure with, or without, PFP included. No flushed members.
Ship Collision	Plated structure with flushed members including secondary members.
Dropped Objects	Plated/beam structure with flushed members.

4.2 Material models

The expected non-linear effects expected in numerical models prepared for ALS design should be captured through appropriate material models. Material properties vary with the carbon content that affects ultimate strength, yield strength and tensile failure levels. Material properties will also vary in thermal analyses where thermal properties need to be considered as a function of temperature. Significant differences in the thermo-physical properties (conductivity, specific heat capacity and thermal strain) of carbon steel and aluminium are noted when exposed to high temperatures; changes in the mechanical properties (Young's modulus and yield stress) are also taking place and should be addressed. Recommended material models often employed for the assessment of action effects are given in the Annex of this Guideline.

Table 4.3 gives the appropriate models to be employed on a hazard-by-hazard basis. For the underlying details with a discussion on temperature-dependent properties, plasticity models and failure criteria see Czujko et al. (2015).

Table 4.3: Non-Linear properties to be considered per accidental action.

Accidental Action	Non-Linear Material Model
Gas Explosion	Plasticity (OTI-92-602; EN-10025-3; EN-10025-6; DNV-RP-C208)
	Failure Criterion (EUROCODE-3; ISO-19902; Kõrgesaar et al., 2014)
Fire/Thermal	Temperature-dependent properties (Kodur et al., 2010; LR, 2014b)
Ship Collision	Plasticity (OTI-92-602; EN-10025-3; EN-10025-6; DNV-RP-C208), Failure Criterion (EUROCODE-3; ISO-19902; Kõrgesaar et al., 2014)
Dropped Objects	Plasticity (OTI-92-602; EN-10025-3; EN-10025-6; DNV-RP-C208), Failure Criterion (EUROCODE-3; ISO-19902; Kõrgesaar et al., 2014)

The relevant material properties of structural steel used in offshore structures are characterized by mechanical properties often taken from open sources like EN-10025-3 (2004)

for thicknesses less than 250mm for grades S275, S355, S420, and S460. EN-10025-6 (2004) should be consulted for steel products of high yield strength with a maximum nominal thickness of less than 150 mm for grades S460, S500, S550, S620 and S690.

4.3 Type of assessments

The available methods of assessment vary with regards to their simplicity, accuracy and ease to ensure the quality of results. Table 4.4 suggests best methods for the assessment of action effects from simplest to most accurate solutions. The adopted solution must consider and analyse the governing properties and sequence of events; this is ensured as computational effort increases.

Assumptions and simplifications based on sound physics used in all assessments must be mentioned with corresponding referecens where appropriate.

For quality assurance purposes a check list must accompany all assessments where cardinal analysis elements are addressed.

Table 4.4: Assessment types applicable to ALS design.

Accidental Action	**Theoretical / Semi-empirical Analytical Sol'ns**	**Numerical Sol'ns (De-coupled)**	**Numerical Sol'ns (Coupled)**
(LOW) → Computational Effort & Accuracy → (HIGH)			
Gas Explosion	SDOF models (w/out strain rate effects) (Biggs, 1964; FABIG-TN4, 1996; FABIG-TN7, 2002; FABIG-TN10, 2007)	Explicit FEA w/ plasticity, strain rate effects† (Czujko and Paik, 2012)	Explicit FEA w/ hydro-code† (Czujko and Paik, 2014)
Fire/Thermal	FABIG-TN1 (1993), FABIG-TN3 (1995)	Implicit/explicit steady state or transient† (Czujko et al., 2015)	Explicit FEA w/ hydro-code† (Czujko and Paik, 2010)
Ship Collision	DNV-RP-C204 (2010)	Explicit FEA w/ plasticity, strain rate effects† (Tabri and Broekhuijsen, 2011)	Explicit FEA w/ hydro-code† (Tabri and Broekhuijsen, 2011)
Dropped Objects	SDOF model, closed-form expressions (Veritec, 1988)	Explicit FEA w/ plasticity, strain rate effects†	Not required
Extr. Environment	SDOF model (Ref)	Implicit/explicit FEA w/ plasticity, strain rate effects†	Not required
Structural Response‡	**Quasi-static**	**Dynamic**	**Dynamic**

† Time-domain solution,
‡ The response of structural components is classified according to the duration of the excitation relative to the fundamental period of the component.

The work of ISSC Committee V.1 on ALS in 2012 and 2015 (Czujko et al., 2012; Czujko et al., 2015) has made use of explicit solvers (decoupled solution) for hydrocarbon explosions and thermal actions respectively. Satisfacotory results have been reported in both cases.

4.4 Acceptance criteria

ISO-19901 (2010) expands acceptance criteria, by adding a ductile capacity limit which incorporates buckling and rupture, and requires that in accidental load analysis all partial safety

factors are reduced to 1.0 and best estimates of yield stress are applied, in conjunction with strain rate and strain hardening effects.

NORSOK-Z-013 (2010) gives risk acceptance criterion related to loss of the main safety function main load carrying capacity (regardless of whether the criterion is 1×10^{-4} or another annual probability) that applies to the global sum of losses on the facility due to each accidental or environmental load category (e.g. the sum of all fires that causes loss of the main load carrying capacity on any part of the facility).

Acceptance criteria can be expressed in various forms as specific measures, or functional requirements, on one studied action at a time. Table 4.5 gives acceptable criteria, based on previous studies, that can be used as acceptance criteria under the effect of accidental actions.

Table 4.5: Example acceptance criteria per accidental action.

Accidental Action	Acceptance Criterion
Gas Explosion	1%–5% strain level (Czujko and Paik, 2014)
Fire/Thermal	Critical deflection (DNV-RP-C204, 2010)
Ship Collision	Deformation energy, critical deformation to avoid leakage of compartments (DNV-RP-C204, 2010)
Dropped Objects	Critical deflection, 5% strain level (ISO-19902, 2007)

In lieu of more advanced analysis, a member shall be conservatively assumed to disconnect when the tensile strains in the extreme fibres of a steel member exceed 5% (ISO-19902, 2007).

CHAPTER FIVE

GAS EXPLOSIONS

5.1 Purpose

The purpose of applying ALS in design is to ensure that acceptable limits of safety are met, safeguard the environment and protect lives from gas explosion hazards. In the ALS design procedure, the assessment of action and action effects includes definition of design explosion actions and the assessment of action effects to guarantee structural integrity, system redundancy, and to determine amount of necessary reinforcement to maintain structural safety.

5.2 ALS design for explosion accidents

The general ALS design procedure given in Figure 2.1 is modified to accommodate specific needs for the evaluation of structural integrity when exposed to explosion actions as shown in Figure 5.1; key workflow elements are discussed in the following pages.

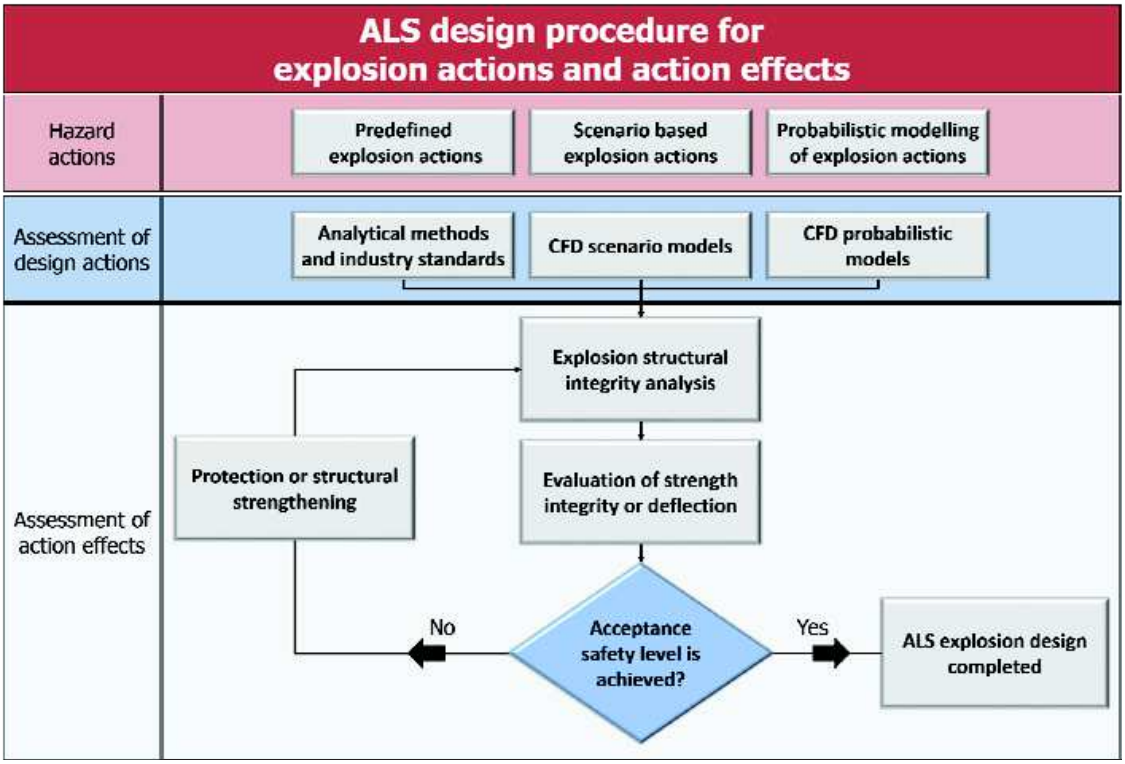

Figure 5.1: ALS design procedure for explosion actions and action effects.

5.3 Types of gas explosion actions

Gas explosion generates different types of actions depending on the size of exposed structures and equipment. The following types of explosion actions have to be considered in design:

a) Explosion overpressure, p_o, dynamic action generated on large surfaces.
b) Drag force, p_d, dynamic action generated on small equipment items and piping.

c) Differential pressure, p_{diff}, global dynamic action generated on large equipment items or enclosures located within the explosion area by explosion wave passing the object.

Overpressure loads result from increase in pressure due to the rapidly expanding combustion process. Description of time dependent overpressure and drag pressure is given in Figure 5.2 and 5.3 respectively.

Drag is a vector quantity in contrast to the overpressure which is scalar, i.e. drag has three independent components. Drag is proportional to square of flow velocity and it can be significant for long and slender objects when the flow speed in the plane normal to object's length is high. Hence, drag should be measured in a plane, not in a direction, referred to as plane drag as shown in Figure 5.3.

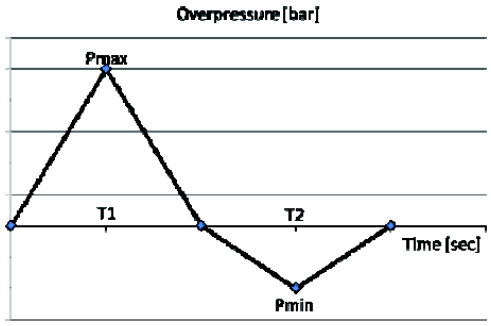

Figure 5.2: Parameters defining design overpressures and drag pressure.

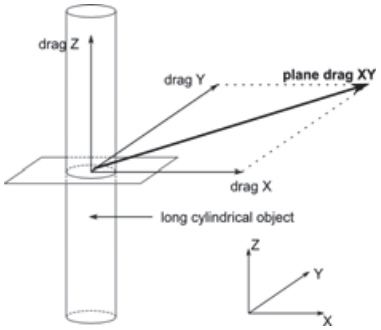

Figure 5.3: Directions of design drag pressure.

5.4 Deterministic models of explosion actions

Most of the predefined gas explosion loads are presented as a space averaged, peak explosion overpressure for typical concept types of installations, and based on limited design data set and operating experiences. Therefore, it is often a conservative value and used in the early phases of design. Deterministic models could follow a series of steps that produce a safe design and then to set DAL loads accordingly. The recommended approach is given below (DNV-OS-A101, 2014).

a) Determine the explosion areas and calculate their volumes (explosion volume).
b) Find the curve letter in Table 5.1 based on congestion, operation, confinement and wind protection.
c) Read off the overpressure in Figure 5.4 using the explosion volume.
d) The pressure pulse duration varies between 0.05 and 0.2 sec.
e) Drag pressure can be set to one-third of the overpressure.

Alternative figures of nominal explosion overpressures for a number of platform types can be found in API-RP2FB (2006) as shown in Table 5.2. The following steps are required in this methodology:

a) Select concept type (fixed jacket or floating facility).
b) Establish conditioning factors to apply (production rate and trains, gas composition. and pressure, module area, aspect ratio and confinement, refer to Table 5.3).
c) Determine nominal overpressures (and associated duration).
d) Apply safety factors to account for data uncertainties.

Table 5.1: Categorization of naturally ventilated offshore oil and gas areas with respect to explosion pressures (DNV-OS-A101, 2014).

Congestion/ density level	Operation	Confinement by balstwalls and solid decks		Typical unit type	DAL on	Weather cladding	Curve no.
		Confinement level	Blastwalls and solid decks				
High to normal	Production	Confined	1 or 2 blastwalls, open or solid deck 6m or more above	FPSO, FLNG, Semi sub, fixed	Blastwall (s)	Windwalls more than 50%	A
						No windwalls	B
		Open	No blastwalls open or deck above (FPSO, FLNG)	FPSO, FLNG, Turrets	Deck	Windwalls more than 50%	B
						No windwalls	D
Less congested	Drilling	Confined	1 or 2 blastwalls, open or solid deck 6m or more above	Drilling rig, Integrated prod/drill	Blastwall (s)	Windwalls more than 50%	B
						No windwalls	C
		Open	No blastwalls open or deck above	Drilling rig	Deck	Windwalls more than 50%	C
						No windwalls	E
Less congested	Tank deck/ crude piping area or similar	Confined	1 or 2 blastwalls, open or solid deck 6m or more above	Tank decks (FPSO, FLNG)	Blastwall (s)	Windwalls more than 50%	E
						No windwalls	F
		Open	No blastwalls open or deck above	Open area on tank deck	Deck	Windwalls more than 50%	F
						No windwalls	G

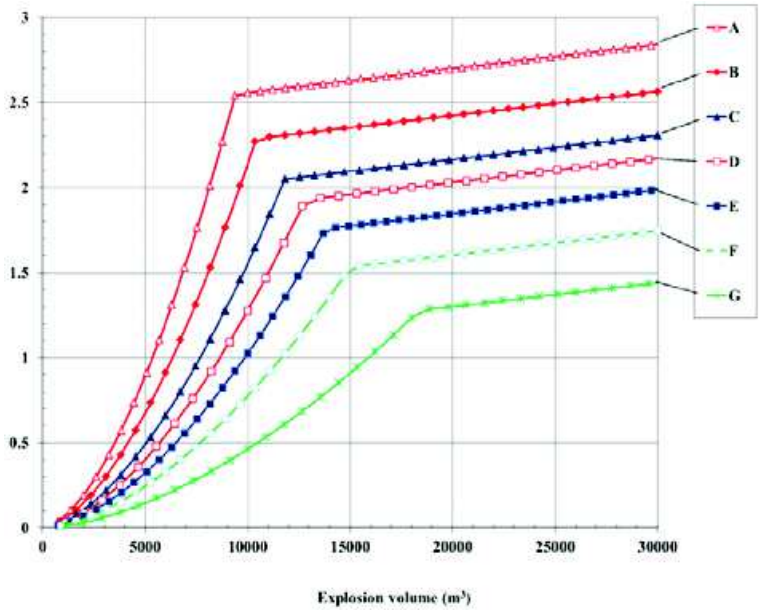

Figure 5.4: Design explosion pressures as a function of the explosion volume; The curves are difined in Table 5.2 (DNV-OS-A101, 2014).

Table 5.2: Nominal overpressures by installation type (API-RP2FB, 2006).

Blast prone area	Nominal overpressure for different offshore installations, [bar]				
	Integrated production/ drilling (Single platform)	Bridge linked production/ drilling (Multiple platforms)	Production only (Single jacket)	Production only (Mono-hull FPSO)	Integrated production/ drilling (TLP/Wet tree)
Well heat/ Drill deck	2.5	2.0	–	–	2.5
Gas separation facility	2.5	1.5	1.5	1.0	1.0
Gas treatment/ Compression facilities	1.5	1.0	1.0	1.0	1.0
Turret (Internal)	–	–	–	3.0	–
FPSO main deck	–	–	–	2.0	–
TLP moon pool	–	–	–	–	2.0
TLP deck box	–	–	–	–	2.5
Other	1.0	1.0	1.0	0.5	0.75

Table 5.3: Load modifiers (API-RP2FB, 2006).

Project parameters		Nominal blast load modifiers
Item	Range/Rate/Qty	
Production rate	Less than 50,000 bbl/day	0.90
	50,000 to 100,000 bbl/day	1.05
	More than 100,000 bbl/day	1.10
Gas compression pressure	Less than 100 bar	1.00
	100 to 200 bar	1.05
	More than 200 bar	1.10
Gas composition	Normal	1.00
	Onerous	1.10
	More onerous	1.35
Production trains	1	0.90
	2	0.95
	3	1.10
Module footprint area	Less than 75,000 sqft	0.90*
	75,000 to 150,000 sqft	1.00
	More than 150,000 sqft	1.10
Confinement	3 sides or more open	0.85
	1 to 2 sides open	0.95
	All sides closed	1.25
Module length to width aspect ratio	Less than 1.0	0.90
	1.0 to 1.7	1.05
	More than 1.7	1.10
*For small and very congested platforms (~10000 sqft), the Load Modifier of 0.9 should not be applied to reduce the nominal explosion overpressure for Module Area. NOTE: Load Modifier should not be applied to wellheads/drilling decks, Moonpools, and FPSO main deck.		

5.5 Probabilistic models for gas explosion actions

Design loads are hard to define by a unique scenario, by doing so one risks overestimating, or underestimating action effects. It is therefore preferable to use a probabilistic approach in determining design explosion loads. The most influential design parameters to be considered in calculating probabilistic explosion loads are:

- Leakage rate and direction with corresponding frequencies;
- Wind speed and direction with corresponding frequencies;
- Ignition source intensity and location with corresponding frequencies;
- Gas clouds size, location and concentration, and so on.

The distribution of explosion loads is defined based on numerous explosion scenarios, which come from a combination of the above parameters simulated by sophisticated analysis methods, like CFD. NORSOK Z-013 (2010) presents the probabilistic approach with CFD simulation for explosion integrated in the process of Quantitative Risk Analysis (QRA). The probabilistic explosion analysis with CFD comprises the following main tasks:

a) Build a 3-D model of the facility.
b) Establish leakage scenarios based on isolatable segments.
c) Present leak frequencies and durations.
d) Perform ventilation simulations for different wind directions and wind speeds in order to determine the ventilation conditions.
e) Perform dispersion simulations with varying leak parameters in order to assess the potential gas cloud build-up from an accidental release.
f) Identify potential ignition sources in the process modules.
g) Perform explosion simulations with varying gas cloud sizes, gas cloud locations and ignition locations to calculate the potential explosion loads.
h) Calculate the exceedance curves for explosion loads at a given location.
i) Determine the dimensioning load with the cut-off frequency of risk acceptance criteria.

Figure 5.5 shows steps in explosion modelling and intermediate results. The design random variables considered in calculating explosion loads are gas leakage rate and direction; wind speed and direction; locations of ignition; gas clouds size, location and concentration.

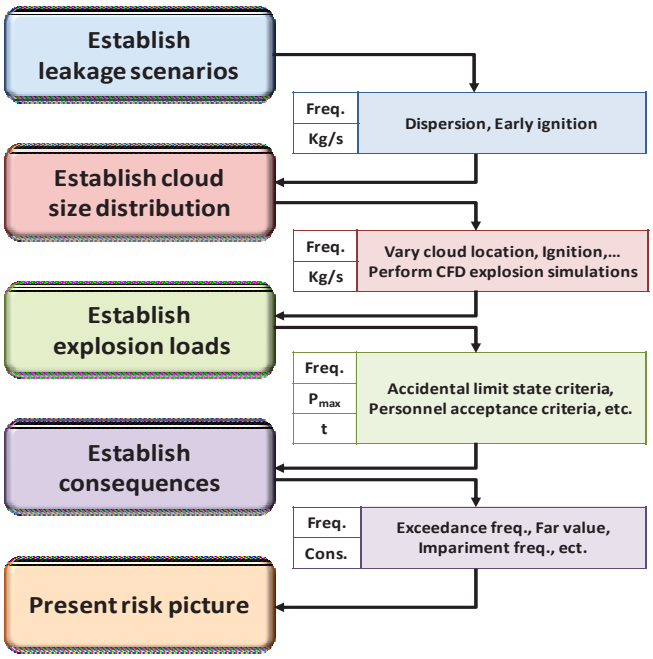

Figure 5.5: Schematics of procedure for calculation of explosion risk (NORSOK-Z-013, 2010).

5.5.1 CFD modelling

Gas explosion loads are affected by the degree of congestion and confinement of layout and also by a compartment's geometry. A numerical model for a CFD analysis needs to include all those details likely to affect congestion and confinement. If geometry details are not available in early design phases, it is essential that all anticipated equipment is identified and modelled based on experience and engineering considerations, e.g., anticipated congestion method.

The boundaries of the computational domain should extend sufficiently so that the different physics involved in each analysis phase, i.e. ventilation, dispersion and explosion, are captured.

5.5.2 Leakage and ignition models

This guideline recommends at least nine initial leak rate categories for detailed explosion simulations. The recommended leak rates are based on a distribution of the orifice sizes and the pressure in the system.

0.1~0.5, 0.5~1, 1~2, 2~4, 4~8, 8~16, 16~32, 32~64, >64 (kg/s)

For initial leak rate categories, the corresponding transient leak rates shall be calculated taking into account the pressure drop due to blow-down and leak, as well as isolation time of the process segment. The topside process segments are divided into isolatable segments bounded by Emergency Shutdown Valves (ESDV), and these can be further broken down based on the operating conditions, compositions, phases and location etc. In the context of the explosion risk analysis, the ESDVs are crucial to ensure a safe isolation and shutdown of the process system in the event of an emergency (i.e. detection of hydrocarbon release).

The failure frequency of each isolatable segment is based on historical data and derived by counting the associated equipment and fittings e.g. vessels, heat exchangers, valves, flanges, instruments and piping, etc. A useful list of recognized failure data sources can be found in NORSOK Z-013 (2010).

In the ignition modelling, a time dependent ignition probability model should be used. The frequency distribution of cloud sizes shall be calculated at the time of ignition, and transient modelling of the gas cloud and its detection is required as input to the ignition model.

The explosion frequency from a leak event can be determined by the leakage scenario frequency by considering the probabilities of ignition.

5.5.3 Wind conditions and ventilation

It is recommended that at least eight wind directions with a frequency and speed distribution should be considered from wind rose data. From ventilation simulation, those wind conditions can be grouped into a few (2 to 4) different ventilation regimes. Based on this information, representative wind conditions could be selected for the dispersion analyses. Proportionality of ventilation rate to the wind speed is acceptable when generating a ventilation distribution in terms of rate, direction and probability.

5.5.4 Dispersion and explosion simulations

Dispersion simulations are performed with varying leak parameters and wind condition to assess the potential gas cloud build-up from an accidental release. The stoichiometric equivalent cloud is used to produce a representative cloud size distribution that is used in the explosion simulations.

Explosion simulations are performed with different gas cloud sizes, location, and ignition locations to calculate the time dependent explosion loads. Overpressure loads should be recorded at monitoring panels and points and expressed as the different types of loads (See Ch. 5.3).

5.5.5 Exceedance curves and DAL

In a probabilistic approach, the gas explosion loads can be expressed in the form of exceedance curves. Exceedance curves are typically plotted with overpressure of linear scale on the horizontal axis, and annual exceedance frequency on a log scale on the vertical axis. An exceedance curve will always be a monotonically decreasing (discrete) function. Exceedance

curves can relate to overpressure at a point, or averaged over a wall, or other load type such as drag pressure or impulse.

From the exceedance frequency curve, the explosion load whose cumulative exceedance frequency corresponds to risk acceptance criteria, i.e. 1.0×10^{-4}/year is selected as the DAL (Dimensioning Accidental Load). In the present industrial practices for offshore explosion analyses, pressure and impulse exceedance curves are considered separately.

5.6 Definition of design actions

5.6.1 Basis for definition of design actions

Dimensioning load shall not cause loss of safety functions or escalation (locally). Unless specific explosion analysis, scenario based or probabilistic assessments are performed, Tables 5.4 and 5.5 apply.

5.6.2 UKOOA and API approach

For the design load of offshore structures in ALS design, there are the two levels of gas explosion actions; the Ductility Level Blast (DLB), and Strength Level Blast (SLB) actions defined as shown in Table 5.4.

Table 5.4: Blast load levels (Oil & Gas UK, 2007 and API RP2FB, 2006).

Load	SLB	DLB
	Reduced blast load	Design level blast load
Event	High-probability (10^{-3}/year), Low-consequence event	Low-probability (10^{-4}/year), High-consequence event
Performance criteria	Elastic response of the primary structure, SCE[1] remaining functional. Restart operation within a reasonable period	Inelastic response of the primary structure, Retaining the integrity of the escape system, No overall collapse with escape possible
Recommended analysis method	Modified code check, SDOF method, static FEA with DAF (Dynamic Amplification Factor)	Dynamic NLFEA

[1] SCE – Safety Critical Elements

5.6.3 ISO and NORSOK approach

According to NORSOK requirements (NORSOK Z-013), facilities shall be designed with due consideration to fire, explosions, impacts, flooding, loss of heading (dead ship scenario) and other relevant accidental events with associated effects. In assessing the risk for accidental events, technical, operational and/or organizational risk reducing measures should be considered.

NORSOK Z-013 defines dimensioning accidental load as the most severe accidental load that the function or system shall be able to withstand during a required period of time, in order to meet the defined risk acceptance criteria. The dimensioning accidental load (DAL) is typically established as the load that occurs with an annual probability of 10^{-4}. Dimensioning accidental action are normally based on safety studies performed within the quantitative risk analysis performed during the desig phase of the project.

5.6.4 Actions to be used in consequence analysis

The design explosion actions for a topside structure are expressed as representative values for different compartments of a topside. Congestion and combustion contents can generate different types of loads, that is, overpressure, drag pressure and differential pressure. An example application of these loads is shown in Table 5.5 while drag coefficients can be equipment-specific values.

Table 5.5: Structural components and calculation basis for a topside structure.

Structure	Explosion action	Calculation basis
Structural members (wall, deck, beam, column, panel)	Overpressure and drag load	-
Piping	Drag load	F_D = Dynamic pressure × Drag coefficient C_d = ½ × ρ × A × v^2 × C_d; C_d = 1.2
		Simplified approach: F_D = ⅓ × Local overpressure
Vessels	Pressure differential load	F_P = ΔP × section area × PDF
Grating floor	Drag load	F_G = Dynamic pressure × Drag coefficient C_d × Permeability factor; C_d =2.0
Large items	Reflected load	F_R = Overpressure × Reflection coefficients; Reflection coefficient = 2.0 for front wall

where, ρ is the fluid density, A is the maximum cross sectional area of the object in a plane normal to v, and v is the large scale fluid velocity ignoring spatial fluctuations in the vicinity of the object. PDF is pressure distribution factor (for cylinders, 2/π) and ΔP is the differential pressure across the obstacle.

For drag dominated structures drag action can be represented as, Czujko (2001):

$$F = F_d + F_p \tag{5.1}$$

where

F_d is form drag contribution proportional to the area, density and velocity square, and depending on Reynolds number and function of Mach number (U/c), where U is velocity of expanding gas and c is speed of sound.

F_p is contribution from the differential pressure.

For small piping and equipment, form drag is a dominant contribution in drag forces. Large equipment, as for example compressors, is mainly subjected to effects of differential pressure. Large items like scrubbers are subjected to both drag components. Table 5.6 is recommended as a basis criterion for the calculation of drag force.

Table 5.6: Limit for equipment size when drag force becomes considerable.

D (m)	F		
	F_d	$F_d + F_p$	F_p
< 0.6	X	–	–
0.6 < D < 2.0	–	X	–
> 2.0	–	–	X

5.6.5 Calculation of drag coefficient

The drag coefficient is dependent on the Reynolds number a shown in Figure 5.6 for a circular cylinder.

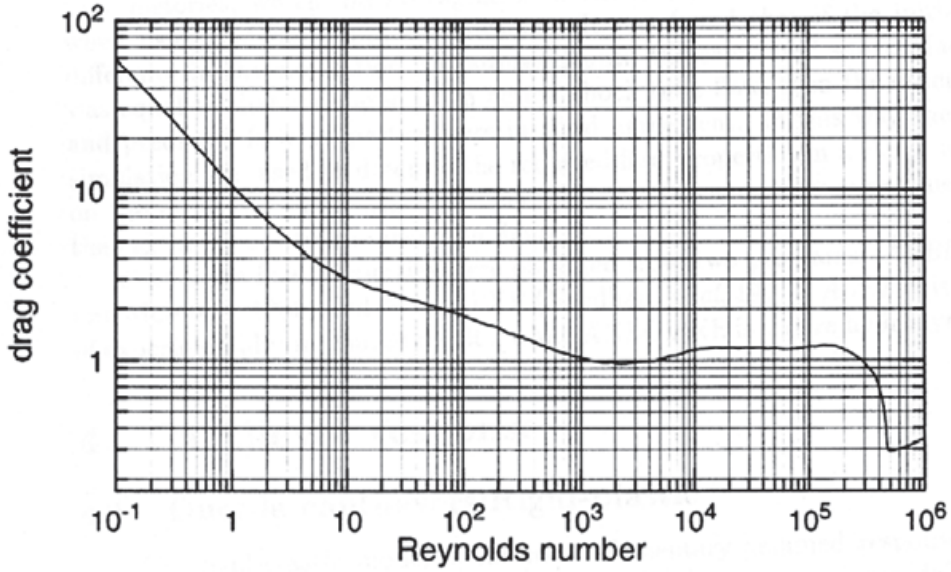

Figure 5.6: Drag coefficient for circular cylinders as a function of the Reynold's number (Schlichting, 1979).

The Reynold's number is:

$$\mathrm{Re} = \frac{\rho \cdot U}{\mu} \tag{5.2}$$

where
ρ is density,
U is velocity,
D is characteristic length (e.g. diameter of a pipe) and μ is dynamic viscosity.

When $\mathrm{Re} > 2\times10^5$, the drag coefficient drops significantly.
When $\mathrm{Re} > 5\times10^5$, the drag coefficient is only about 0.25 × Re in the range $10^3 \sim 2\times10^5$.
The dynamic viscosity μ is 6×10^{-5} for burned gases and 1.78×10^{-5} for air.
By using $\mathrm{Re} = 5\times10^5$ as a "transition" limit, one may write for burned gases:

$$5\cdot10^5 = 0.17\cdot U\cdot D/(6\cdot10^{-5}) \tag{5.3}$$

From Equation (5.3), for $U \cdot D > 176$ the drag coefficient will be low, typically 0.3, otherwise it will be high, typically 1.2.

The velocity U for burned gases is measured to be above 300 m/s for basically all cases and may attain values up to 700 m/s, or even higher. The characteristic length (diameter D) of the exposed object is then;

$$D > \frac{176}{300} = 0.6m \tag{5.4}$$

The pipe diameter dependent drag coefficient are given in Table 5.7.

Table 5.7: Drag coefficients.

D (m)	C_d	
	Single pipe	Pipe rack
< 0.6	1.20	1.30
> 0.6	0.30	1.20

5.7 Assessment of actions effects

The structural design for the time dependent gas explosion load has to consider the dynamic and non-linear structural behavior.

The dynamic response of structural components can conveniently be classified into three categories according to the duration of the explosion pressure pulse τ, relative to the fundamental period of vibration of the component, T as shown in Table 5.8. The gas explosion loading of offshore facilities is usually within the dynamic loading regime.

For non-linear structural response, especially for large explosion loads like DLB load, non-linear effects like large displacements, load re-distribution and material property changes should be considered in the analysis procedure.

Table 5.8: Structural analysis methods with acceptance criteria for dynamic loads.

Loading regime τ/T	**Dynamic response**	**Non-linear response**	
		Strength level analysis (Design code)	Ductility level analysis
Impulsive $\tau/T \leq 0.3$	Energy method	Strength limits (linear elastic analysis based on LRFD or ASD code with modified factors for nonlinear behavior)	Deformation limits (ductility ratio, failure strain or deflection for nonlinear analysis)
Dynamic $0.3 < \tau/T < 3.0$	Dynamic analysis with SDOF or MDOF(FE) method		
Quasi-static $\tau/T \geq 3.0$	Static or Energy method		

The response to explosion loads can be determined by non-linear dynamic finite element analysis, or by simple calculation models based on Single Degree Of Freedom (SDOF) analogies.

5.7.1 SDOF method

In the simple calculation models, the component is transformed to a single spring-mass system exposed to an equivalent load pulse by means of suitable shape functions for the displacements in the elastic and elastic-plastic range. The shape functions allow calculation of the characteristic resistance curve and equivalent mass in the elastic and elastic-plastic range as well as the fundamental period of vibration for the SDOF system in the elastic range. Provided that the temporal variation of the pressure can be assumed to be triangular, the maximum displacement of the component can be calculated from design charts for the SDOF system as a function of pressure duration versus fundamental period of vibration and equivalent load amplitude versus maximum resistance in the elastic range. The maximum displacement must comply with ductility and stability requirements for the component.

5.7.2 Non-linear dynamic finite element analysis

When a structure cannot be idealized to an SDOF, the MDOF (Multi Degree of Freedom) method is used to consider its dynamic response. Dynamic non-linear finite element analysis (NLFEA) is a powerful tool to calculate the complicated structural response of the explosion.

NLFEA has the capability to account for non-linear and rate dependent material behaviour, geometric non-linearity, load re-distribution, large displacements, local and global instability in the structural response simulation. To guarantee the validity of results, the type and size of finite elements, boundary conditions, plasticity models and failure strain limits. need to be considered during the assessment process. For a thorough discussion see Czujko et al. (2015).

5.7.2.1 Structural models for FEA

The degree of detail of FE models for ALS design is often adhering to the following:

- Global response: coarse mesh with primary members only.
- Local response: medium-size mesh with primary and secondary members.
- Detailed response: fine mesh, often controlled by tertiary members (flange width, web height, bracket size and other tertiary structural elements. Submodelling may also be necessary.

Failure modes like yielding or buckling can be captured as long as a sufficiently fine mesh and the proper element types are in place. The boundary conditions should be applied in a realistic manner, at a sufficient distance from the point of interest to minimize any Poisson effects.

5.7.2.2 Application of explosion loads for FEA

Gas explosion loads are represented as uniform pressures for shell elements, and line loads when acting on beam elements. In a local analysis, the pressure can be treated as uniform over the whole model. However, in a global analysis, the spatial variation of the load should be accounted for (see coupled solutions, Section 4.3).

5.8 Acceptance criteria for action effects analysis

Performance standards for an explosion event dictate that at least one escape route must be available following the event for all survivors. A temporary refuge or safe mustering area must be available to protect those not in the immediate vicinity of an explosion, and to survive the event without injury. Table 5.4 shows the performance criteria according to the load level of SLB and DLB.

Specific acceptance criteria for failure or damage of structural members and systems under explosion loads is closely dependent on the analysis method and level of refinement. Strength criteria (e.g. yield strength, bucking strength), or deflection criteria (e.g. plastic strain limit, ductility ratio, deformation limit) are typically used as shown in Table 5.8.

5.8.1 Strength limit

Using LRFD or ASD code, structural failure is defined as the state that the design load, or load effects, exceed the design strength. For gas explosion design with plastic regimes, modified factors on loading and strength must be adopted considering an extreme event.

5.8.1.1 Modified factors for design code

Recommended modified factors for design codes are shown in Table 5.9.

5.8.1.2 Strain rate effects

Due to rapid rate of changes of strain in steel materials under gas explosion events, the material properties change in a dynamic state. The most important effect is the increase of yield stress due to strain rate effects. The Cowper-Symonds relation can be used to account for the non-linear strain rate effects as given in Equation 5.5.

$$\frac{\sigma_d}{\sigma_y} = 1 + \left(\frac{\dot{\varepsilon}}{D}\right)^{1/P} \tag{5.5}$$

where

σ_d is dynamic yield stress, σ_y = static yield stress, ε̇ = equivalent plastic strain rate

D, q is material-depended coefficients asdefined in Table 5.10

Table 5.9: Appropriate modified factors for design codes (FABIG IGN 1993 & Oil & Gas UK 2007).

Design code	Factors	Load or strength	Values
LRFD	Load factor	Dead loads, storage and other permanent loads	1.0
		Variable loads	0.33(BS 5950-1:2000) ~ 1.0
		Blast loads	1.0
		Environmental loads	Can be ignored
	Resistance factor	Yield strength	Divided by 1.0 with strain rate effect (×1.2)
ASD	Overstress factor	Yield strength	Approaching yield (utilization factor × 1.5) with full plastic section (×1.12)

Table 5.10: Coefficients D and P for dynamic yield stress (Jones, 1989; Paik and Wierzbicki, 1997; Burgan, 2001).

Material	D (s^{-1})	q
Mild steel	40.4	5
High tensile steel	3200	5
Aluminium alloy	6500	4
α-Titanium (Ti 50A)	120	9
Stainless steel 304	100	10
Stainless steel 316L	240	4.74
Stainless steel 2304	3489	5.77
Stainless steel 2205	5958	6.36

5.8.2 Deformation limit

The following criteria for the deflection limit in ALS design are recommended herein:

- No part of the structure impinges on critical operational equipment.
- The deformations do not cause collapse of any part of the structure that support SCE within the required endurance period.

5.8.2.1 Strain limit

Failure strains of typical materials encountered in offshore facilities are suggested in Table 5.11 and 5.12.

Table 5.11: Critical strength and strain for different steel materials (NORSOK N-004).

	Mild steel	HT 32 Steel	HT 36 Steel
Yield stress (MPa)	235	315	355
Critical strain for rupture (%)	20.0	16.7	15.0
Critical strength for rupture (MPa)	327	416	461

Table 5.12: Strain limits for different classes of steel section (FABIG IGN 1993).

Type of section		Strain limit
Tension member		5%
Bending or compression member		–
BS 5950	Euro code	
Plastic section	Class I	5%
Compact	Class II	3%
Semi-compact	Class III	1%
Other sections		$\leq \varepsilon_y$ (yield stress)

5.8.2.2 Ductility limit

The above strain limit can be transformed to a limiting deflection, i.e., to a ductility ratio as defined by:

$$\text{Ductility ratio, } \mu = y_{max} \text{ (Total deflection)} / y_{el} \text{ (deflection at elastic limit)} \quad (5.6)$$

Typical values often used for design pruproses are re-created in Table 5.13.

Table 5.13: Ductility ratio for beams with no axial restraint (NORSOK N-004).

Boundary conditions	Loads	Cross-section type		
		Class I	Class II	Class III
Cantilevered	Concentrated	6	4	2
	Distributed	7	5	2
Pinned	Concentrated	6	4	2
	Distributed	12	8	3
Fixed	Concentrated	6	4	2
	Distributed	4	3	2

5.9 Choice of design approach for explosion design

The design approach consists of the combination of a method of analysis with a means of strength assessment. Table 5.14 shows various approaches for offshore topside structures under gas explosion loads. The SDOF method is a simple calculation method, while dynamic NLFEA deserves more pre-processing, analysis and post-processing time.

Table 5.14: Choice of design approach for topside structures under gas explosion loadings.

Design stage	Analysis method	Dynamic behavior	Nonlinear behavior	Acceptance criteria	Structural model	Tools
Basic	① SDOF method	- Intrinsic capability (or by DAF from response charts) - Enhanced yield stress (strain rate effect, ×1.2	- Intrinsic capability - Enhanced yield stress (full plastic section, ×1.12) - Strain hardening (ultimate tensile strength /1.25)	- Ductility ratio	- Member by member - Plate only or Stiffened plate idealized as beam	- Response charts, - Spread sheets, - SATEL
Basic	② Linear static FE analysis	- Intrinsic incapability and considered by DAF - Enhanced yield stress (strain rate effect, ×1.2)	- Intrinsic incapability and partially considered by modified code check - Enhanced yield stress (full plastic section, ×1.12) - Strain hardening (ultimate tensile strength /1.25)	- Yield Strength with modified code check (utilization factor ×1.5 for ASD)	- Framed - Plate only - Stiffened plate (idealized stiffeners)	- USFOS - SACS
Detail	③ Nonlinear static FE analysis	- Intrinsic incapability and considered by DAF - Enhanced yield stress (strain rate effect, ×1.2)	- Intrinsic capability	- Strain limit (or ductility ratio)	- Framed - Plate only - Stiffened plate(idealized stiffeners)	- USFOS - SACS (unstable after full plastic state)
Detail	④ Dynamic nonlinear FE analysis	- Intrinsic capability	- Intrinsic capability	- Strain limit (or ductility ratio)	- Framed - Plate only - Stiffened plate(idealized stiffeners)	- USFOS - SACS (linear dynamic with mode superposition, unstable after full plastic state)
Detail	⑤ Dynamic nonlinear FE analysis	- Intrinsic capability	- Intrinsic capability	- Strain limit (or ductility ratio)	- All structures	- ABAQUS - LS-DYNA

CHAPTER SIX

FIRES

6.1 Purpose

This purpose of fire assessment of structure using ALS methodology is to document structural fire integrity and redundancy when exposed to accidental fire actions and to determine amount of PFP primary and secondary structures.

The amount of PFP is determined based on a combination of thermal and structural response analyses using detailed heat transfer and non-linear assessment of fire action effects.

The thermal analyses calculate the time dependent temperature distribution on the structural members. The temperature distribution are used as input to the structural response analysis to study the effect of the fire loads.

The procedure for PFP optimization follows two steps. First, Design Fire Loads will be used to determine where PFP is needed. Then, Fire Scenarios will be run in order to determine the amount of PFP necessary.

6.2 ALS procedure for fire redundancy analysis

The ALS structural fire assessment generally follows a three step approach.

1. Definition of design fire loads by:
    a. Using standard predefined fire heat and temperatures, given in Sec. 6.5.1 and 6.5.2.
    b. Performing CFD fire analysis for fire scenarios selected using process system probability of failure, given in Sec. 6.5.3.
    c. Development of fire load exceedance curve applying probabilistic methods, as given in Sec. 6.6. This includes screening of identified hydrocarbon isolatable sections and fire hazards, probability, fire type, their potential leak locations and rate, based on their damage potential to the structure.
2. Fire thermal load calculation: The thermal load calculation is based on a heat transfer analysis of structural members using fire and radiation heat flux input for fire scenarios to be investigated. This defines the member thermal loading in form of temperature profile and time histories.
3. Structural assessment and fire mitigation: this includes detailed structural analysis and PFP design for each topsides module.

The ALS procedure for the fire redundancy analysis is illustrated in Figure. 6.1.

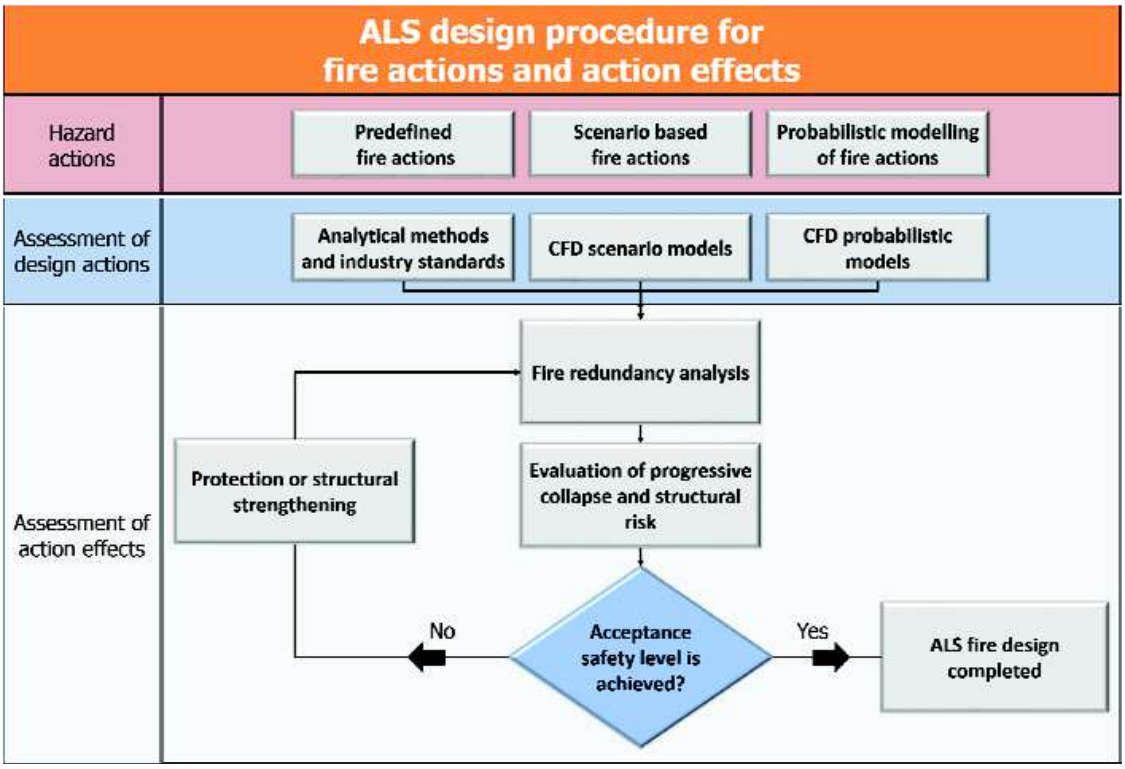

Figure 6.1: ALS design procedure for definition of fire action an action effects.

6.3 Type of fires

Following fire types shall be considered within fire safety design/ALS of offshore installations:

1. Gas jet fires
2. Two-phase jet fire
3. Pool fires on an installation
4. Hydrocarbon pool fires on the sea
5. Gas fires from subsea releases

6.4 Fire actions

The following actions resulting from fire needs to be distinguished and considered in the assessment of fire action effects:

- Radiation from flame to the surroundings
- Convection from the hot combustion products passing over an object surface
- Conduction
- Smoke load (soot and carbon monoxide) formed during an inefficient combustion of hydrocarbons

6.5 Deterministic models of fire actions

The determination of fire actions to be used in association with ALS design process can be based on:

1. Application of standard fire curves, ISO-834-1 (1999), EN-1363-1 (1999), etc.
2. Prescribed temperature and radiation, NORSOK, ISO, UKOOA
3. Temperature and radiation form CFD analysis

6.5.1 Standard fire curves

Table 6.1: Standard fire curves.

Type of fire curves	Reference	Equation
UL-1709 fire curve	UL-1709 (1994)	$\theta_g = \begin{cases} 218.6t & 0 \le t < 5 \\ 1093 & t \ge 5 \end{cases}$
Cellulosic fire curve	ISO-834-1 (1999)/ EN-1363-1 (1999)	$\theta_g = 20 + 345\log(8t+1)$
Hydrocarbon fire curve	ISO-834-2 (2009)/ EN-1363-2 (1999)	$\theta_g = 20 + 1080(1 - 0.325e^{-0.167t} - 0.675e^{-2.5t})$
Hydrocarbon Modified fire curve	-	$\theta_g = 20 + 1280(1 - 0.325e^{-0.167t} - 0.675e^{-2.5t})$
NOTE: θ_g = gas temperature near the steel member in °C; and t = time in minutes.		

Figure 6.2 shows the comparison between different definitions of fire curves.

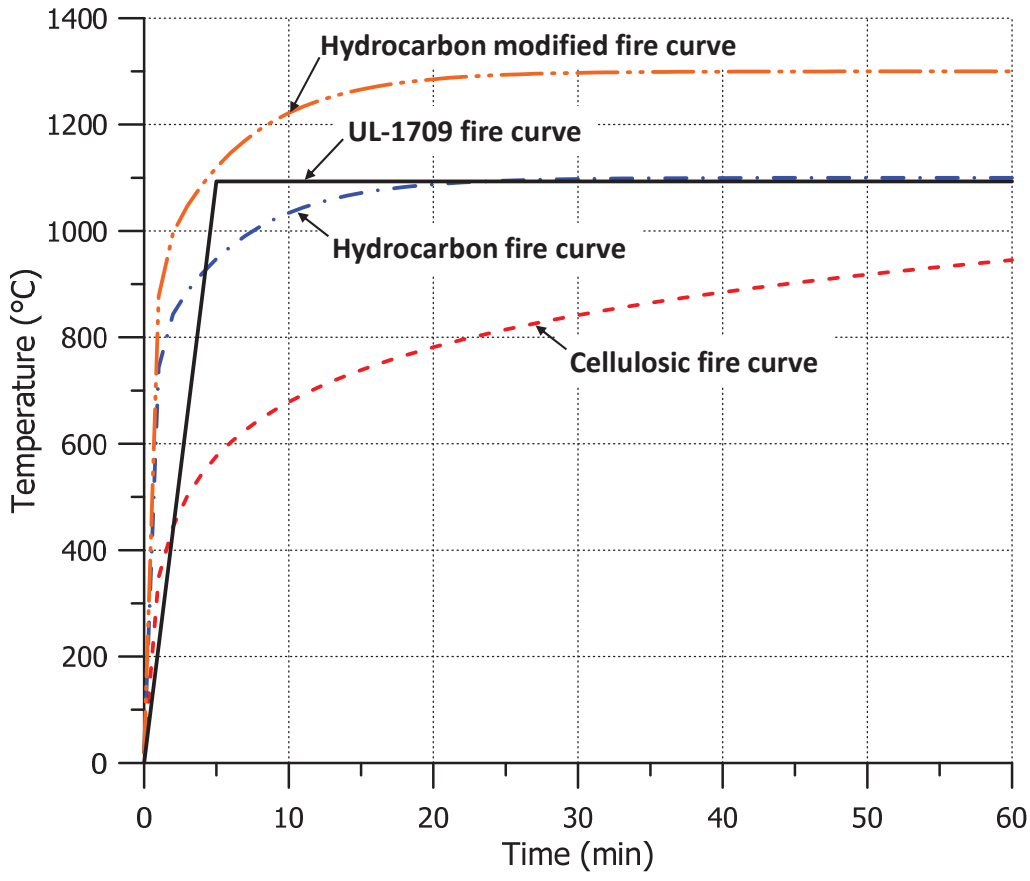

Figure 6.2: Standard fire curve.

6.5.2 Prescribed temperature and radiation

Unless specific fire analysis is performed, following heat actions are recommended by, NORSOK-S-001 (2008).

Table 6.2: Heat flux values.

Heat load type	Unit	Jet fire		Pool fire
		For leak rates m> 2 kg/s	For leak rate 0.1 kg/s <m< 2 kg/s	
Local peak heat load	kW/m^2	350	250	150
Global average heat load	kW/m^2	100	0	100

Table 6.3: Definitions of temperatures and radiation for jet fires (UKOOA/HSE-152-RP-48, 2006).

Characteristic	Unit	Size			
		Small	Medium	Large	Major
Size	kg/s	0.1	1	10	> 30
Flame length	m	5	15	40	65
Fraction of heat radiated, F		0.05	0.08	0.13	0.13
CO level	% v/v	< 0.1	< 0.1	< 0.1	< 0.1
Soot concentration	g/m^3	~ 0.01	~ 0.01	~ 0.01	~ 0.01
Total heat flux*	kW/m^2	180	250	300	350
Radiative flux	kW/m^2	80	130	180	230
Convective flux	kW/m^2	100	120	120	120
Flame temperature, T_f	K	1560	1560	1560	1560

* Due to confinement: Increased heat loadings up to 400 kW/m^2.
(280 W/m^2 radiative, 120 kW/m^2 convective, $T_f = 1600K$, $\varepsilon_f = 0.75$, $h = 0.09$)

Table 6.4: Definitions of temperatures and radiation for pool fires. (UKOOA/HSE-152-RP-48, 2006).

Characteristic	Unit	Methanol pool	Hydrocarbon pool diameter	
			Small	Large
Typical pool diameter	m	5	< 5	> 5
Flame length	m	equal to pool diameter	twice pool diameter	twice pool diameter
Mass burning rate	kg/m^2s	0.03	Crude: 0.045-0.06 Diesel: 0.055 Kerosene: 0.06 Condensate: 0.09 C3/C4s: 0.09	Crude: 0.045-0.06 Diesel: 0.055 Kerosene: 0.06 Condensate: 0.10 C3/C4s: 0.12
Fraction of heat radiated, F		0.15	0.25	0.15
CO level	% v/v	negligible	< 0.5	< 0.5
Soot concentration	g/m^3	negligible	0.5 – 2.5	0.5 – 2.5
Total heat flux	kW/m^2	35	125	250
Radiative flux	kW/m^2	35	125	230
Convective flux	kW/m^2	0	0	20
Flame temperature, T_f	K	1250	1250	1460

6.5.3 Fire scenario identification

The selection of fire scenarios for CFD analysis shall be based on the basis of the leak frequency above 10^{-4} normally documented in the Fire Risk Analysis (FRA) report.

Fire mitigation measures such as Partial Isolation and Blowdown Failure (IF-BDF), Isolation and Blowdown Success (IS-BDS) and Isolation Success and Blowdown Failure (IS-BDF) needs to be considered

The criticality of fire scenario can be calculated from the fire scenario's frequency versus its consequence. Here, the fire consequence C_F is defined as a product of leak rate R_L and a fire duration D_L as below;

$$C_F = R_L \cdot D_L \tag{6.1}$$

6.5.4 CFD analysis

CFD fire analysis shall be carried out using the commercial CFD codes as for example Kameleon FireEx, FLACS Fire, Fluent or Ansys.

Results of CFD analysis provide time variant temperatures and radiations in the whole CFD analysis model.

Manual conversion of CFD analysis data is pruned to large errors and therefore should be avoided in the ALS design process. Special purpose verified interfaces shall be used to convert CFD fire analysis results into the non-linear structural analysis models.

A leak classification often used is:

- Small leaks – typically 0.1 kg s^{-1}
- Medium leaks – typically 1 kg s^{-1}
- Large leaks – typically 10 kg s^{-1}
- Major failures – typically >30 kg s^{-1}

For high pressure gas releases, these correspond to failure sizes of the order of 1, 10, 30 and 100 mm diameter respectively.

6.6 Probabilistic models of fire actions

This chapter presents the probabilistic model to determine the fire design loads. The probabilistic approach, in association with probability exceedance curves, was employed based on the results of the fire simulations for selected fire scenarios.
The EFEF JIP method introduced by Czujko and Paik (2010) to determine fire design loads comprises the following seven steps.

1. Establish a table listing the fire frequency, maximum temperature, and maximum heat dose for all of the scenarios considered.
2. Based on the table established in Step 1, rearrange the order of scenarios in such a way that the scenario with the lowest maximum temperature comes first and that with the highest maximum temperature comes last. Then, calculate the cumulative fire frequency.
3. Again based on the table established in Step 1, rearrange the order of scenarios in such a way that the scenario with the smallest maximum heat dose comes first and that with the largest maximum heat dose comes last, and then calculate the cumulative fire frequency.
4. Based on the table established in Step 2, calculate the exceedance frequency (probability) associated with the maximum temperature. This is equal to the total frequency (probability) minus the cumulative frequency at the corresponding maximum temperature.
5. Based on the table established in Step 3, calculate the exceedance frequency (probability) associated with the maximum heat dose. This is equal to the total frequency (probability) minus the cumulative frequency at the corresponding maximum heat dose.
6. Determine the fire design loads in terms of the maximum temperature at an acceptable level of exceedance fire frequency (e.g., 10^{-4}) using the exceedance curve, as shown in Figure 6.3(a).
7. Finally, determine the fire design loads in terms of the maximum heat dose at an acceptable level of exceedance fire frequency (e.g., 10^{-4}) using the exceedance curve, as shown in Figure 6.3(b).

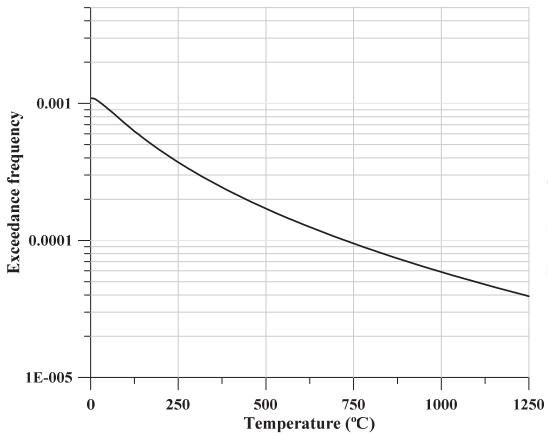

Figure 6.3(a): Exceedance curves for maximum gas temperature.

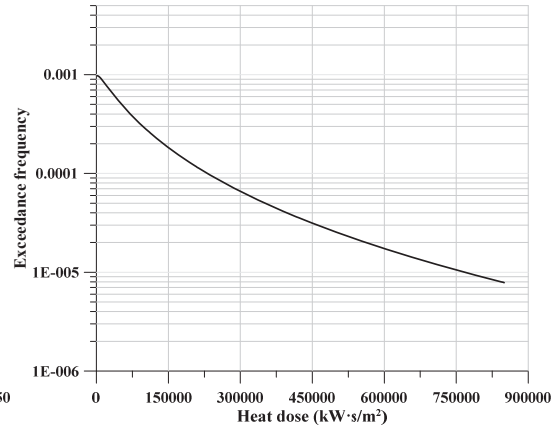

Figure 6.3(b): Exceedance curves for maximum heat dose (flux).

6.7 Definition of design actions

Dimensioning load shall not cause loss of safety functions or escalation (locally). The following principles shall apply:

- Fire loads, (e.g. heat loads). Unless specific fire analysis is performed, Table 6.1 applies;

When the dose methodology is used for establishing the dimensioning incident fire dose, e.g. 10^{-4} or 10^{-5} per year dose, the design fire action, dose, has to be decoded to a corresponding incident heat flux and duration giving the same dose. This approach does not solve the

fundamental problem of uniqueness mentioned earlier as the product of two parameters may be arranged in numerous (potentially infinite) ways to get the same result. Different combinations, i.e. dimensioning accidental fire loads with durations, will have different consequences.

One way to handle this challenge is to decode the dimensioning incident fire dose to more than one design event (heat flux as a function of time) with the same heat dose. As a minimum, a low heat flux scenario and a high heat flux scenario must be defined when using the heat dose approach. This is especially important when evaluating the risk of rupture of process equipment exposed to fires as this occurrence is very sensible to high heat fluxes in the beginning of the fire where there has not been any significant reduction in pressure due to blowdown yet. For process equipment the time to rupture is vital to determine if the escalation is acceptable or not, and as previously discussed dose cannot be used to derive heat-up durations.

A probabilistic risk assessment methodology described in Appendix A in FABIG-TN11 (2010) combines the dose methodology with the conservative approach of selecting the point with the highest heat flux for each particular fire. Then a curve relating the accumulated fire frequency versus incident dose can be established. From this the dimensioning incident fire dose can be found, e.g. 10^{-4} or 10^{-5} per year.

6.8 Assessment of actions effects

6.8.1 Basic heat transfer considerations

The incident thermal radiation, q (kW/m^2), to an object from a fire can be described as:

$$q = V \cdot E \cdot \tau \tag{6.2}$$

where

V is the view factor of the flame by the receiver,
E is the average surface emissive power of the flame (kW/m^2),
τ is the atmospheric transmissivity.

The view factor is a function of the flame shape. Consequently, most integral or empirical mathematical models will assume some kind of simplified flame shape which is then used to calculate the view factor. The flame average surface emissive power is also a function of the flame shape. Therefore, average surface emissive powers used by the model will not necessarily be the same as those measured during an actual fire.

In the far field, (typically more than 2 flame lengths away) the flame shape is not critical, so a simplified approach can be taken using the 'point source' model, whereby the difficulties of defining a flame shape and associated average surface emissive power can be avoided. In this approach, the fraction of the heat of combustion of the fuel radiated to the surroundings is defined as:

$$F = \frac{E \cdot A}{Q} = \frac{E \cdot A}{\dot{m} \cdot H} \tag{6.3}$$

where

A is the surface area of the flame (m2),
Q is the net rate of energy release by combustion of fuel (kW),
ṁ is the rate of fuel combustion (kg/s),
His the net calorific value (kJ/kg).

The incident radiation received in the far field at a distance, d (m), from the fire is then expressed as:

$$q_d = \frac{\tau \cdot F \cdot \dot{m} \cdot H}{4 \cdot \pi \cdot d^2} \tag{6.4}$$

The thermal load per unit area to an object engulfed by fire will be a combination of radiation from the flame (q_r) and convection from the hot combustion products (q_c) passing over the object surface. Hence the thermal load can be written as:

$$q_{total} = q_r + q_c = \varepsilon_s \sigma(\varepsilon_f T_f^4 - T_s^4) + h(T_f - T_s) \quad (6.5)$$

where, ε_f , ε_s are the emissivity of the flame and surface respectively, σ is the Stefan-Boltzman constant (5.6697×10^{-11} kW/m^{2}K^4), T_f , T_s are the flame and surface respectively (K), h is the convective heat transfer coefficient (kW/m^{2}K).

The heat dose concept can be used in order to get a unique way of sorting the fire scenarios from the CFD-simulations based on received energy. The incident heat dose is found by integrating the incident heat flux, $q_{inc}(t)$, over time, D_{inc}, i.e.

$$D_{inc} = \int q_{inc}(t)dt \quad (6.6)$$

For selected scenarios it is possible to sort values the of Dinc into an ascending or descending order that can then be used for establishing a value of Dinc corresponding to for instance a return period of 10^{-4} or 10^{-5} years. This will give one indication of severity in terms of received energy. But the heat dose does not solve all of the challenges of establishing dimensioning fire events since as:

1. It is the net absorbed dose by an object that is relevant for the temperature increase of the object. This is in principle to be calculated for each object type depending on material type, object thickness etc. The net absorbed heat flux will decrease with time as the object temperature rises.
2. The time to reach a given temperature is not determined by the net absorbed dose but by the net absorbed flux as a function of time (as high heat flux will quicker heat the material). Hence dose cannot be used for the calculation of time until the critical temperature is attained.

The very small radiation exchange of the surface with the surrounding ambient atmosphere has been ignored. It has been assumed that both the flame and surface can be considered as diffuse grey bodies, meaning that absorptivity and emissivity can be assumed equivalent. Many materials, including steel and most PFP materials, approximate to diffuse grey surfaces. Hence, for thermal response purposes, the hemispherical total absorptivity/emissivity of the target material is assumed to be independent of the nature of incident radiation and the spectral properties of the fire.

Below tables show the typical value of emissivity of the flame and convective heat transfer coefficient for jet fire and pool fire.

Table 6.5: Typical value of ε_f and h for jet fires (UKOOA/HSE-152-RP-48, 2006).

Characteristic Jet fire	Unit	Size			
		Small	Medium	Large	Major
Flame emissivity, ε_f	-	0.25	0.4	0.55	0.7
Convective heat transfer coefficient, h	kW/m^{2}K	0.08	0.095	0.095	0.095

Table 6.6: Typical value of ε_f and h for pool fires (UKOOA/HSE-152-RP-48, 2006).

Characteristic Pool fire	Unit	Methanol pool	Hydrocarbon pool diameter	
			Small	Large
Flame emissivity, ε_f	-	0.25	0.9	0.9
Convective heat transfer coefficient, h	kW/m^{2}K	-	-	0.095

6.8.2 Modelling of structures

The non-linear structural model for fire redundancy analysis is normally established by conversion from the linear structural model developed for the operation in-place conditions.

When USFOS package is used to perform fire redundancy analysis, the conversion can be performed using STRUMAN, built-in utility software, to convert linear structural models to USFOS format.

For the models developed for the local structural fire redundancy analysis care shall be taken to correctly represent boundary conditions affecting thermal expansion of the structure and correct representation of stiffness of joints with adjacent parts of the structure not included in the model.

6.8.3 Carbon steel structural materials

Material model for strength assessments was assumed to be bilinear elastic – plastic, described by the material constants.

To perform the thermal and structural response analysis of structures under fire loads, material properties should be defined as temperature dependent. Figure 6.4 presents the reduction factors for yield stress and elastic modulus at elevated temperature defined according to Eurocode (EN-1993-1-2, 2005).

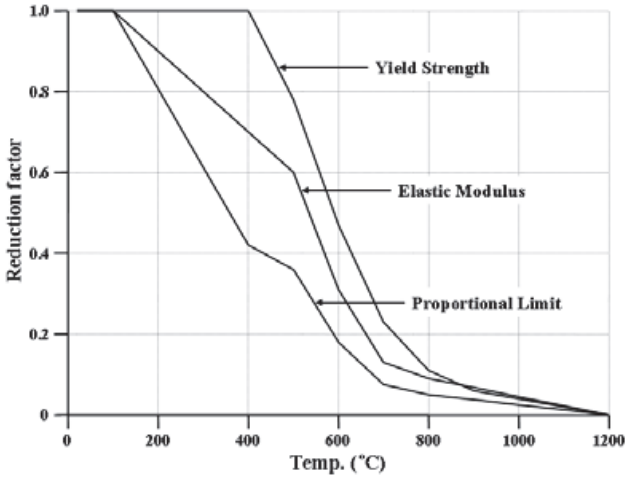

Figure 6.4: Reduction factors at elevated temperatures.

The carbon steel material curves for elevated temperatures specified in Eurocode were used in the thermal and structural analysis. Figure 6.5 shows the curves for specific heat capacity and thermal conductivity, respectively (EN-1993-1-2, 2005). The surface emissivity of steel was set to 0.8 for all structural members exposed to fire.

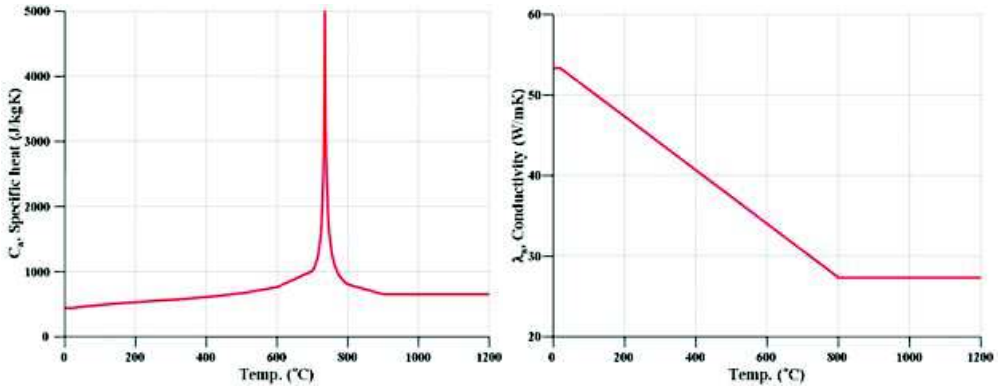

Figure 6.5: Thermal properties of steel: specific heat capacity (left) and conductivity (right).

6.8.4 Aluminium structural materials

The aluminium material model for strength assessments was assumed to be bilinear elastic – plastic, described by the material constants.

Figure 6.6 presents the reduction factors for yield stress and elastic modulus at elevated temperature defined according to Eurocode (EN-1999-1-2, 2007).

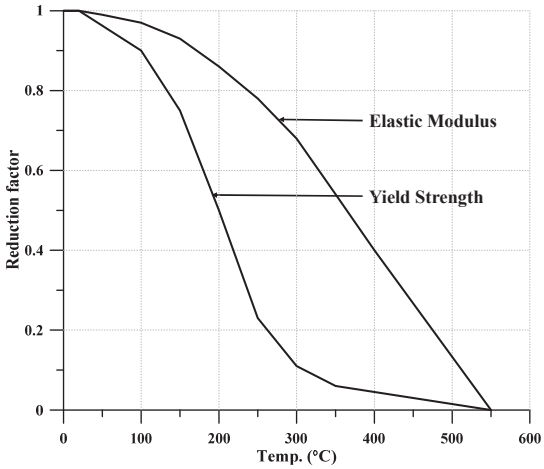

Figure 6.6: Reduction factors of aluminium at elevated temperatures.

Figure 6.7 shows the aluminium material curves according to elevated temperatures for specific heat capacity and thermal conductivity, respectively (EN-1999-1-2, 2007).

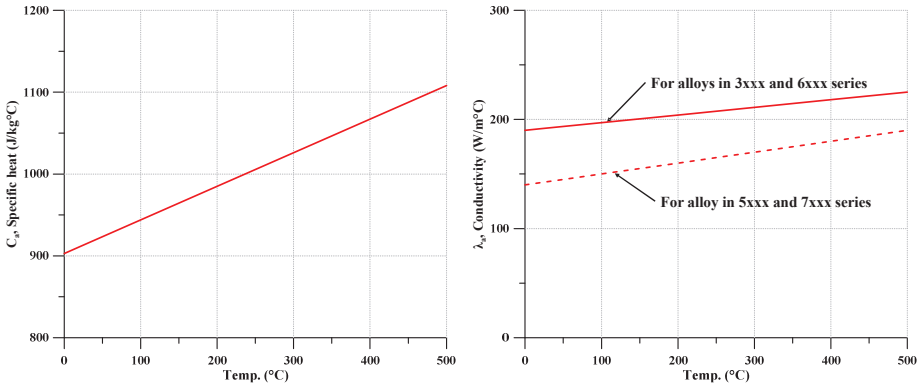

Figure 6.7: Thermal properties of aluminium: specific heat capacity (left) and conductivity (right).

6.8.5 Passive Fire Protection materials for load bearing structures

The fire protection material applied to a structural member was to remain unaffected and retain its fire performance if subjected to fire loads. The chosen spray-on fire protection material was Chartek 7. The thermal characteristics of Chartek 7 shown in Figure 6.8 was used in this study (IPC, 2000).

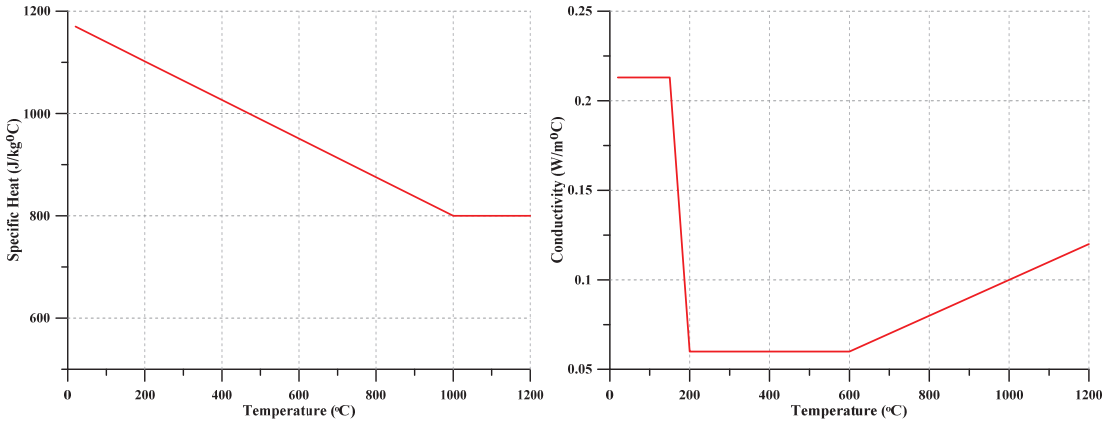

Figure 6.8: Thermal characteristics of Chartek 7: specific heat (left) and conductivity (right).

6.9 Fire redundancy analysis

Two methods for the assessment of fire redundancy analysis can be applied:

1. Direct Heat Application (DHA) method
2. Push-down method

6.9.1 Direct heat application method

The Direct heat application method is the most complete and complex analysis procedure. It mimics the real physical process closely and is considered to produce the "true" behavior of the structure. The procedure of direct heat application method is as follows;

- All the functional (in-place) load cases are combined into a combination load case. The combination load case is first applied.
- Secondly, the temperature is incremented stepwise according to the thermal evolution. Temperature associated with the fire duration is applied and simulate up to the total fire duration time.

As thermal expansion is included in this method, compressive members will buckle but still contribute to the resistance of the system. At certain stages, the degradation of members subjected to heating may require a significant redistribution of forces in the system in order to carry the functional loads. Numerically, this is characterized by negative current stiffness matrix. In a real system this will cause the structure to displace dynamically to a new equilibrium state. In static analysis it may be necessary to perform intermediate unloading of the functional loads followed by reloading to the equilibrium state.

Advantage of this method is that it predicts the real physical process of fire accidents closely and drawback of Direct heat application method is that it only provides information of whether the structure survives the fire history or not. The margin to failure at the various time instances is not known.

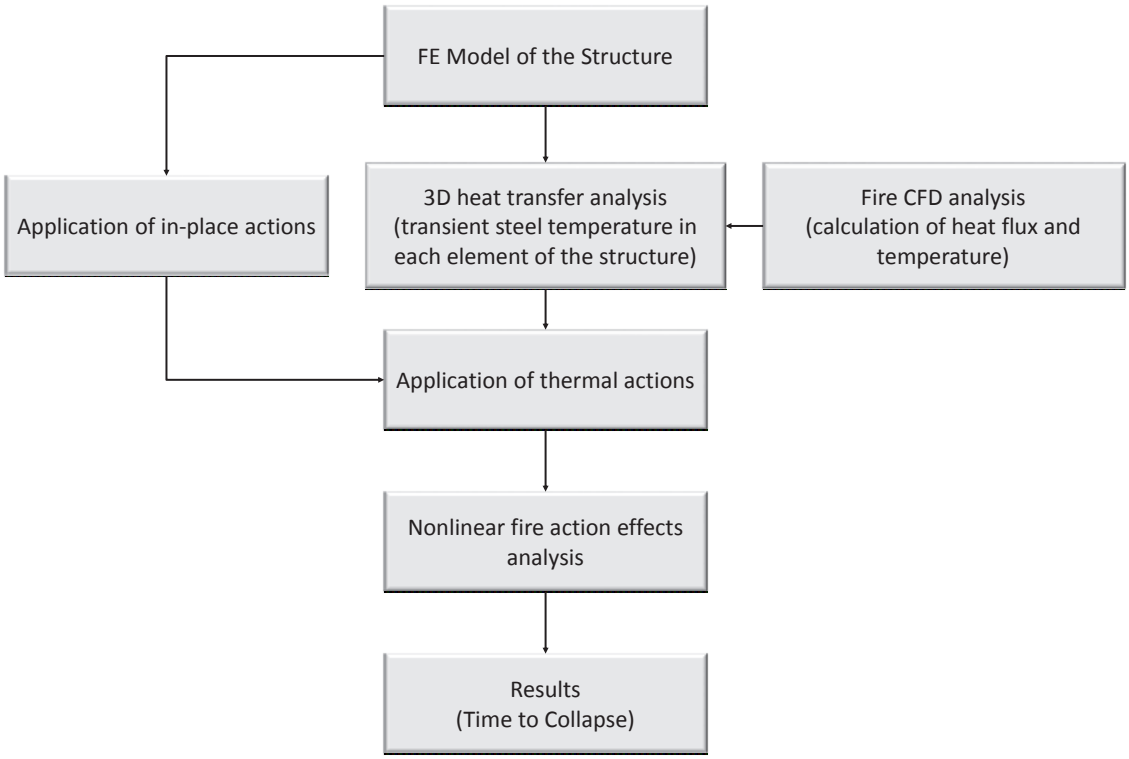

Figure 6.9: Direct heat application method.

6.9.2 Push-down method

The primary objective of the Push-down method is to obtain information of the ultimate strength of the structure when the functional loads are increased beyond the nominal load level when the structure is exposed to the maximum temperature distribution and the associated collapse mechanism.

The procedure of Push-down method is as follows:

1. The temperature is applied in the structure model considering different fire duration (e.g. 5 min, 10 min, 20 min, 30 min, etc.) and the material properties are modified according to the temperature level attained at specific fire duration.
2. For any specific fire duration, the functional loads are increased until collapse is triggered. The peak resistance of structure for this fire duration is noted.
3. The similar procedure stated at step 2 is followed for another fire duration and the peak resistance for that fire duration is noted. This procedure is followed up for other fire duration cases as well.
4. The peak resistance noted at step 2 & 3 is plotted versus fire duration time. This single curve describes the performance of the structure during fire, i.e. how the ultimate resistance degrades. The demand for resistance is = 1.0, i.e. when the functional loads are applied 100%.

The push-down method is illustrated in Figure 6.10. The advantage of Push-down method is that it gives more information about the safety margin as a function of time and how the performance of the structure change over time. The calculation complexity is reduced significantly and this procedure is favorable because it allows the removing members from the structural system with extreme temperatures, those members who has a minor contribution to the load carrying, but may cause numerical ill-conditioning and numerical problems. A drawback of Push-down method is that it does not consider the thermal expansion of material. But, the thermal induced deformations is considered in terms of the initial deformations defined in Eurocode-2 Curve C.

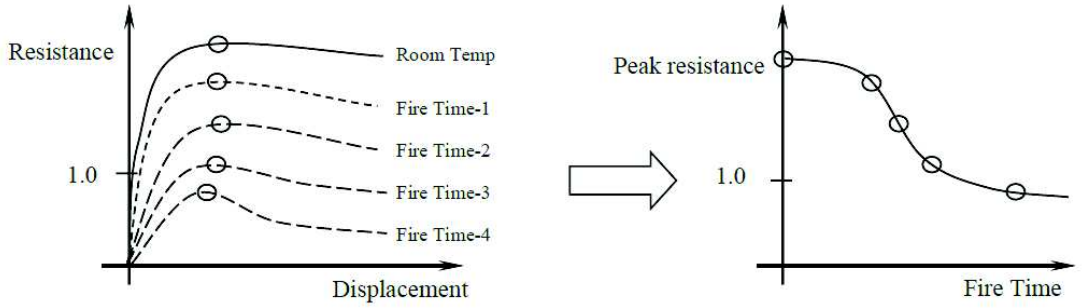

Figure 6.10: Push-down analysis method.

6.10 PFP design and optimization

Practical design of PFP on offshore platforms is conducted in the following steps:

- Perform heat transfer analysis by solving the transient heat balance equation to generate temperature field for the structure exposed to fire. All structural elements are assumed to be unprotected from fire exposures, i.e. no passive fire protection (PFP) and members are fully engulfed by the fire.
- Apply in-place loads and temperature field obtained from heat transfer analysis in the progressive collapse analysis and consider the reduction of mechanical properties at elevated temperature.
- The passive fire protection shall be specified if the progressive collapse analysis results in failure of primary structural members or, when critical, to secondary structural members.
- After necessity of PFP is detected, its effect is included in the design model by changing the thermal property of affected members.
- The progressive collapse limite state shall be applied to optimize amount of PFP.

The procedure for design and optimization of PFP is illustrated in Figure 6.11.

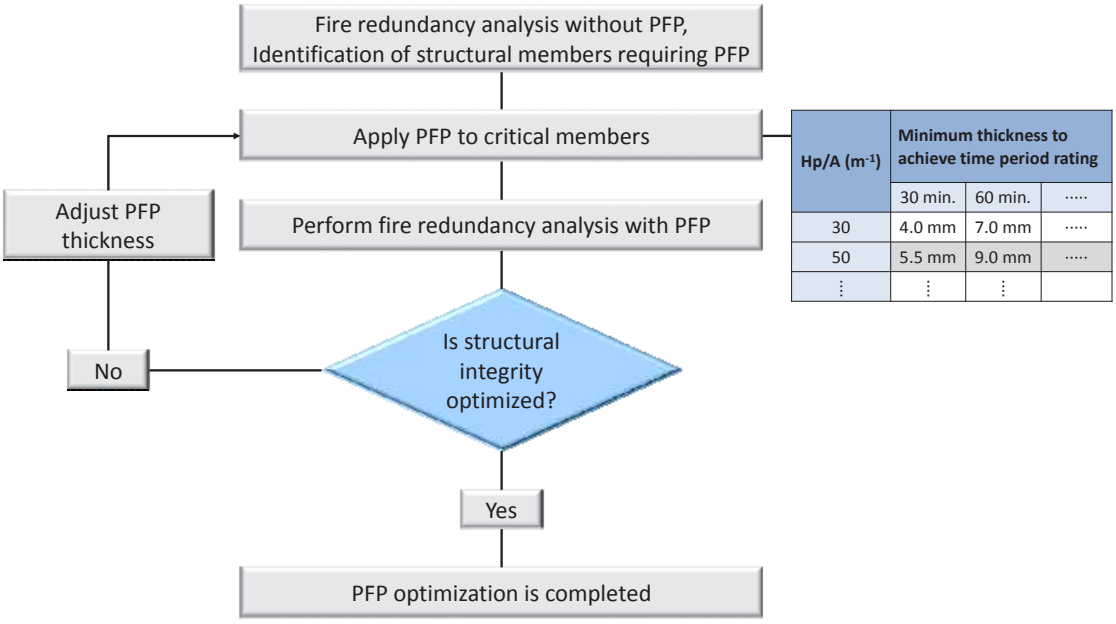

Figure 6.11: The procedure of PFP design and optimization.

6.11 Design considerations

6.11.1 Topside, main structures

The primary effects of a fire on an individual structural member are the elevation of the member's temperature and thermal expansion. As the temperature increases, a reduction in its strength, stiffness and thermal expansion will be observed. The rate of material degradation depends on many factors including structural member material strength and stiffness at elevated temperatures, applied loading (thermal and structural), and the presence of active and passive fire protection. The member response to a fire may result in a variety of failures including (but not limited to) member yielding, buckling, formation of plastic hinges, exceeding deformation limits, connection failures, etc.

6.11.2 Passive fire protection barriers

6.11.2.1 Functional requirements

Functional requirements for PFP materials include the period of resistance, expressed in time, to a certain fire exposure before the first critical point in behavior is observed.
The functional requirements of PFP barriers may be split into three categories:

- Stability — to maintain the load-bearing capacity (structural capability) of a structural member or a fire barrier
- Integrity — to maintain the integrity of a fire barrier by preventing the transmission of flame, smoke, hot and toxic gases;
- Insulation — to keep the unexposed side of a barrier cool when the other surface is exposed to a fire.

Standard fire tests should be used to qualify PFP materials and systems. ISO-834-1 (1999) is a recognized standard for testing of PFP performance in cellulosic and pool fires. There is no recognized fire test at present for jet fires, but a small-scale interim fire test procedure is given in (OTI-95-634, 1996).

Consideration should also be given to resistance to explosion effects, when establishing the functional requirements for PFP materials.
Blast walls and decks with superimposed PFP must be assessed for the integrity of the PFP following deflections of the structure during an explosion.

6.11.2.2 Classification of hydrocarbon fire barriers

A hydrocarbon fire protection barriers shall be designed from incombustible materials and satisfies the following criteria:

a) it is sufficiently reinforced,
b) it prevents the spread of flames and smoke for at least two hours of the standardised fire test,
c) it is designed so that the average temperature and the temperature of any single point on the unexposed side do not rise more than 140°C and 180°C, respectively, above the original temperature within the following timeframes:
   - Class H-120: 120 minutes,
   - Class H-60: 60 minutes,
   - Class H-0: 0 minutes,

And insulation materials are fire-tested at an institution that is internationally or nationally recognised in the specific discipline.

All H-Class fire bariers shall maintain stability and integrity within 120min.

6.11.2.3 Coat-back

A joint industry study (Thurlbeck, 2006) of the effects of coat-back on the primary member temperature demonstrated the following:

- The required coat back length should be determined based on the local average temperature which can be tolerated in the primary member at the attachment location. As the coat-back

temperature increases this temperature reduces. However, beyond 150 mm, any further reduction is small.

- The ratio of the cross sectional area of the attachment to that of the primary member was found to have a significant influence on the temperature. The ratio of the section factors (Hp/A) has secondary significance.
- The effect of the attachment on the temperature increased with increasing fire resistance period. Thus, to maintain the same temperature in the primary member a longer coat-back length would be required for a 2 hour duration than for 1 hour.
- Within the limits of the study, it was found that the section shape (of both the primary member and attachment) had negligible effect.

The properties of fire protection material have a small effect on coat-back length.

CHAPTER SEVEN

SHIP COLLISIONS

7.1 Purpose

The purpose of collision assessment of the structure using ALS methodology is to document structural crashwortyness and the structural capacity to absorb collision loads without severe consequences such as loss of global load carrying capacity, structural collapse, structural damage leading to oil spill, critical loss of buoyancy etc. The collision analysis is to guide the structural and layout modifications, and additional strengthening required to mitigate the consequences.

The collision analysis is conducted with predefined collision energy levels or with certain predefined collision scenarios. The structural consequences are evaluated using either time-domain or displacement-controlled analysis using non-linear finite element method or simple elastic-plastic methods. The analysis provides the extent of collision damage the structures undergo while absorbing the collision energy.

Once the accidental actions are defined, the overall goal of the design against accidental actions is to achieve a system where the main safety functions of the installation are not impaired.

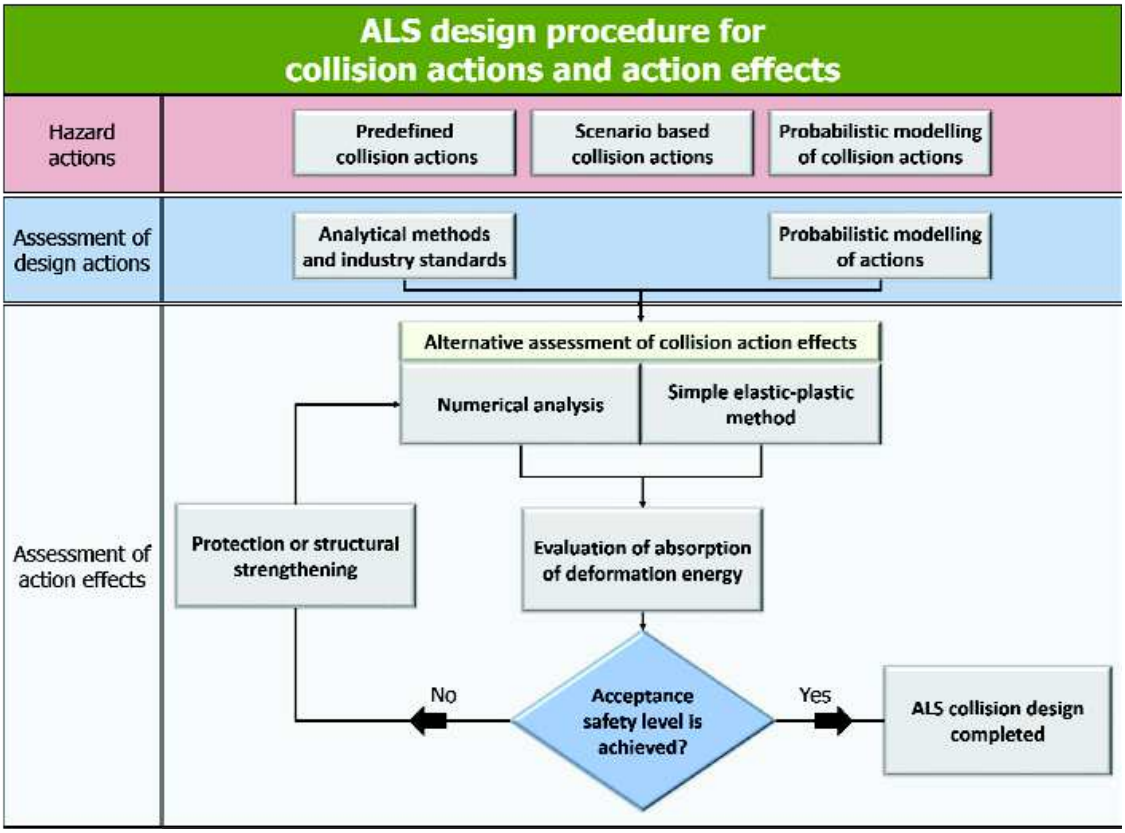

Figure 7.1: ALS Procedure for the ship collision assessment.

7.2 ALS procedure for collision analysis

The principle schema for ALS collision analysis procedure is shown in Figure 7.1. The main steps of the ALS procedure are the following:

1. Definition of the collision actions as
   a. Deterministic energy levels,
   b. Prescribed scenarios defined on the basis of relevant masses, velocities and directions of ships or aircraft that may collide with the installation,
   c. Probabilistic methodologies to determine the possible collision energy levels by mapping the vessel traffic and operational pattern in the relevant area and evaluating the possible events.
2. Description of actions as
   a. Collision scenario described in a simulation environment such as non-linear finite element method,
   b. Collision energy to be absorbed by deforming structures,
   c. Predefined force-deformation relationships.
3. Evaluation of action effects via
   a. Non-linear dynamic finite element analysis,
   b. Energy considerations combined with simple elastic-plastic methods.
4. Assessment of accidental consequences and comparing to acceptance levels.

The following rules are mainly referred when discussing the ALS procedures in subsequent sections:

– NORSOK N-003 for general requirements for accidental actions;
– NORSOK Z-013 for the risk analysis guidelines;
– NORSOK N-004 for the definition of actions and action response;
– Lloyd's guidelines (LR, 2014) for general requirements for risk analysis, actions and action response.

7.3 Collision mechanics and energy

The ship collision action is characterized by kinetic energy, governed by the mass of the ship, including its hydrodynamic added mass and the speed of the ship at the instant of impact (NORSOK-N-004, 2004).

If a moving body collides with a fixed object such as fixed platform, all the available kinetic energy is absorbed via structural deformations and thus, the deformation energy can be evaluated as:

$$E_s = \frac{1}{2}(m_s + a_s)\cdot v_s^2 \tag{7.1}$$

where

E_s is the kinetic energy of the vessel equal to the collision energy;
a_s is ship added mass coefficient, typically a_s = 1.4 for a broadside collision, a_s = 1,1 for a bow/stern collision (ISO-19902, 2007);
m_s is the vessel mass;
v_s is the velocity of vessel at impact.

If also the struck body is allowed to move, NORSOK-N-004 (2004) provides a simple equation for the collision energy based on the momentum conservation:

$$E_s = \frac{1}{2}(m_s + a_s)\cdot v_s^2 \cdot \frac{\left(1-\frac{v_i}{v_s}\right)^2}{1+\frac{m_s + a_s}{m_i + a_i}} \tag{7.2}$$

where

E_s is the collision energy;
a_S is ship added mass coefficient, typically a_s = 1.4 for a broadside collision, a_s = 1.1 for a bow/stern collision (ISO-19902, 2007);
a_i is added mass coefficient of the installation or the struck ship;
m_s is the vessel mass;
m_i is mass of the installation or the struck ship;
v_s is the impact speed;
v_i is the velocity of installation or the struck ship;

For articulated columns, the collision energy is evaluated as (NORSOK N-004):

$$E_s = \frac{1}{2}(m_s + a_s) \cdot \frac{\left(1 - \frac{v_i}{v_s}\right)^2}{1 + \frac{m_s \cdot z^2}{J}} \tag{7.3}$$

where

E_s is the collision energy;
a_S is ship added mass coefficient, typically a_s = 1.4 for a broadside collision, a_s = 1.1 for a bow/stern collision (ISO-19902, 2007);
a_i is added mass coefficient of the installation;
m_s is the vessel mass;
m_i is mass of the installation;
v_s is the impact speed;
v_i is the velocity of installation;
J is mass moment of inertia of installation (including added mass) with respect to effective pivot point;
z is distance from pivot point to point of contact.

Collision scenarios, defined via the masses (m_s and m_i) and velocities (v_s and v_i) of the colliding bodies, their relative position, geometry and structural configuration, should be established via risk analysis.

7.4 Probabilistic models of actions

Several rules (ISO, NORSOK and API) provide general guidance to conduct the risk assessment process. In collision risk assessment it is important to consider all the vessels that travel in the vicinity of the offshore installations using appropriate traffic monitoring systems (such as AIS), surveys and databases.

NORSOK-Z-013 (2010) requires the risks from two types of collisions to be considered:

- Ships/vessels ramming the installation (powered as well as drifting).
- Collision between the installation and floating units located nearby (flotels, crane vessels, etc.).

Lloyd's guidelines (LR, 2014a) extends the list to more detailed collision scenarios:

- Passing vessel powered collision
- Passing vessel drifting collision
- Powered collision on approach
- Collision while alongside installation/target
- Grounding

LR Guidelines (LR, 2014a) and NORSOK-Z-013 (2010) also define the type of vessels to be considered in the traffic survey and the risk assessment:

- Passing merchant & supply vessels
- Visiting (service) vessels
- Fishing vessels
- Offshore/shuttle tankers
- Floating installations

- Naval and submarine vessels
- Ferries

The most probable impact location should be determined by risk analysis with due account of the factors that affect the exact location like tidal changes, and vessel motions sea states (NORSOK-N-003, 2007). The most probable impact locations and impact geometry should be established based on the dimensions and geometry of the structure and vessel and should account for tidal changes, operational sea-state and motions of the vessel and structure which has free modes of behaviour. Unless more detailed investigations are done for the relevant vessel and platform, the impact zone for supply vessels should be considered to between 10 m below low astronomical tide and 13 m above high astronomical tide.

Impact scenarios should be established representing bow, stern and side impacts on the structure as appropriate (NORSOK-N-003, 2007). If a central impact (impact action through the vessel's centre of gravity) is physically possible, this impact situation should be analysed.

In the early phases of platform design, the mass of supply ships should normally not be selected less than 5 000 tons and the speed not less than 0,5 m/s and 2 m/s for ULS and ALS design checks, respectively (NORSOK-N-003, 2007). A hydrodynamic (added) mass of 40 % for sideways and 10 % for bow and stern impact can be assumed.

ISO-19902 (2007) requires that the collision events shall represent both a fairly frequent condition, during which the structure should only suffer insignificant damage, and a rare event where the emphasis is on avoiding a complete loss of integrity of the structure. Two energy levels shall be considered:

a) *low energy level,* representing the most frequent condition, based on the type of vessel that would routinely approach alongside the platform (e.g. a supply boat) and that would have a velocity representing normal manoeuvring of the vessel approaching, leaving, or standing alongside the platform;
b) *high energy level,* representing a rare condition, based on the type of vessel that would operate in the platform vicinity, drifting out of control in the worst sea state in which it would be allowed to operate close to the platform.

Level a) above represents a serviceability limit state to which the owner can set his own requirements based on practical and economic considerations, while level b) represents an ultimate limit state in which the structure is damaged but progressive collapse shall not occur.

For each possible collision type, the collision scenarios should be established together with appropriate collision frequency. LR (2014a) discusses several different collision scenarios and presents the generic equations for the evaluation of collision frequency and energy. In general, the collision frequency is defined as follows:

$$f_c = N \times f \tag{7.4}$$

where

f_c is collision frequency (year);
N is number of arrivals per year (visits per year);
f is collision frequency (per visit)

However, especially for collision frequency, it is suggested to use generic historical collision frequency per visit that is adjusted to the area subject to analysis based on the area-specific statistics, if available. LR guidelines (LR, 2014a) and NORSOK-Z-013 (2010) suggest several databased for the statistical accidental data:

Petroleum Safety Authority Norway	www.psa.no
Health and Safety Executive UK	www.hse.gov.uk
IHS Fairplay	www.ihs.com
Norwegian Maritime Authority	www.sjofartsdir.no
The International Association of Oil and Gas Producers	www.ogp.org.uk
COAST traffic database	

More comprehensive risk analysis can, for example, be based on Bayesian Belief Networks or The Monte Carlo simulation techniques. Examples for collision risk analyses for a certain sea regions can be seen in (Goerlandt et al., 2012; ADN, 2013; Montewka et al., 2014).

As a result of the risk analysis, the following data should be obtained:

- Collision type
- Participating ships/installations/others
- Mass and velocity data
- Collision configuration (impact point along the hull, angle between the colliding object, relative position etc.)
- Structural arrangement of the colliding bodies (not required for those, which can be considered rigid)
- Frequency or probability of the specific collision scenario and arrangement

7.5 Definition of design actions

Risk analysis provides the description of collision scenarios together with the exceedance probabilities. According to NORSOK-N-003 (2007), ALS design checks should be made with impact events corresponding to exceedance probabilities of 10-4.

Design actions can be defined by setting up a numerical simulation that defines the contact between the colliding bodies or by using predefined force-deformation curves that are available for supply vessels up to 5000 tons and for tankers ~ 125,000 dwt.

When the duration of the collision is short compared with the periods governing the motion and the rate of loading is relatively small, the damage caused in the collision in structures with free modes may be determined in two steps (NORSOK-N-003, 2007):

1) First the distribution of impact energy between kinetic rotation and translation energy and deformation energy, can be determined by momentum and energy considerations, see Chapter 7.3.
2) Then local damage to vessel and installation can be determined so that the energy absorbed by the two structures corresponds to the energy that is to be absorbed as deformation energy.

If the impact duration is long compared with the relevant local or global periods of structural vibration, structural analysis to determine the energy absorption and damage can be done by a quasi-static method of analysis. Otherwise, a dynamic structural analysis should be carried out. This analysis can be based on action - indentation curves obtained by laboratory tests and analysis, as outlined in NORSOK-N-004 (2004).

7.5.1 Numerical evaluation of the design actions

Guidelines for the determination of structural capacity by non-linear FE analysis can be found in DNV-RP-C208. The contact between the structures is to be modelled to capture the exact contact area and its development during the collision process. The simulation itself can be conducted either in quasi-static displacement controlled manner or dynamically.

Quasi-static displacement controlled approach suffices for practical studies where the impact duration is long compared to the periods of structural vibrations. In the displacement controlled simulations the striking ship penetrates the installation or struck ship along the prescribed path. The local damage to vessel and installation can be determined so that the energy absorbed by the two structures corresponds to the energy that is to be absorbed as deformation energy i.e. the energy defined by relationships in Chapter 7.3.

Dynamic simulations are to be conducted in a way that realistic collision speed and its change during the collision process are modelled. The speed can be defined from the momentum and energy considerations or by modelling the exact masses and inertias of the colliding bodies.

7.5.2 Predefined force-deformation relationships

For the collision with supply vessels with a displacement of 5000 tons, the force-deformation relationships are given in NORSOK-N-004 (2004) for broad side -, bow-, stern end and stern corner impact for a vessel with stern roller. The curves for broad side and stern end impacts are

based upon penetration of an infinitely rigid, vertical cylinder with a given diameter and may be used for impacts against jacket legs (D = 1.5 m) and large diameter columns (D = 10m). The curve for stern corner impact is based upon penetration of an infinitely rigid cylinder and may be used for large diameter column impacts.

For supply vessels and merchant vessels in the range of 2-5000 tons displacement, the force deformation relationships are given in NORSOK-N-004 (2004) and may be used for impacts against jacket legs with diameter 1.5 m – 2.5 m. The force deformation relationships given are for conventional supply ship without e.g. bow reinforcements for operations in ice. The curve for bow impact is based upon collision with an infinitely rigid, plane wall and may be used for large diameter column impacts, but should not be used for significantly different collision events, e.g. impact against tubular braces.

Force-deformation relationships for tanker bow impact are given in NORSOK-N-004 (2004) for the bulbous part and the superstructure, respectively. The curves may be used provided that the impacted structure (e.g. stern of floating production vessels) does not undergo substantial deformation i.e. strength design requirements are complied with, see Chapter 7.7. If this condition is not met interaction between the bow and the impacted structure shall be taken into consideration. Non-linear finite element methods or simplified plastic analysis techniques of members subjected to axial crushing shall be employed.

In addition to resisting the total collision force, large diameter columns have to resist local concentrations (subsets) of the collision force, given for stern corner impact. The tabulated values for the concentrated force together with the contact area are given in Table A.3-1 and Table A.3-2 in NORSOK-N-004 (2004).

7.6 Assessment of actions effects

The energy absorbing mechanisms during the collision should be evaluated (ISO-19902, 2007). Typically, local member denting, elastic and plastic deflection of the impacted member, global elastic and plastic response of the whole structure, and denting of the ship or platform are the main mechanisms.

7.6.1 Numerical analysis

In a rigorous impact analysis, the collision actions should be evaluated based on a dynamic time simulation. Under certain conditions, quasi-static analysis can be exploited, see Chapter 7.5. Due to the large degree of non-linearity involved in ship collision analyses, explicit numerical solvers are typically used. Non-linear solvers like USFOS, Ls-Dyna, Ansys and Abaqus are preferred for these problems where the loss of stiffness at large displacements and member collapse is considered.

Any structure needs to be modelled with sufficient detail so that a satisfactory response is captured when the loads are applied. Accidental and ultimate limit state analysis has to capture geometrical and material non-linearities. Some general guidelines for modelling can be found in DNV-RP-C208 (2013) and Ultiguide (DNV, 1999).

The non-linear FE analysis is typically conducted using shell elements. Increased mesh resolution is to be used in the areas where non-linear deformations and effects are assumed to occur i.e. the collision zone. At least five integration points though material thickness are to be used to describe the shell thinning. The stiffeners should in minimum be modelled having at least one element for the web and either a beam of two shell elements for the flange in order to take into account the buckling or tripping.

The extent of the collision models should be selected such that there are not plastic deformations in the vicinity of the boundary conditions.

The implemented elements should capture common failure modes (tension yielding, bending/compression failure, stability failure, post-buckling load shedding in neighbor members, interaction with local buckling) at all times. Yield and fracture modelling requires careful consideration on element size in order to capture high stress concentrations in the facture zone. Typically, several elements should be present in the yield zone to achieve good strain estimates (DNV-RP-C208, 2013).

Selected material models should describe elastic-plastic material behaviour. Most FE codes will assume that true values (not engineering) are being used in the material input data. Guidance to convert engineering to true values is provided in DNV-RP-C208 (2013).

The material certificates are to be obtained for the determination of material properties. The certificates should present the engineering stress-strain curves until the material failure. In load levels where the material undergoes large degrees of membrane stretching, shell thinning needs to be considered as the plasticity level increases.

ALS design often involves the ductile fracture. A reliable fracture criterion should be established. DNV-GL has published the recommended practices for the determination of structural capacity of non-linear FE analysis methods (DNV-RP-C208, 2013) suggesting material curves both for engineering stress-strain and true stress-strain space. The material curves are defined until the necking that is assumed to initiate once the ultimate strain value is reached. As the material possesses significant resistance after the necking, the material curves should be extended beyond the necking until the failure. The failure strain should be scaled according to the element size, see for example Ehlers and Varsta (2009), Scharrer et al. (2002) and Zhang et al. (2004). To evaluate the critical thru thickness strain at the moment of fracture, an empirical criterion is presented by Scharrer et al. (2002) and Zhang et al. (2004):

$$\varepsilon_f(l_e) = \varepsilon_g + \varepsilon_e \cdot \frac{t}{l_e} \tag{7.5}$$

where ε_g is the uniform strain and ε_e is the necking strain, t is the plate thickness and l_e is the individual element length. It is commonly recommended that the ratio l_e/t is not less than 5 for shell element. The values of uniform and necking strain achieved from thickness measurements related to the calculated stress states given in Scharrer et al. (2002) are 0.056 for the uniform strain and 0.54 for the necking strain in the case of shell elements.

Additional information on material properties can be found in the Material Database presented in Annex 1.

7.6.2 Simple elastic-plastic methods

NORSOK N-004 defines several elastic-plastic relationships for the response of ship bow, tubular members and beams. These relationships can be used for a simplified analysis together with energies and force-deformation curves presented above. The following relationships are provided:

1. Energy dissipation in ship bow:
   Tabulated values are presented for normal bows without ice strengthening.
2. Force-deformation relationships for denting of tubular members:
   Graphs and equations are presented for the resistance to indentation of unstiffened tubes
3. Force-deformation relationships for beams:
   - *Plastic force-deformation relationships including elastic, axial flexibility*
   - *Bending capacity of dented tubular members*

In NORSOK-N-004 (2004) guidelines are given to account and assess the strength of connections and adjacent members. The resistance of connections should be taken from ULS requirements in NORSOK-N-004 (2004) for tubular joints and EUROCODE-3 (1993) or NS-3472 (2001) for other joints. NORSOK-N-004 (2004) also present the criteria for local buckling, lateral stability at yield hinges, tensile fracture and tensile fracture in yield hinges and resistance of large diameter, stiffened columns is presented in the form of closed form equations.

7.7 Design considerations

With respect to the distribution of strain energy dissipation there may be distinguished between, see Figure 7.2 (NORSOK-N-004, 2004):

- strength design
- ductility design
- shared-energy design

Strength design implies that the installation is strong enough to resist the collision force with minor deformation, so that the ship is forced to deform and dissipate the major part of the energy.

Ductility design implies that the installation undergoes large, plastic deformations and dissipates the major part of the collision energy.

Shared energy design implies that both the installation and ship contribute significantly to the energy dissipation.

The aim of the design against accidental actions is to achieve a system where the main safety functions of the installation are not impaired. This implies the absorption of the deformation energy in a way that the load bearing function of the installation shall remain intact with the damages imposed by the ship collision action. Furthermore, it has to be verified that the residual strength of the installation with damage caused by the accidental load is sufficient to accommodate the functional loads and design environmental loads.

While the strength design would be desirable for the installation, it is not always feasible in practical applications. In most cases ductility or shared energy design is used. For example, the collision between the tanker and the side of the FPSO: the relative strength of the intruding bow exceeds that of the FPSO side and the FPSO absorbs most of the energy i.e. behaves as a ductile design. However, strength design may in some cases be achievable with little increase in steel weight by positioning the additional steel either to a possible impact location or in a way to prevent buckling due to local damage.

The occurrence of fracture can be minimized by preventing the local stress concentrations by reducing the strong or very stiff points within the structure. This allows the development of deformations behind these hard points and the energy is absorbed over larger area.

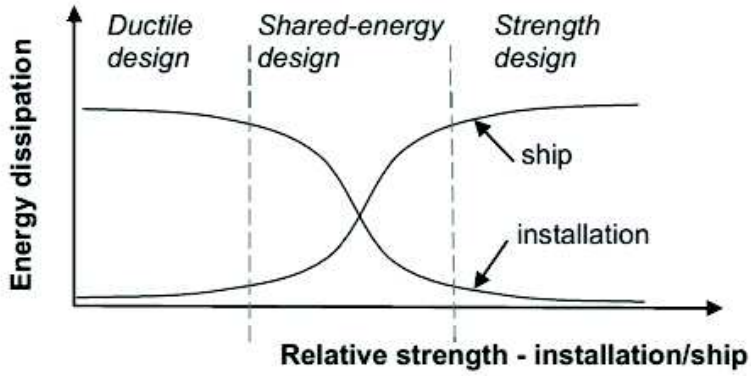

Figure 7.2: Energy dissipation for strength, ductile and shared energy design (NORSOK-N-004, 2004).

CHAPTER EIGHT

DROPPED OBJECTS

8.1 Probabilistic models of actions

The purpose of a dropped objects analysis is to evaluate the effectiveness of a protection system or remaining strength of a structural member subject to dropped object actions. The design procedure for ALS actions and action effects is shown in Figure 8.1. The intention of the analysis is to evaluate if hazardous, vulnerable areas, safety critical systems on deck or subsea, conform with acceptable safety levels after the application of risk control options. The following sections detail the probabilistic action models, action assessment methods and the ALS design procedure for dropped object actions and action effects. Impact actions may be dictated by the owner/operator, may be based on a case-by-case study, or based on probabilistic methods. Evaluating the performance of a vulnerable area subject to dropped object actions may be completed numerically, or by elastic-plastic methodology. Once the action effects are evaluated, the residual strength of the impacted member may be assessed to ensure if the design function is met.

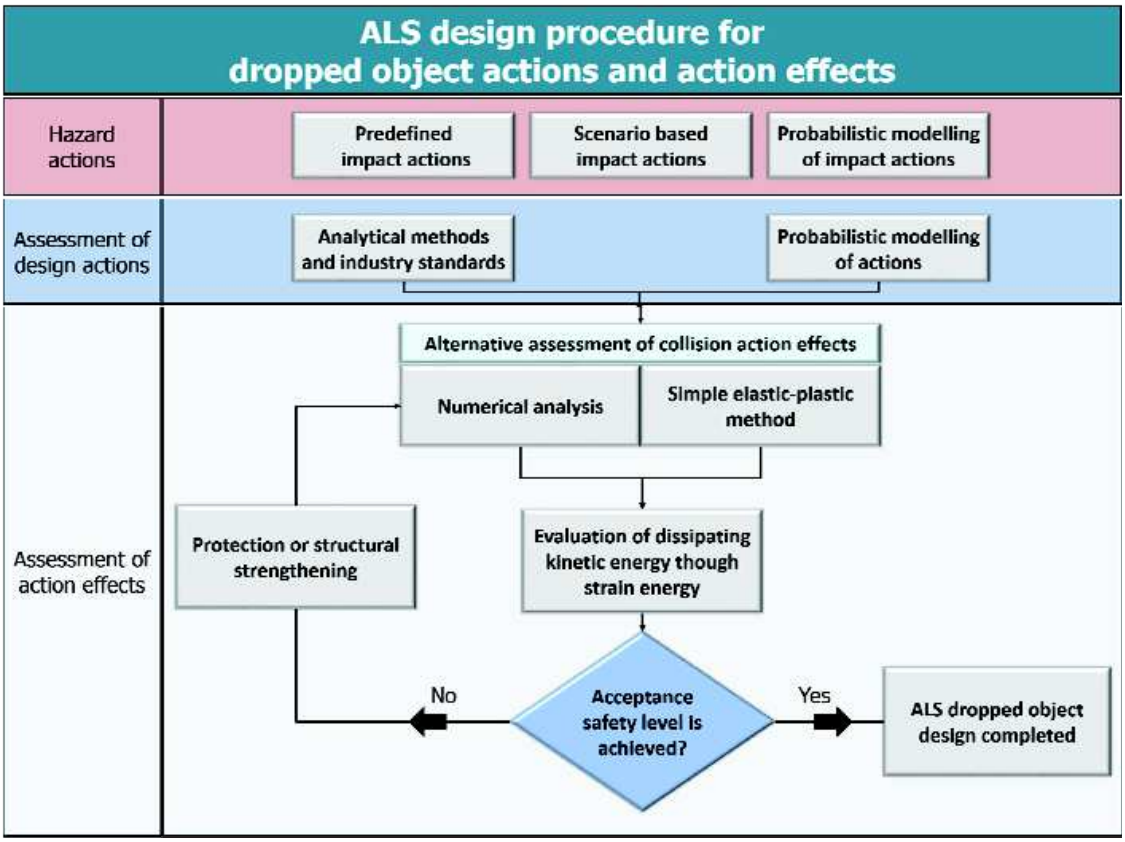

Figure 8.1: ALS design procedure for dropped objects.

8.2 Identification of dropped object hazard

8.2.1 General definitions

A Dropped Object Study (DOS) is normally carried out as a part of overall risk assessments of the facility. DOS can be classified in two parts based on the dropped location: 'onboard' or 'overboard' of the facility. The DOS for onboard actions is further categorized based on the object's movement, i.e. 'Dropped' or 'Swung' study. For each study, the necessary data to carry out the risk assessment and underlying assumptions are different.

8.2.2 Facility Layout

The facility layout including a crane's working radius and laydown area(s) of the studied deck(s) should be available. The crane type and lifting capacity should also be provided together with all data likely to affect the crane's operational profile. Figure 8.2 is an example of an FPSO's layout.

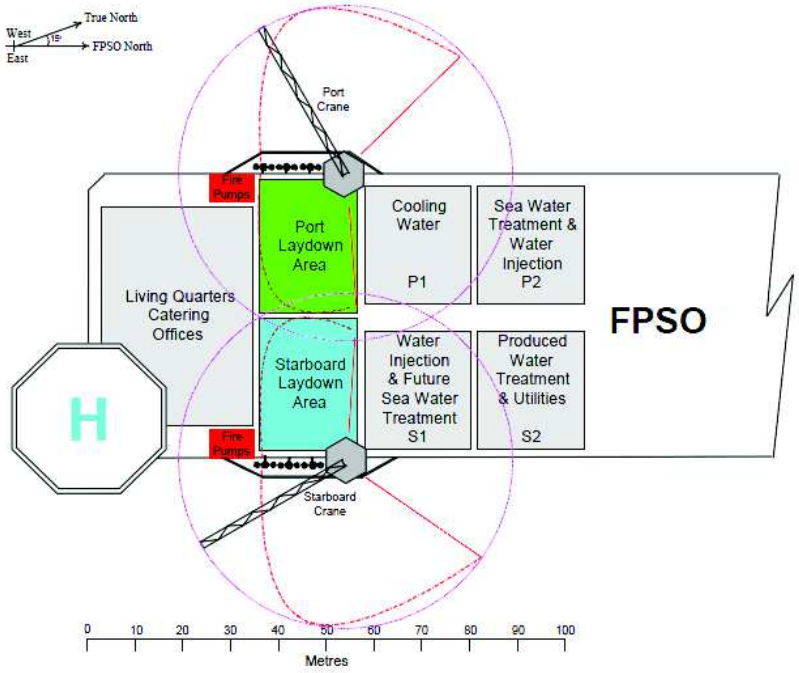

Figure 8.2: Typical offshore unit layout.

8.2.3 Object lift schedules

Operating schedules of the cranes should be prepared in a tabulated format like the one in Table 8.1. These tables should contain the equipment type being lifted, crane location (number), delivered location, equipment dimension, weight and lifting frequency per year etc. from field lifting and operating plans. The plans should cover lifters to move important equipment as well as main cranes.

Table 8.1: Object lift schedules (example).

No.	Equipment	Vessel appoach	Crane	Lifting from	Lifting to	Units or times	Equipment dimension			Dry weight (Ton)	Lifting frequence (per unit year)
							L (m)	W (m)	H (m)		
1	10ft. container	Platform south	South	Supply deck	Top deck	3	3	2.4	2.6	10.1	5.2
⋮	⋮	⋮	⋮	⋮	⋮	⋮	⋮	⋮	⋮	⋮	⋮

8.2.4 Onboard dropped objects

8.2.4.1 Frequency

The frequency of dropped objects onboard an offshore unit on annual basis can be estimated by the following expression:

$$F_{dpy} = F_{lpy} \cdot P_{dpl} \quad (8.1)$$

where,

F_{dpy} is dropped frequency per year;
F_{ipy} is lifting frequency per year;
P_{dpl} is dropped probability per lifting

The International Association of Oil & Gas Producers (OGP-434-8, 2010) provides various dropped object probabilities depending on load weight, lifting device and dropped location for mobile units and fixed installations. OREDA (SINTEF, 2009) also suggests reliability data of an offshore crane system. The mechanical lifting failures report of OGP contains dropped object probabilities for mobile units as shown in Table 8.2, and in Table 8.3 for fixed installations. The probabilities are classified in accordance with load weight, lifting device and dropped location (installation, sea and vessel). Based on the object lift schedule (see Section 8.2.3), proper probabilities can be selected. For example, the dropped probability per lift, P_{dpl}, of an object less than 1 tonne for fixed installation onto installation is 3.8×10^{-5} per lift using a main crane.

Table 8.2: Dropped object probabilities for mobile units (per lift) (OGP-434-8, 2010).

Dropped Object Probabilitlies for Mobile Units (per lift)					
Load weight	**Lifting device**	**Drop onto:**			**total**
		Installation	Sea	Vessel	
<1 te	Main crane	3.2×10^{-5}	8.8×10^{-6}	1.1×10^{-5}	4.1×10^{-5}
	Drilling derrick	1.7×10^{-5}	7.3×10^{-7}	6.1×10^{-8}	1.8×10^{-5}
	Other device	8.6×10^{-5}	1.1×10^{-5}	0	9.7×10^{-5}
1-20 te	Main crane	3.1×10^{-6}	2.0×10^{-6}	3.0×10^{-6}	5.4×10^{-6}
	Drilling derrick	3.6×10^{-6}	4.6×10^{-7}	0	4.0×10^{-6}
	Other device	7.6×10^{-6}	2.9×10^{-6}	0	1.1×10^{-5}
20-100 te	Main crane	1.2×10^{-5}	7.1×10^{-6}	9.5×10^{-6}	2.0×10^{-5}
	Drilling derrick	1.8×10^{-6}	0	0	1.8×10^{-6}
	Other device	1.9×10^{-6}	0	0	1.9×10^{-6}
>100 te	Main crane	2.8×10^{-4}	0	0	2.8×10^{-4}
	Drilling derrick	4.7×10^{-3}	1.4×10^{-3}	0	6.1×10^{-3}
	Other device	4.9×10^{-4}	2.4×10^{-4}	0	7.3×10^{-4}
All	Main crane	8.5×10^{-6}	3.3×10^{-6}	4.6×10^{-6}	1.2×10^{-5}
	Drilling derrick	1.1×10^{-5}	6.7×10^{-7}	3.0×10^{-8}	1.1×10^{-5}
	Other device	4.5×10^{-5}	6.5×10^{-6}	0	5.2×10^{-5}
Total	All	1.2×10^{-5}	1.4×10^{-6}	9.4×10^{-7}	1.4×10^{-5}

Table 8.3: Dropped object probabilities for fixed installations (per lift) (OGP-434-8, 2010).

Dropped Object Probabilitlies for Mobile Units (per lift)					
Load weight	**Lifting device**	**Drop onto:**			**total**
		Installation	Sea	Vessel	
<1 te	Main crane	3.8×10^{-5}	6.9×10^{-6}	1.1×10^{-5}	4.5×10^{-5}
	Drilling derrick	1.7×10^{-5}	1.2×10^{-7}	1.2×10^{-7}	1.7×10^{-5}
	Other device	1.0×10^{-4}	4.2×10^{-6}	6.1×10^{-7}	1.0×10^{-4}
1-20 te	Main crane	4.7×10^{-6}	1.7×10^{-6}	5.1×10^{-6}	7.9×10^{-6}
	Drilling derrick	2.7×10^{-6}	1.5×10^{-7}	0	2.9×10^{-6}
	Other device	1.4×10^{-5}	0	7.4×10^{-7}	1.5×10^{-5}
20-100 te	Main crane	1.0×10^{-5}	6.2×10^{-6}	1.6×10^{-5}	2.0×10^{-5}
	Drilling derrick	1.2×10^{-6}	0	0	1.2×10^{-6}
	Other device	2.6×10^{-5}	0	0	2.6×10^{-5}
>100 te	Main crane	9.3×10^{-5}	0	0	9.3×10^{-5}
	Drilling derrick	0	0	0	0
	Other device	6.1×10^{-4}	0	0	6.1×10^{-4}
All	Main crane	1.0×10^{-5}	2.8×10^{-6}	6.4×10^{-6}	1.5×10^{-5}
	Drilling derrick	9.6×10^{-6}	1.2×10^{-7}	6.1×10^{-8}	9.7×10^{-6}
	Other device	5.7×10^{-5}	2.0×10^{-6}	5.8×10^{-7}	6.0×10^{-5}
Total	All	1.4×10^{-5}	8.8×10^{-7}	1.6×10^{-6}	1.6×10^{-5}

8.2.4.2 Consequence

If the drag on a falling object is neglected, the potential energy of an object at the point of release is virtually equal to the kinetic energy at impact i.e.:

$$\text{Impact Energy} = \frac{1}{2}mv^2 \approx mgh \tag{8.2}$$

where, m is the mass of the object, v is the velocity of an object at impact, g is the acceleration due to gravity, and h is the object height above the impact surface.

It is practical in the offshore industry, to consider that the absorbed impact energy ratio by the target (struck body) ranges from 75% to 100% (worst case scenario).

8.2.5 Onboard swinging objects

8.2.5.1 Frequency

For the most of statistical databases, the probability of swung objects is often included in the probability of dropped objects making it difficult to acquire a database that only includes the impact probability of swung objects . For swung objects the impact frequency is usually calculated as a conditional probability times the dropped object frequency. The assumed conditional probability can be based on figures from a statistical database or previous experience.

8.2.5.2 Consequence

Impacts from swung objects are assumed to occur either (a) as a result of the crane's slew on a target during horizontal rotation, or (b) due to the load developing a swing during vertical lifting/lowering. Depending on the studied scenario, the following equations are used to estimate the potential impact energies associated with swinging loads.

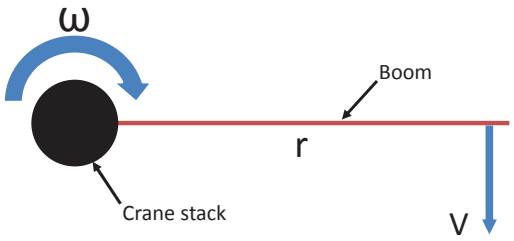

Figure 8.3: Crane component description (top view).

If the slew speed of a crane is N rpm, then the velocity v, of the crane load at a swing radius of r metres is as follows:

$$v[m/s] = \omega \times r = \frac{2\pi N}{60} \times r \tag{8.3}$$

The maximum impact energy is then equal to the kinetic energy of the slewed object, i.e.:

$$E = \frac{1}{2} mv^2 \tag{8.4}$$

where, m is the mass of the load, v is the maximum swing velocity.

For loads with a swinging component (e.g. pendulum motion due to the effects of wind or rotational acceleration by sudden stop), the impact energy is:

$$E = m\,g\,h \tag{8.5}$$

where, h is the maximum lift height due to the swing that can be obtained in two different ways.

To acquire h use the maximum swing angle theta shown in Figure 8.4; the maximum lift height due to swing h can be expressed as:

$$h = L \times (1 - \cos\theta) \tag{8.6}$$

where, L is cable length (m), and θ (theta) is maximum swing angle to the vertical.

Alternatively, one can use the horizontal translation x of the load as depicted in Figure 8.5. The maximum lift height due to swing h can be expressed as:

$$h = L - (L^2 - x^2)^{1/2} \tag{8.7}$$

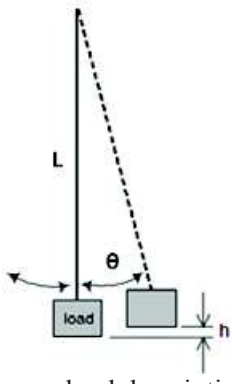

Figure 8.4: Swung load description with swing angle θ (theta) (side view).

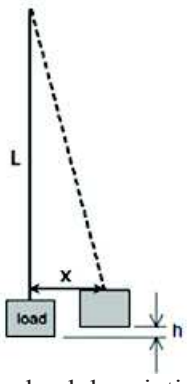

Figure 8.5: Swung load description with translation distance x (side view).

The impact energy in both cases can be estimated from the potential energy due to lateral slew velocity or from the potential energy at the swing peak.

8.2.6 Overboard dropped objects

8.2.6.1 Frequency

The frequency of hit can be estimated based on the number of lifts (DNV-RP-F107, 2010), the drop frequency per lift and the probability of hit to the exposed sections of subsea lines and equipment. For a certain ring around the drop point, the hit frequency is estimated by the following:

$$F_{hit,sl,r} = N_{lift} \cdot f_{lift} \cdot P_{hit,sl,r} \tag{8.8}$$

where,

$F_{hit,sl,r}$ is frequency of hit to the subsea line within a certain ring (per year);
N_{lift} is number of lifts;
f_{liftt} is frequency of drop per lift;
$P_{lhit,sl,r}$ is probability of hit to a subsea line or equipment within a certain ring, Eq. 8.9.

The total frequency of hit to a subsea line or equipment is assessed by summarizing the hit frequencies to the pipeline within each ring around the drop point as shown in Figure 8.6. Within a certain ring, the probability of hit to a pipeline or umbilical with an object, Phit,sl,r, can be described as the exposed area which gives a hit within a ring divided on the total area of the ring, multiplied with the probability of hit within the ring.

$$P_{hit,sl,r} = P_{hit,r} \cdot \frac{L_{sl} \cdot (D + B/2 + B/2)}{A_r} \tag{8.9}$$

where,

$P_{hit,sl,r}$ is probability of hit on subsea line (sl) within a certain ring, r;
$P_{hit,r}$ is probability of hit within the ring, Eq. 8.11;
L_{sl} is length of subsea line within the ring (m);
D is diameter of subsea line (m), see Figure 8.7;
B is breadth of falling object (m), see Figure 8.7;
A_r is area within the ring (m^2), see Figure 8.6

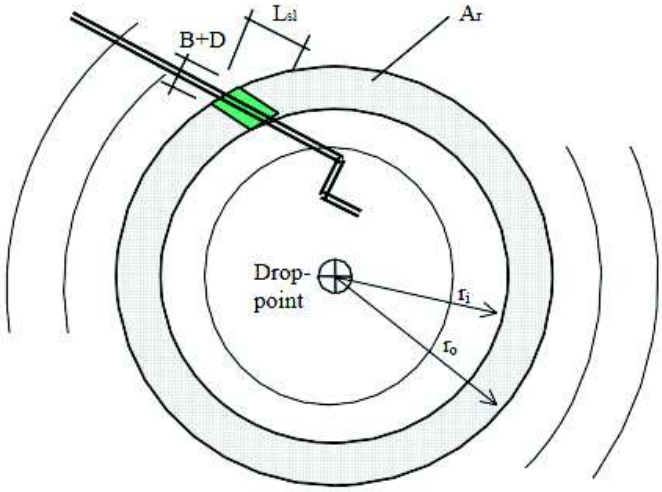

Figure 8.6: Probability of hit within a ring, defined by inner radius, r_i, and outer radius, r_o, from the drop point.

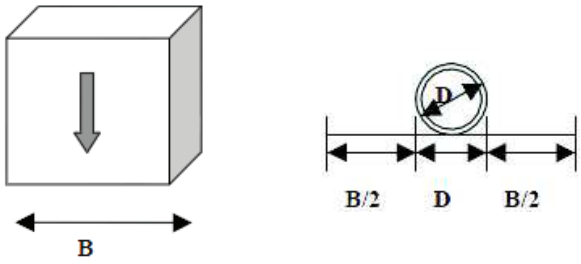

Figure 8.7: Definition of hit area.

For containers and massive objects, B can be set to the average of the two shortest sides, and for tubular objects, B can be set equal to the diameter for front impact and equal to the length for side impacts.

The probability that a sinking object will hit the seabed within a distance r from the vertical line through the drop point is then:

$$P(x \le r) = \int_{-r}^{r} p(x)dx \tag{8.10}$$

The actual extent of the vulnerable items on the seabed, e.g. pipeline, within each ring can be incorporated by dividing the probability in several "rings", see Figure 8.6. The probability of hit within two circles around the drop point, $P_{hit,r}$ with inner radius r_i and outer radius, r_o, can be found by:

$$P_{hit,r} = P(r_i < x \le r_o) = P(x \le r_o) - P(x \le r_i) \tag{8.11}$$

The breadth of each ring can be taken at 10 metre intervals. The hit probabilities within each of these rings may then be calculated for different deviation angles and the actual sea depth.

The normal distribution of Eq. 8.8 is defined as:

$$p(x) = \frac{1}{\sqrt{2\pi}\delta} \exp\left(-\frac{1}{2}\left(\frac{x}{\delta}\right)^2\right) \tag{8.12}$$

where,

- $p(x)$ is probability of a sinking object hitting the seabed at a distance x from the vertical line through the drop point;
- x is horizontal distance at the seabed (metres);
- δ is lateral deviation (metres), see Table 8.4 and Figure 8.8

Table 8.4: Angular deviation of object category.

No.	Description	Weight (tonnes)	Angular deviation (α) (deg)
1	Flat/long shaped	< 2	15
2		2-8	9
3		> 8	5
4	Box/Round shaped	< 2	10
5		2-8	5
6		> 8	3
7	Box/Round shaped	>> 8	2

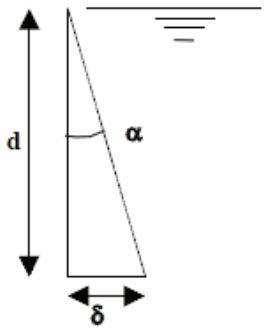

Figure 8.8: Symbols used in eq. 8.12.

8.2.6.2 Consequence

The kinetic energy of a dropped object is directly proportional on on the mass and the velocity of the object (DNV-RP-F107, 2010). Furthermore, the sinking velocity depends on the shape of an object and its mass in water.

The terminal velocity is found when the object is in balance with respect to gravitation forces, displaced volume and flow resistance. When the object has reached this balance, it falls with a constant velocity, i.e. terminal velocity. This can be expressed by the following equation:

$$\left(m - V \cdot \rho_{water}\right) \cdot g = \frac{1}{2} \rho_{water} \cdot C_D \cdot A \cdot v_T^2 \tag{8.13}$$

where,

m is mass of the object (kg);
g is Gravitation acceleration (9.81 m/s^2);
V is volume of the object (the volume of the displaced water) (m^3);
ρ_{water} is density of water (i.e. 1025 kg/m^3);
C_D is drag-coefficient of the object;
A is projected area of the object in the flow-direction (m^2);
V_T is terminal velocity through the water (m/s)

The kinetic energy of the object, E_T, when terminal velocity has been reached is:

$$E_T = \frac{1}{2} m v_T^2 \tag{8.14}$$

Combining Eq. 8.13 and Eq. 8.14 gives the following expression for the terminal energy:

$$E_T = \frac{mg}{C_D A}\left(\frac{m}{\rho_{water}} - V\right) \tag{8.15}$$

In addition to the terminal energy, the kinetic energy that is effective upon impact, E_E, includes the energy of added hydrodynamic mass, E_A. The added mass may become significant for large volume objects such as containers. The effective impact energy becomes:

$$E_E = E_T + E_A = \frac{1}{2}(m + m_a) v_T^2 \tag{8.16}$$

where,

m_a is the added mass found by $m_a = \rho_w \cdot C_a \cdot V$

The drag and added mass coefficients depend on the object geometry. The drag coefficients will affect the object's terminal velocity, whereas the added mass takes part only as the dropped object strucks an asset and is brought to a stop. Guidance for both values are given in Table 8.5.

Table 8.5: C_d and C_a coefficients for sinking objects.

Category no.	Description	C_d	C_a
1, 2, 3	Slender shape	0.7–1.5	0.1–1.0
4, 5, 6, 7	Box shaped	1.2–1.3	0.6–1.5
All	Misc. Shapes (spherical to complex)	0.6–2.0	1.0–2.0

It is recommended that a value of 1.0 initially be used for C_d, after which the effect of a revised drag coefficient should be evaluated.

8.3 Probabilistic models of actions

The process for assessing accidental loadings from dropped objects follows in principle the risk assessment traditionally used in the offshore industry. An example of a typical risk assessment procedure is provided in DNV-RP-F107 (2010). A typical dropped object risk assessment utilizes the general arrangement of the topside and subsea detailing the process equipment, piping and crane range of motion. The general arrangement will provide the analyst with a general understanding of the critical drop zones. The general arrangment will also provide identification of the hazardous areas and safety critical elements susceptible to damage from dropped objects likely to be caused from mechanical handling activities.

A comprehensive register of all lifts including crane capacity, the type of object, shape, weight, and lift frequency per year is also required. This data will be used to establish the drop frequency per lift using drop frequency tables (DNV-RP-F107, Table 9 for example). For objects falling in water, the likelihood of striking a single point is computed by including probability of excursion. Based on the shape of the dropped object, the amount of excursion is assumed to be normally distributed and defined as:

$$p(x) = \frac{1}{\sqrt{2\pi}\delta} e^{\frac{1}{2}\left(\frac{x}{\delta}\right)^2} \tag{8.17}$$

where, the horizontal distance from the seabed and lateral deviation in meters are represented using x and δ, respectively.

The likelihood of a dropped object landing within a distance r, off the drop point may be computed from:

$$P(x \le r) = \int_{-r}^{r} p(x)dx \tag{8.18}$$

Generally, the hit area may be split into different rings with a likelihood of impact computed within each ring expressed as:

$$P_{hit,r} = P(r_i < x \le r_o) = P(x \le r_o) - P(x \le r_i) \tag{8.19}$$

In order to determine the hit frequency as a function of energy, the analyst must solve the following steps:

1. Determine the likelihood of hitting a ring by Eq. 8.19.
2. Determine the probability of hit to a structure within a ring by Eq. 8.9.
3. Calculate the hit frequency by Eq. 8.8.
4. Compute the hit frequency for all potential dropped object mass and shapes.
5. Compute the conditional probability of each dropped object mass and shape hitting an object using Eq. 8.9 for each hit probability.
6. Sum the conditional hit frequencies for each mass and shape to provide a single hit frequency associated with an impact energy.
7. Plot hit frequency as a function of impact energy similar to Figure 8.9.

From this figure, the analyst can determine what impact energy to design the structure to absorb given a likelihood of occurrence. The likelihood of occurrence less than 10^{-2} is considered an accidental action (including dropped objects) as per DNV OS-F101. It is the discretion of the operator, owner or regulator to define the acceptable likelihood of occurance of a dropped object event.

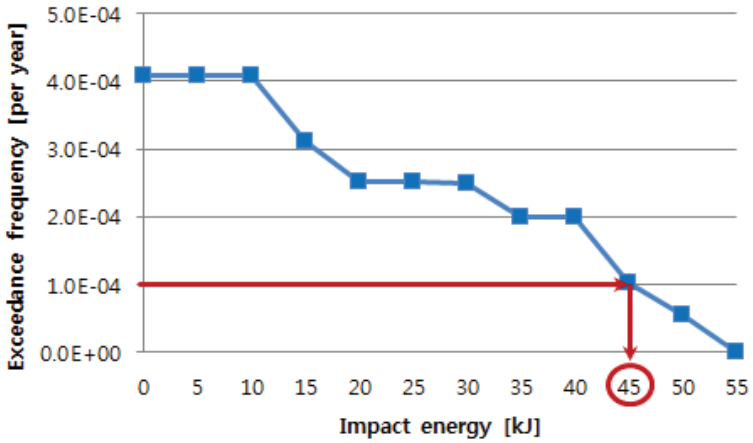

Figure 8.9: Impact energy levels associated with accumulated annual hit frequencies.

8.4 Definition of impact actions

The impact energy of a dropped object is characterized by its kinetic energy; a function of its cumulative mass and velocity. The mass and height of a dropped object is directly related to the safe working load of the lifting appliance. Typically at sea level, a minimum of 5MJ of impact energy is developed for cranes with a lifting capacity of 30 tonnes or more (NORSOK N-004). Below sea level, the impact energy may be assumed the same as at sea level. For cranes of lower capacity, a reduced impact energy may be determined.

The protection of process equipement and safety systems may have a predefined impact design condition. This will generally be provided in the platform design guidance. The parameters of the design condition will directly specify the total kinetic energy to be absorbed during the impact event, shape of the dropped object or impact area as well as hit angle. The design specification may also define what proportion of strain energy is absorbed by the dropped object and struck body as well. Conservatively, the struck object is required to absorb all of the kinetic energy by strain energy.

The kinetic energy of a dropped object has been defined in Eq 8.4, where the velocity of the dropped object is expressed from Eq. 8.20.

$$v = \sqrt{2gs} \tag{8.20}$$

where s is the distance travelled from the object drop point in air. For objects dropped into water, the subsea impact velocity may account for the loss of momentum when impacting the water surface if the velocity at contact is sufficiently less than terminal velocity.

The momentum loss at the impact with the water surface is a function of the impact duration $t_{d,}$ and impacting force $F(t)$ expressed as:

$$m\Delta v = \int_0^{t_d} F(t)dt \tag{8.21}$$

The velocity after impact is:

$$v = v_o - \Delta v \tag{8.22}$$

Once submerged, the velocity profile of the dropped object can be expressed using Figure 8.10 where s is the distance travelled in water, v is the velocity of the body in water, s_c and terminal velocity v_t are defined as:

$$s_c = \frac{v_t^2\left(1+\frac{a}{m}\right)}{2g\left(1-\frac{\rho_w V}{\rho_w C_d A_p}\right)} \tag{8.22}$$

$$v_t = \sqrt{\frac{2g(m - \rho_w V)}{\rho_w C_d A_p}} \tag{8.23}$$

where the water density, hydrodynamic drag coefficient, object mass, projected cross-sectional area and object displacement are ρ_w, C_d, m, A_p, and V, respectively.

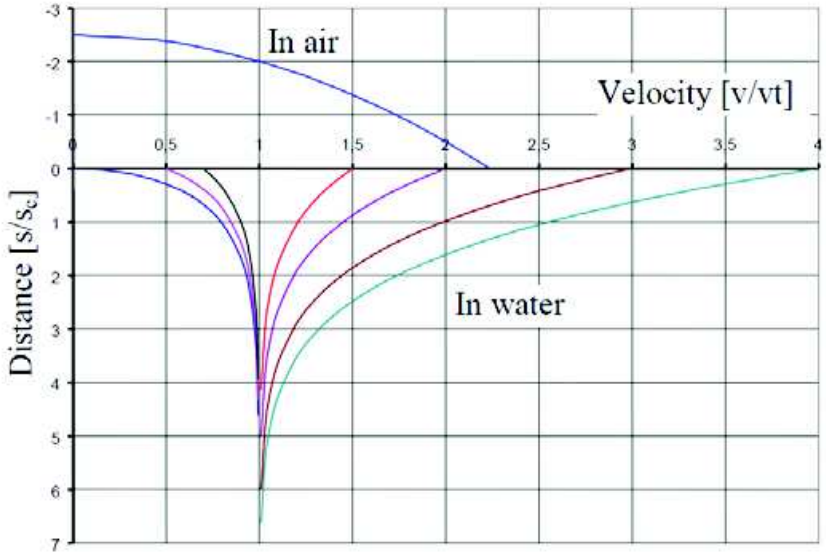

Figure 8.10: Falling object velocity profile (reproduced from NORSOK N-004).

8.5 Assessment of actions effects

The evaluation of structures subject to dropped object events require the kinetic energy be dissipated as strain energy in the struck component and possibly also in the dropped object itself. Generally, this involves large plastic strains and significant damage to the struck component. Consideration should be made to limit the amount of deflection developed in process equipment such as risers and gas pipes subject to dropped object actions. Deck penetration and shutdown of safety critical systems should also be avoided. In order to evaluate the amount of deflection and potential damage resulting from an impact event, the strain energy during impact must be calculated. The strain energy calculation may be completed using elastic-plastic empirical calculations or numerically using non-linear finite element analysis.

There are several commercially available non-linear finite element analysis packages available including Ansys, Abaqus, LS-DYNA and NASTRAN which are well suited for a dropped object analysis. It is important the analyst understands the inherent analysis parameters required to accurately represent the impact scenario and energy dispersion. The analysis parameters include and are not limited to:

- Load and boundary conditions.
- Contact definition between struck and striking objects.
- Numerical integration type.
- Hourglassing and other energy controls.
- Material constituitive model.
- Element formulation.

The total strain energy (the area under the force-displacement curve) in the struck structure must be equivalent to the kinetic energy of the dropped object at impact. Generally, the dropped object is considered rigid and the strain energy of the impacted object is computed. It is often practical to compute the strain energy of the struck and dropped object to predict a less conservative estimate of structural damage.

The force-displacement curve for a struck component may be developed incrementally using empirical formulations specific to the type of struck component. NORSOK N-004 (2004) provides force-deformation relationships for the denting of tubular members and stiffened

plates with and without axial flexibility. The force-displacement curves may be used to compute the total strain energy, the capability to develop a plastic hinge mechanism from local buckling, and the tensile fracture at a specific displacement value should be known. Emperical formulations are provided in NORSOK N-004 (2004) for local buckling and tensile fracture evaluations. As per NORSOK N-004, the impacted object must be sufficiently stiff to absorb the kinetic energy through strain energy and meet stability and ductility requirements (local buckling and tensile fracture shall be avoided). For structural components which sustain significant damage, a reevaluation of the global structure without the struck member should be completed. The total-strain energy and deformation of a struck member may also be computed using numerical methods. This is the preferred method of analysis if the analyst would like to reduce possible conservatisms in the emperical predictions and provide an accurate prediction of the deformed configuration. Computing the deformed shape numerically is an ideal analysis method when the dropped object and impacted structure are complex.

A numerical representation of the impact event must consider an accurate representation of the struck body and adjacent structure. All structure (striking and struck bodies) which are likely to develop large strains shall be represented using shell elements. In the event where the striking body is defined as rigid, the struck structure shall be modeled with shell elements to provide an accurate representation of the impacting area. The level of refinement is a function of the size of the dropped object and struck body. The numerical model must be sufficienty refined to represent the stiffness of the structure and capture local buckling and tensile fracture.

The numerical model is generally loaded by defining an initial velocity to the striking body which properly represents the kinetic energy of the impact event. The mass of the striking body may be represented as a single lumped mass positioned at the centre of gravity and attached to the striking surface using rigid links. For analyses like the scenario based approach which utilize the strain energy in the striking object and the struck body, it is important not to artificially stiffen the dropped object using rigid links. An accurate representative of the structural stiffness and mass dispersion may be required. The boundary conditions are generally applied on the struck body sufficiently far from the impacted area so that any developed strain levels are not influenced.

The constituitive material model must properly represent elastic-plastic deformation and follow the guidance detailed in the Annex of this Guideline. The loading rate for impact events may be high enough to justify applying a strain-rate sensitive consitituitive model. Caution should be used when employing strain-rate constituitive models since strain-rate sensitivity varies with strain direction (compressive, tensile, bending, and shear).

8.6 Design considerations

The design considerations of equipment, structure and conduit systems subject to dropped object loads are focused on dissipating the kinetic energy of the impacting object through strain energy. This is done through developed plasticity in the deformation of the struck structure. Limitations on the magnitude of deformation are a typical requirement of equipment and structural design. These limitations are implemented to ensure equipment operational requirements are achieved and secondary hazards are prevented.

It is recommended to provide resistance to dropped objects by using redundant framing and adequate material toughness. The assessment of action events is used to determine the required strength of the struck structural configuration. The design evaluation requirements may be different based on the structure's intended design. Protection systems used to shield safety critical equipement from dropped objects are required to sustain the impact loads without meeting local or global structural load requirements. The dropped object analysis will suggest if any local reinforment or protection is required. Other structural elements such as decking, tubular members and piping are required to sustain the dropped object impact loading and have sufficient residual strength to resist local and global loads. These local members must be evaluated in their deformed state to sufficiently meet strength requirements. NORSOK N-004 (2004) provides guidance on joint, bracing and adjacent member design of impacted components as well as empirical formualtions describing the bending moment reduction of dented tubulars.

CHAPTER NINE

EXTREME ENVIRONMENTAL LOADS

9.1 Purpose

The purpose of an ALS assessment is to verify structural integrity during extreme/abnormal wind and wave scenarios. The severity of the loading scenario is based on the platform type. Mobile units such as MODU, FSPO's and Jackup structures have the ability mitigate the likelihood of experiencing an extreme loading event by relocating. Fixed offshore platforms however, must sustain extreme loading scenarios and achieve a level of reduced operational functionality.

The analysis procedure for an extreme/abnormal environmental loading scenario follows the work flow shown in Figure 9.1. The wave and/or wind action loads are first defined using Metocean data specific to the installation location. Based on the type of structure, structural region of interest and design requirement, the action assessment requirements are determined and structure is evaluated. The follow sections will briefly explain the actions, action defintions and action assessment.

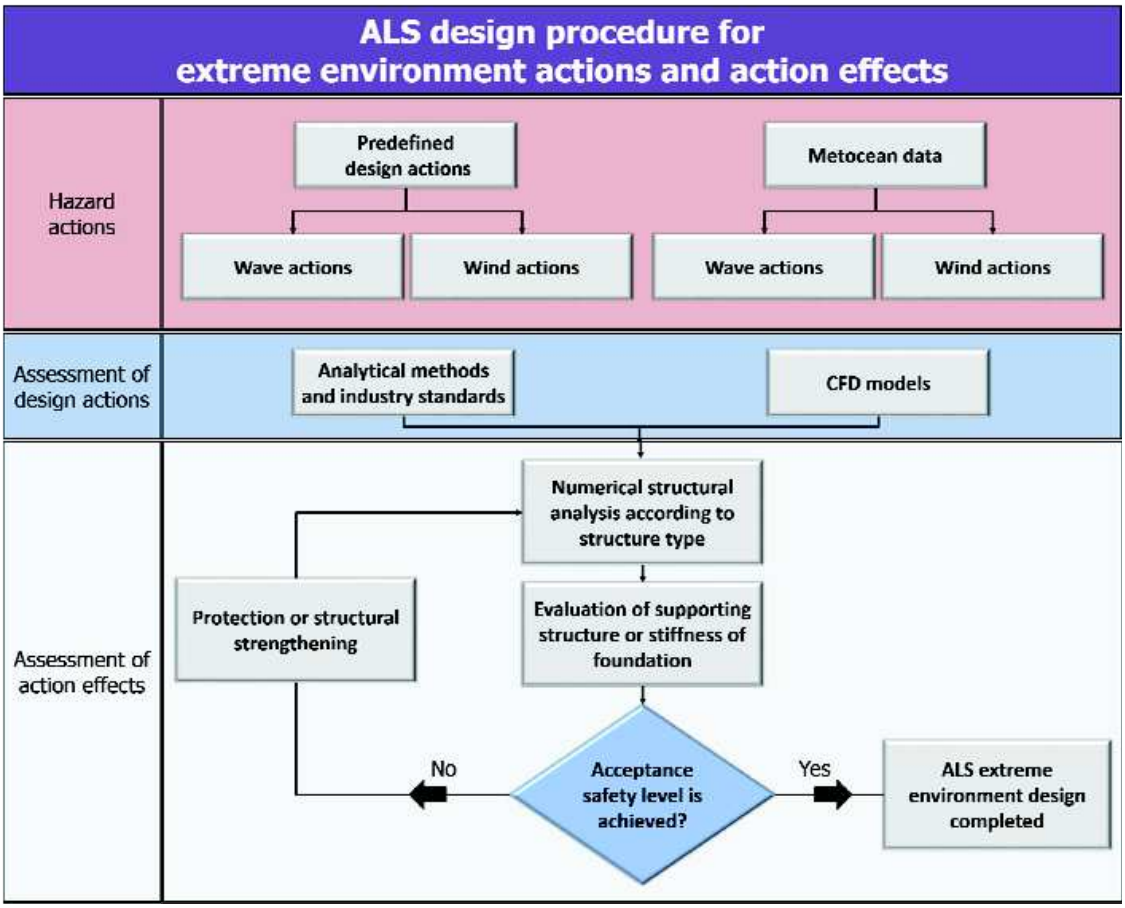

Figure 9.1: ALS assessment procedure for extreme wave and wind loads.

9.2 Probabilistic models of actions

The amplitude and likelihood of an abnormal wave or wind loading event may be determined using a risk assessment. Guidelines for hazard identification and risk assements of offshore structures may be found in Germaniicher Lloyd and NORSOK-N-006 (2009). Although general assessment guidance is provided, the acceptance criteria is not provided in probabilistic terms. The ISO-19906 (2010) provides an ALS acceptance criteria which considers an abnormal environmental action to have a return period of 10,000 years. An alternative return period of an abnormal environmental action may be defined by the owner with sufficient validation and regulatory approval.

The environmental conditions governing the ULS and ALS design requirements are defined by the owner. In order to define the conditions, one must use the metocean database with appropriate parameters given the location of the installation, platform mobility and operating period. The abnormal wind and wave data for rare conditions (1,000 or 10,000 year recurrence period) is not provided in the metocean database. To define the extreme actions one must use extrapolation and hindcasting methods. The accuracy of the extrapolation is generally a function of the data set length. Further information about the metocean database is provided in ISO-19901 (2010).

9.2.1 Wind actions

The statistical terms that define the wind design actions are typically the wind speed standard deviation and mean as well as the mean direction in the length and time scale. It is also important to qualify the wind parameters by elevation above sea level since the mean wind speed and direction will vary with height. The standard reference height for a wind parameter definition is typically 10 m above mean sea level. Generally, the wind speed may be classified as sustained wind speeds or gust wind speeds. Depending on the wind definition (normal, extreme or abnormal) the gust duration and spatial variation may vary.

The wind actions on a particular structure vary based on the type of offshore structure as well as area of the structure above the water. The wind profile varies with elevation and typically does not govern the global response of an offshore structure. It may however, have a significant influence on the local response of a structural component. The gust wind speed may be the most appropriate loading definition for the local structural response analysis.

Offshore structures which develop a dynamic response to the wind loads is required to account for the wind speed variation in time and space. This requires information on the wind turbulence intensity, frequency spectrum and spatial coherence. Physical testing and computational fluid dynamics is the most accurate way of determining the accurate wind actions. Where only two-dimensional wind speed variations are available, the frequency spectrum for wind speeds in the mean direction is used. The frequency spectrum may only be applied to steady state wind conditions. In order to define the spatial variation of the wind speed between two points P_1 and P_2, a coherence function is used. A recommended coherence function is defined in ISO-19901 (2010) as:

$$F_{Coh}(f, P_1, P_2) = \exp\left\{-\frac{1}{U_{wo}}\left[\sum_{i=1}^{3}(A_i)^2\right]^{\frac{1}{2}}\right\} \tag{9.1}$$

where,

A_i is a function of frequency and position of P_1 and P_2.

If the assessed structure is slender, it may be subject to vortex induced vibration (VIV) when exposed to steady state wind conditions. It is important to account for VIV's during installation and transportation in addition to operational conditions.

9.2.2 Wave actions

Wave actions may be defined using a single regular/periodic wave or as a linear random wave model. The real sea state however, is best described using a random wave model which is composed of many small individual regular waves described by their heading, amplitude and incident frequency. An individual regular wave may be suficient for some quasi-static structural

assessments however, a compliant structure with a dynamic response may require a wave frequency spectrum. The ALS design sea state may be specified using:

- Long-term statistical distributions using oceanographic parameters.
- Short-term descriptions of different design sea states and currents to describe a wave spectrum with a given heading, incident frequency/period and significant wave height,
- Individual design waves and currents specifying wave height, period and wave theory.

9.3 Definition of design actions

9.3.1 Wind actions

The extreme wind velocity may be defined by extrapolating physical measurements at the installation site or wind tunnel tests. In the event data from measurements and tests are unavailable, a characteristic wind speed at 10 m above sea level of 44m/s and 48m/s for one hour and ten minute average, respectively (NORSOK-N-003, 2007). Additional empirical formulations to compute the characteristic wind velocity for heights greater than 10 m above sea level and different averaging periods may also be computed using NORSOK-N-003 (2007).

The wind action may be simplified as a force load which is dependent on the characteristics of the installaction. To assess local structural components, the analyst shall use the wind gust velocity to determine wind action. The duration of the wind gusts used for the calculation are a function of the size of the structure:

- Structural components with maximum dimension less than 50 m may use 3.0 s wind gusts to determine static wind force.
- Structural components with maximum dimension greater than 50 m may use 15.0 s wind gusts to determine static wind force.
- Combined extreme wind, wave and current actions may use 1 min mean wind speed or longer.

When extreme wind actions are expected to develop low-frequency excitation, the analyst must use an energy density spectrum. NORSOK-N-003 (2007) provides the expression for a one sided energy density spectrum of the longitudinal velocity fluctuations.

The global structural response of a fixed or floating platform may not be sensitive to wind gusts and can therefore assume wind actions are static. The static mean wind action force, F, is expressed as (NORSOK-N-003, 2007):

$$F = \frac{1}{2} \cdot \rho \cdot C_s \cdot A \cdot U_m^2 \cdot \sin \alpha \tag{9.2}$$

where, ρ, C_s, A, U_m and α are the mass density of air, shape coefficient, area of the member normal to with direction of the wind, wind speed and angle between the wind direction and axis of the exposed structure, respectively. For structures which are sensitive to the dynamic wind actions (compliant installations, catenary anchored installations, flare booms, tension leg installations, flare booms and high towers) the wind velocity is based on a 1 hour period. For these structures, the wind action is the sum of the fluctuating velocity component and mean velocity, expressed as:

$$F = \frac{1}{2} \cdot \rho \cdot C_s \cdot A \cdot \left[U_m \cdot u(t)\right]^2 \cong \frac{1}{2} \cdot \rho \cdot C_s \cdot A \cdot \left[U_m^2 + 2 \cdot U_m \cdot u(t)\right] \tag{9.3}$$

The spatial variation may be included in the analysis of large structures by accounting for coherence (Equation 9.1).

9.3.2 Wave Actions

The design and abnormal wave of an offshore platform typically has an exceedance probability of 10^{-2} and 10^{-4}, respectively. The dynamic response of the platform has a significant influence on the design and abnormal wave parameters. The dynamic response of fixed platforms is limited and the highest wave is typically the critical design condition. The significant wave height corresponding to the design wave is the significant wave height factored by 1.9. The

significant wave height is obtained from long-term statistics of a three hour sea state duration. Once the significant height of the design wave is determined, the wave period, T, should be varied between:

$$\sqrt{6.5 \cdot H_{100}} \le T \le \sqrt{11 \cdot H_{100}} \tag{9.4}$$

For the abnormal or extreme wave, detailed documentation on the wave derivation shall be provided. In the event sufficient details are unavailable, the designer use a significant wave height of 1.25 times the H_{100} with a increased corresponding period by 5% (NORSOK-N-003, 2007).

For compliant offshore structures which are sensitive to wave dynamics, the wave length and steepness may define the design wave rather than height. Conservatively, the wave period with the greatest splitting forces may be used to define the design wave significant wave height. The design wave height may be expressed by:

$$H_d = \begin{Bmatrix} 0.22T^2 & ; for\ T \le 6 \\ \dfrac{T^2}{4.5 + 0.02(T^2 - 36)} & ; for\ T > 6 \end{Bmatrix} \tag{9.5}$$

It is important to note that the methods of determining the design wave need to be calibrated using stochaistic analysis (NORSOK-N-003 (2007) clause 10). The model used to determine the extreme design wave kinematics are a function of the wave length to water depth ratio. Stokes 2nd order or higher theory for ratios greater than 0.15 and Stream function theory for shallower depths. Some engineering approximations of extreme wave kinematics may obtain an acceptable level of accuracy by using Wheeler stretching (vertical extrapolation of particle velocities above the mean water level).

9.4 Assessment of actions effects

Assessing the action effects of wind and waves to an offshore structure is directly influenced by the structure type.

Fixed steel structures (ISO-19902, 2007): Assessment must evaluate the structure linear elastically and account for geometric and material non-linearities in the structure-foundation interaction. The environmental actions are treated quasi-statically since dynamic amplification of fixed platforms is small. The structure in question is required to meet clauses 13, 14, 15 and 17 of ISO-19902 (2007) with all action and resistance factors set to 1.0.

Fixed concrete structures (ISO-19903, 2006): Similar to Fixed steel structures, the platform is evaulated by setting all resistance and action factors set to 1.0.

Floating structures (monohulls, semi-submerisbles and spars) (ISO-19904-1, 2006): Assessment must verify the structural integrity, stability and watertightness when subject to ALS action loads. When actions result in damage, the vessel must maintain station under specified environmental conditions sufficiently long to provide safe:

- Evacuation of personnel
- Control over movement or motion of the structure
- Temporary repairs
- Fire fighting
- Control of cargo outflow liable to cause environmental damage or pollution

The residual strength of the damaged condition must be verified using non-linear or simplified analysis methods. Simplified methods include plastic hinge or yield-line mechanisms. The action and resistance factors for the residual strength verification are set to unity.

Jack-ups (ISO-19905-1, 2012): An ALS assessment is required to fulfill the ULS requirements of a platform by developing a strength ratio. A strength ratio is calculated by scaling the abnormal sea condtions until failure occurs within the structure or foundation. The scale factor corresponding to the failed condition of the platform is the strength ratio.

Arctic structures (ISO-19906, 2010): The structure and foundation must be verified to have adequate reserve capacity and energy dissipation capabilty in the inelastic region. By using

non-linear analysis methods and setting all action factors to 1.0, the structure and foundation piles must be verified to be sufficiently designed to avoid complete loss of integrity. The assessment allows the structural components to act inelastically and consider all design conditions in combination with ice actions.

Generally, the design and extreme wind and wave actions are defined by the owner in the structural design guidance and specific to the structure and location. Assessing the structure subject to wind and wave action effects can be done using third party offshore analysis package suitable for analysis requirements.

The global analysis of fixed installations are typically completed using beam element based finite element programs which idealize the wind and wave loading as distributed loads along the exposed jacket and topside structure. These programs require the user to create a beam model of the jacket and topsides structure with member joints idealized as nodal positions. How the user defines the wind and wave actions within the user interface, is specific to the program and may vary between software packages. It is important for the user to understand how the program simplifies the loading to ensure the analysis will capture the required physics of the problem. Local analysis of platform members subject to wave and wind loads may require additional structural detail within the FE model to capture a detailed stress state. The use of shell elements for local analyses is more appropriate than beam elements.

Global analysis of compliant structures are slightly more complex than fixed platforms due to their dynamic response to wave loads. The software programs suited for compliant structures have the capability to account for unique wetted surfaces and complex member-hull connections. The hull structure is typically represented using shell elements with intermediate stiffening and topside structure idealized using beam elements. Since the wetted hull may be constructed using shell and beam element formulations, it important to ensure the analysis software can compute/apply hydrodynamic loads to each element type.

9.5 Design considerations

Design of offshore platforms subject to extreme/abnormal wind and wave events must be sufficiently strengthened to sustain the wind and wave actions with or without damage. The platform may be considered undamaged if the design strength of the platform subject to abnormal wind and wave actions can meet an ULS environmental actions evaluation (NORSOK N-004). The platform may be sufficiently designed to meet the ALS action requirements if:

$$Q_{10}^{-2} \cdot \gamma_{f10}^{-2} \cdot \gamma_{M10}^{-2} \geq Q_{10}^{-4} \cdot \gamma_{f10}^{-4} \cdot \gamma_{M10}^{-4} \tag{9.6}$$

where, Q_{10}^{-2}, γ_{f10}^{-2}, and γ_{M10}^{-2} represent wave/current base overturning moments and shear, load factor and material factor for the ULS, respectively. The terms Q_{10}^{-2}, γ_{f10}^{-2}, and γ_{M10}^{-2} represent wave/current base overturning moments and shear, load factor and material factor for the ALS, respectively.

In the event damage to the platform is expected, the damaged condition shall be evaluated to sustain environmental actions specific to regulatory, geographical and owner requirements. The damaged condition evaluation of fixed offshore platforms shall include the residual strength of dented tubulars as per ISO-19902 (2007) Clause 13,14,15 and 17 or NORSOK-N-004 (2004) Clause 10. In general, the platform shall sustain environmental actions with duration period sufficiently long such that:

1. All personnel to evacuate and/or all pollution risk to be removed.
2. Repairs to all damages can be made.
3. Structure remains fit-for-purpose.

In the event regulatory, geographical or owner requirements do not define after damage design requirements, ISO-19902 (2007) recommends the after damage design return period. The recommended after design return period is twice the conservative time required to repair the platform to as-built condition with a minimum period of one year.

CHAPTER TEN

REFERENCES

ADN 2013. The european agreement concerning the international carriage of dangerous goods by inland waterways.

API-2A-LRFD 1993. API Recommended Practice 2A-LRFD. American Petroleum Institute.

API-RP2FB 2006. Recommended Practive for the Design of Offshore Facilities against Fire and Blast Loading. American Petroleum Institute.

ASCE 2010. *Design of Blast-Resistant Buildings in Petrochemical Facilities*, The ASCE Task Committee.

Biggs, J. M. 1964. *Introduction to structural dynamics*, McGraw-Hill College.

Burgan, B. 2001. Elevated temperature and high strain rate properties of offshore steels. UK: HSE.

Czujko, J. 2001. *Design of offshore facilities to resist gas explosion hazard: engineering handbook*, CorrOcean ASA.

Czujko, J., Brubak, L., Czaban, J., Johnson, M., Kim, G. S., Pahos, S. J., Tabri, K., Tang, W. Y., Wægter, J. & Yamada, Y. 2015. Accidental limit states. ISSC Committe V.1.

Czujko, J., Buannic, N., Ehlers, S., Hung, C. F., Klæbo, F., Pahos, S. J., Riley, M., Vredeveldt, A. V., Tang, W. Y. & Wægter, J. 2012. Damage Assessment following Accidents. ISSC Committe V.1.

Czujko, J. & Paik, J. K. 2010. Explosion and fire engineering of FPSOs (Phase II): Definition of gas explosion design loads. Final Report No. EFEF JIP-04-R1, Research Institute of Ship and Offshore Structural Design Innovation, Pusan National University, Busan, Korea.

Czujko, J. & Paik, J. K. 2012. Hydrocarbon explosion-assessing and managing hydrocarbon explosion and fire risks in offshore installations. *Marine Technology.* SNAME.

Czujko, J. & Paik, J. K. 2014. New robustness assessment method for ALS design of structures subjected to hydrocarbon explosion loads. The ICTWS 2014 7th International Conference on Thin-Walled Structures, 29 Sep–2 Oct 2014, Busan, Korea.

DNV-OS-A101 2014. Safety Principles and Arrangements. Det Norske Veritas.

DNV-OS-C101 2014. General design of offshore steel structures (LFRD Method). Det Norske Veritas.

DNV-RP-C204 2010. Desgn against accidental loads. Det Norske Veritas.

DNV-RP-C208 2013. Determination of structural capacity by non-Linear FE analysis methods. Det Norske Veritas.

DNV-RP-F107 2010. Risk Assessment of Pipeline Protection. Det Norske Veritas.

DNV 1999. Ultiguide: best practice guidelines for use of non-linear analysis methods in documentation of ultimate limit states for jacket type offshore structures. Det Norske Veritas.

Ehlers, S. & Varsta, P. 2009. Strain and stress relation for non-linear finite element simulations. *Thin-Walled Structures,* 47, 1203-1217.

EN-1363-1 1999. Fire-resistance Tests – General Requirements. European Committee for Standardization CEN.

EN-1363-2 1999. Fire-resistance Tests – Alternative and Additional Procedures. European Committee for Standardization CEN.

EN-1993-1-2 2005. Design of steel Structures – Part 1-2. *General Rules- Structural Fire Design.* European Committee for Standardization CEN.

EN-1999-1-2 2007. Design of aluminum structures – Part 1-2. *Structural Fire Design.* European Committee for Standardization CEN.

EN-10025-3 2004. Hot Rolled Products of Structural Steels- Part 3. *Part 3:Technical Delivery Conditions for Normalized/nomalized Rolled Weldable Fine Grain Structural Steels.* European Committee for Standardization.

EN-10025-6 2004. ot Rolled Products of Structural Steels. *Part 6: Technical delivery conditions for flat products of high yield trength structural steels in the quenched and tempered condition.* European Committee for Standardization.

Eurocode-3 1993. Design of steel structure. European Committee for Standardization.

FABIG-IGN 1992. Interim Guidance Notes for the Design and Protection of Topside Structures against Explosion and Fire. Steel Construction Institute.

FABIG-TN1 1993. Fire resistant design of offshore topside stuctures. Steel Construction Institute.

FABIG-TN3 1995. Use of ultimate strength techniques for fire resistant design of offshore structures. Steel Construction Institute.

FABIG-TN4 1996. Explosion resistant design of offshore structures. Steel constuction institute.

FABIG-TN7 2002. Simplified methods for analysis of response to dynamic loading. Steel Construction Institute.

FABIG-TN10 2007. An advanced SDOF model for steel members subject to explosion loading: material rate sensitivity. Steel Construction Institute.

FABIG-TN11 2010. Fire loading and Structural Response. Steel Construction Institute.

Goerlandt, F., Ståhlberg, K. & Kujala, P. 2012. Influence of impact scenario models on collision risk analysis. *Ocean engineering,* 47, 74-87.

IPC 2000. Chartek 7 fireproofing – fire exposure case studies. International Protective Coatings.

ISO-834-1 1999. Fire-resistance Tests – Elements of Building Construction – Part 1: General Requirements. International Organization for Standardization.

ISO-834-2 2009. Fire-resistance Tests – Elements of Building Construction – Part 2: Guidance on Measuring Uniformity of Furnace Exposure on Test Samples. International Organization for Standardization.

ISO-13702 2015. Petroleum and natural gas industries - Control and mitigation of fires and explosions on offshore production installations - Requirements and guidelines. International Organization for Standardization.

ISO-19900 2013. Petroleum and natural gas industries – General requirements for offshore structures. International Organization for Standardization.

ISO-19901 2010. Petroleum and natural gas industries - Specific requirements for offshore structures - Part 3: Topsides structure. International Organization for Standardization.

ISO-19902 2007. Petroleum and natural gas industries – fixed steel offshore structures. International organization for standardization.

ISO-19903 2006. Petroleum and natural gas industries – fixed steel offshore structures. International organization for standardization.

ISO-19904-1 2006. Petroleum and natural gas industries - Floating offshore structures - Part 1: Monohulls, semi-submersibles and spars. International Organization for Standardization.

ISO-19905-1 2012. Petroleum and natural gas industries - Site-specific assessment of mobile offshore units - Part 1: Jack-ups. International Organization for Standardization.

ISO-19906 2010. Arctic offshore structures. International Organization for Standardization.

Jones, N. 1989. *Structural impact*, Cambridge University Press.

Kõrgesaar, M., Romanoff, J. & Tabri, K. 2014. Simulating ductile fracture in large scale shell structures – influence of mesh size and damage induced softening. *In revision.*

Kodur, V., Dwaikat, M. & Fike, R. 2010. High-Temperature Properties of Steel for Fire Resistance Modeling of Structures. *Journal of Materials in Civil Engineering,* 22, 423-434.

LR 2014a. Guidance notes for collision analysis. Lloyd's Register.

LR 2014b. Guidance notes for fire loadings and protection. Lloyd's Register.

Montewka, J., Ehlers, S., Goerlandt, F., Hinz, T., Tabri, K. & Kujala, P. 2014. A framework for risk assessment for maritime transportation systems—A case study for open sea collisions involving RoPax vessels. *Reliability Engineering & System Safety,* 124, 142-157.

NKB 1978. Structure for building regulations. Stockholm: Nordic Committee on Building Regulations (NKB).
NORSOK-N-003 2007. Action and action effects. Standard Norway.
NORSOK-N-004 2004. Design of Steel Structure. Standard Norway.
NORSOK-N-006 2009. Assessment of structural integrity for existing offshore load-bearing structures. Standard Norway.
NORSOK-S-001 2008. Technical Safety. Standard Norway.
NORSOK-Z-013 2010. Risk and Emergency Preparedness Assessment. Standard Norway.
NS-3472 2001. Steel structures - Design rules. Norway: Norwegian standard.
Oil & Gas UK 2007. Fire and Explosion Guidelines. Oil & Gas UK.
OGP-434-8 2010. Mechanical lifting failures. International Association of Oil & Gas Producers.
OTI-92-602 1992. The effects of high strain rates on material properties. London, UK: HSE.
OTI-95-634 1996. Jet-fire resistance test of passive fire protection materials. HSE.
Paik, J. K., Czujko, J., Kim, J. H., Park, S. I., Islam, M. S. & Lee, D. H. 2013. A new procedure for the nonlinear structural response analysis of offshore installations in fires. *Transactions of Society of Naval Architects and Marine Engineers,* 121.
Paik, J. K., Czujko, J., Kim, S. J., Lee, J. C., Kim, B. J., Seo, J. K. & Ha, Y. C. 2014. A new procedure for the nonlinear structural response analysis of offshore installations in explosions. The Society of Naval Architects and Marine Engineers (SNAME 2014), Houston, USA.
Paik, J. K. & Wierzbicki, T. 1997. A benchmark study on crushing and cutting of plated structures. *Jounal of Ship Research,* 41, 147-160.
Scharrer, M., Zhang, L. & Egge, E. D. 2002. Collision calculations in naval design systems. *Report Nr. ESS*.
Schlichting, H. 1979. *Boundary layer theory,* NY, USA, McGraw-Hill.
SINTEF 2009. *Offshore Reliability Data Handbook (OREDA),* Nøvik, Norway, OREDA participants.
Tabri, K. & Broekhuijsen, J. 2011. Influence of ship motions in the numerical prediction of ship collision damage. 3rd Int. Conf. on Mar. Struct.–MARSTRUCT, 391–7.
Thurlbeck, S. 2006. Acceptance criteria for damaged passive fire protection coatings, Report No. MMU013-P2-R-01. MMI Engineering Ltd.
UKOOA 2003. Fire and explosion guidance. *Part 1: Avoidance and mitigation of explosions.* London, UK: UK offshore operators association.
UKOOA/Hse-152-RP-48 2006. Fire and Explosion Guidance. *Part 2: Avoidance and Mitigation of Fires.* Laurencekirk, Scotland: fireandblast.com ltd.
UL-1709 1994. Standard for rapid rise fire tests of protection materials for structural steel. Underwriters Laboratories.
Veritec 1988. Design guidance for offshore steel structures exposed to accidental loads. Høvik, Norway.
Zhang, L., Egge, E. D. & Bruhns, H. 2004. Approval procedure concept for alternative arrangements. *3th International conference of collision and grounding of ships (ICCGS).* Tokyo, Japan.

- Reference websites

Access Steel	www.access-steel.com
Eurocodes - building the future	http://eurocodes.jrc.ec.europa.eu
Eurocodes expert	www.eurocodes.co.uk
NCCI-UK	www.steel-ncci.co.uk
Stainless steel design software	www.steel-stainless.org/software

CHAPTER ELEVEN

ANNEX. MATERIAL MODELS FOR THE USE IN ALS DESIGN

11.1 Introduction

Offshore structures exposed to hazards as defined above may undergo highly non-linear structural deformations, including rupture. Therefore, finite element analyses of these events require the input of appropriate material relations including failure representing the local material behaviour. Depending on the hazard to be analysed and the materials found on the offshore structures a selection of recommended material models can be made, see Table A1. The physical origin of these material models will be briefly presented, followed by numerical implementation possibilities as well as comments, hints and shortcomings arising from the use of those models as well as concerns of guidelines and standards. However, hazard simulations utilizing the recommended material models and input parameters can be used for basic physical checks, but they may not be applicable in general.

Table A1: Recommended material models and associated hazards.

Hazard \ Material	Steel	Aluminium	Foam, Isolator, Rubber	Ice	Air	Water	Explosives	Risers, umbilical or power cables	Composite	Concrete	Seabed
Hydrocarbon explosions	■	■	■					■	■	■	
Hydrocarbon fires	■	■	■					■	■	■	
Underwater explosions	■	■	◆		■	■	■		◆	◆	◆
Wave Impact	■	■	■			■		◆	■		
Water-In-Deck	■	■	■			■			■		
Dropped Objects	■	■	■			◆		◆	■	■	■
Ship Impact	■	■	■	■				◆	■	■	◆
Earthquakes	■	■	■			◆		■	■	■	■
Ice, Iceberg	■	■		■		■		■	■	■	
Flooding	■	■	■		■	■			■		

■ - recommended, ◆ - recommended where applicable

The material modelling represents a crucial part of all numerical simulations, because it predefines how the material is assumed to behave during the simulations. Hence, the ability of the material model to represent the physical behaviour accurately directly influences the accuracy of the simulation results and their reliability. Furthermore, the correct physical behaviour may be represented well by the underlying assumptions of the material model, because it can correspond well to the physical experiment done to obtain the properties of the material in question. However, whether or not this experiment or the correspondence represents the true material behaviour remains often a question, e.g. a classical tensile experiment is a material test by agreement even though a structural test is carried out. Hence, the utilization of such experimentally based material models using small structural tests can lead to inconsistent results when applied to general structures. Furthermore, it remains often questionable whether the obtained material model corresponds to the discrete mathematical model, i.e. the finite element mesh, of the structure to be analysed. Hence, a material model should be unique and

usable for any mesh size or conditions and should therefore not affect the results with a change in discretization of the simulation domain. In the past, often the term 'true' material model was utilized, which is however misleading as it implies that it is 'true' by all means and could be universally applied. In fact, all material measures are 'true' with respect to their determination scale, i.e. the engineering measure obtained by a tensile experiment is true with respect to the specimens' gauge length.

Hence, this chapter seeks to provide appropriate guidance to identify the material model to be used with the associated hazard according to Table A1 in such a way that it is consistent with the discretized, respectively meshed, simulation domain. Furthermore, engineering based best practices are provided as well as the associated shortcomings. The nomenclature of the numerical implementation used in the material input cards can be found in Hallquist (2007). The effects the material models account for, e.g. strain rate, temperature or damage criteria, will be provided alongside a selection of references relevant to the given material. Thereby, this database of material models will clarify common questions and uncertainties associated with the use of material models.

11.2 Guidelines and standards

ISO 19902 Ed 1 requires that the expected non-linear effects, including material yielding, buckling of structural components and pile failures, should be adequately modelled and captured. Strain rate effects should be considered as well as temperature dependency. NORSOK standard N-003 and DNV Recommended Practices DNV-RP-C204 suggest the use of the temperature dependent stress-strain relationships given in NS-ENV 1993 1-1, Part 1.2, Section 3.2. To account for the effect of residual stresses and lateral distortions compressive members should be modelled with an initial, sinusoidal imperfection with given amplitudes for elastic-perfectly plastic material and elasto-plastic material models. General class rules or CSR commonly state that an appropriate material model should be used; possibly in the form of a standard power law based material relation for large deformation analysis of steel structures. Additionally, some specify critical strain values to be used independent of the mesh size, which should, however, be sufficient, may be specified.

Hence, these guidelines and standards fail to provide a clear guidance for the analyst and may easily lead to diverse results simply by choosing different, yet not necessarily physically correct, material parameters.

11.3 Material model database

11.3.1 Steel

Commonly, the nonlinear material behaviour is selected in the form of a power law; see, for example, Alsos et al. 2009 and Ehlers et al. (2008). The power law parameters can be obtained from standard tensile experiments; see Paik (2007). However, with this approach agreement between the numerical simulation and the tensile experiment can only be achieved by an iterative procedure for a selected element size chosen a priori. Hence, the procedure needs to be repeated if the element size is changed.

Furthermore, the determination of the material relation alone does not necessarily suffice, as the failure strain, i.e. the end point of the stress versus strain curve, depends in turn on the material relation. However, a significant amount of research has been conducted to describe criteria to determine the failure strain, for example by Törnqvist (2003), Scharrer et al. (2002), Alsos et al. (2008), and to present their applicability (e.g. Tabri et al. 2007 or Alsos et al. 2009). However, all of these papers use a standard or modified power law to describe the material behaviour, and none of these papers identifies a clear relation between the local strain and stress relation and the element length.

Relations to obtain an element length-dependent failure strain value are given by Peschmann (2001), Scharrer et al. (2002), Törnqvist (2003), Alsos et al. (2008) and Hogström et al. (2009). These curve-fitting relations, known as Barba's relations, are obtained on the basis of experimental measurements. However, they define only the end point of the standard or modified power law. Hence, Ehlers et al. (2008) conclude that the choice of an element length-dependent failure strain does not suffice in its present form.

Therefore, Ehlers and Varsta (2009) and Ehlers (2009a) presented a procedure to obtain the strain and stress relation of the materials, including failure with respect to the choice of element size using optical measurements. They introduced the strain reference length, which is a function of the discrete pixel recordings from the optical measurements and corresponds to the finite element length. As a result, they present an element length dependent material relation for NVA grade steel including failure, see Figure A1.

Moreover, Ehlers et al. (2010) identified that a constant strain failure criterion suffices for crashworthiness simulations of ship structures and that the strain rate sensitivity of the failure strain and ultimate tensile force is less than three per cent, see Figure A2. Hence, for moderate displacement speeds the strain rate influence is negligible.

An example input card following the LS-DYNA nomenclature for a piece wise linear material (mat_24) is given in Table A2.

Table A2: Piecewise linear steel material model.

*MAT_PIECEWISE_LINEAR_PLASTICITY								
$#	mid	ro	e	pr	sigy	etan	fail	tdel
	1	7850.00	2.06E+11	0.3000	3.423E+8	0.000	0.661000	0.000
$#	c	p	lcss	lcsr	vp			
	0.000	0.000						
$#	eps1	eps2	eps3	eps4	eps5	eps6	eps7	eps8
	0.006	0.02612	0.04019	0.06865	0.15071	0.345	0.64477	0.74
$#	es1	es2	es3	es4	es5	es6	es7	es8
	3.423E+8	3.530E+8	3.731E+8	4.219E+8	4.901E+8	5.827E+8	6.621E+8	6.737E+8

However, the material behaviour, that is the change in the yield stress, at higher strain rates, $\dot{\varepsilon}$, can be calculated according to the Cowper-Symonds relation

$$1 + \left(\frac{\dot{\varepsilon}}{C}\right)^{1/p}$$

where, *C, p* are the strain rate parameters and may be chosen as 40.4/sec and 5 for mild steel, respectively. Additionally, effects on elevated temperatures may be accounted for by scaling the global yield stress as a function of the temperature, see Figure A3. The increase in yield- and ultimate strength at cryogenic temperatures, i.e. –100 and –163°C, is presented by Yoo et al. (2011) for mild stainless steel.

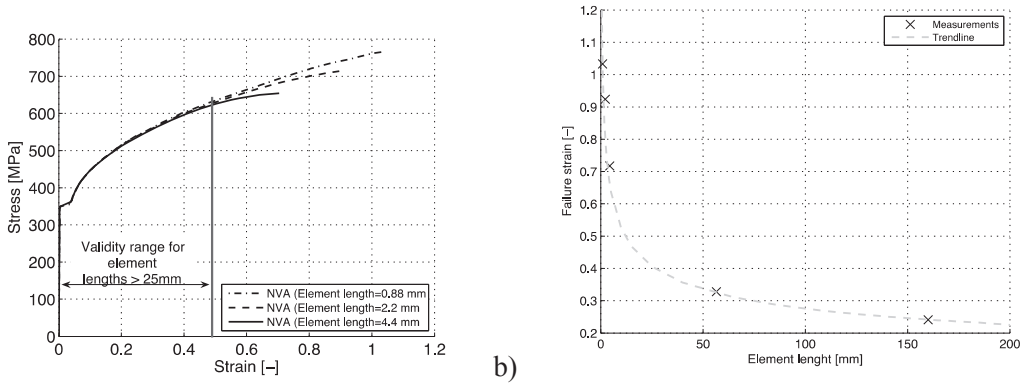

a) b)

Figure A1: NVA grade steel: measured local strain and stress relation (a) and failure strain (b) (Ehlers 2009b).

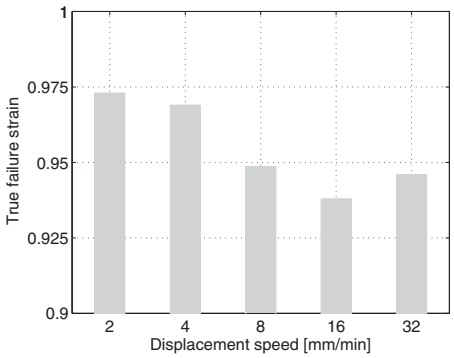

Figure A2: Influence of the displacement speed on the failure strain (Ehlers et al. 2010).

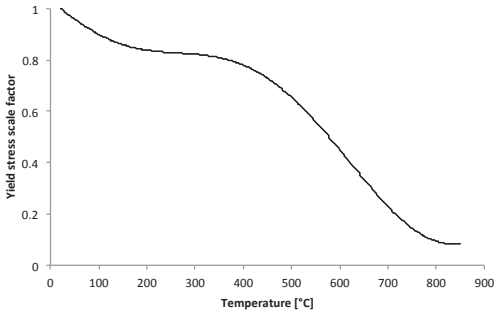

Figure A3: Global yield stress scale factor versus temperature for mild steel.

Definitial of thermal properties of materials requires additional keycards compared to the definition of basic material properties. A working example is presented in Table A3. *PART keyword should include the definitions for the basic material properties (marked with 355 in Table A3) and additional thermal material definition (marked with 2 in Table A3). Basic material definition is via *MAT_ELASTIC_PLASTIC_THERMAL, that defines gives the mechanical properties such as steel density and temperature dependent Young's moduli, Poisson's ratio, coefficients of thermal expansion, yield stresses and plastic hardening moduli. A maximum of eight temperatures with the corresponding data can be defined with a minimum of two points is needed. Keyword *MAT_THERMAL_ISOTROPIC_TD_LC allows additional isotropic thermal properties such as steel conductivity (tclc) and steel specific heat (hclc) to be specified by load curves. Finally, keyword *MAT_ADD_THERMAL_EXPANSION is used to apply the thermal expansion to a certain part according to a specified curve (curve no. 100 applied to the part no. 1 in Table A3). It should be noted that the latter overwrites the thermal expansion coefficients defined in *MAT_ELASTIC_PLASTIC_THERMAL keyword.

Table A3: Definition of thermal properties for steel (temperature in K).

*PART								
Part 1 (Section 1, MAT 355, thermal material 2)								
$#	pid	secid	mid	eosid	hgid	grav	adpopt	tmid
	1	1	355	0	0	0	0	2
*MAT_ELASTIC_PLASTIC_THERMAL								
$#	mid	ro						
	355	7.8500e-9						
$#	t1	t2	t3	t4	t5	t6	t7	t8
	273	293	373	673	773	973	1073	1473
$#	e1	e2	e3	e4	e5	e6	e7	e8
	2.1e5	2.1e5	2.1e5	1.47e5	1.26e5	2.73e5	1.89e5	201
$#	pr1	pr2	pr3	pr4	pr5	pr6	pr7	pr8
	0.3	0.3	0.3	0.3	0.3	0.3	0.3	0.3
$#	alpha1	alpha2	alpha3	alpha4	alpha5	alpha6	alpha7	alpha8
	0	0	0	0	0	0	0	0
$#	sigy1	sigy2	sigy3	sigy4	sigy5	sigy6	sigy7	sigy8
	355	355	355	355	277	82	39	1
$#	etan1	etan2	etan3	etan4	etan5	etan6	etan7	etan8
	200	200	200	200	200	200	200	200
*MAT_THERMAL_ISOTROPIC_TD_LC								
$#	mid	tro	tgrlc	tgmult				
	2	7.8500E-9						
	hclc	tcl						
	3	4						

```
*DEFINE_CURVE_TITLE
Steel CONDUCTIVITY (TCLC), temperature in K
$#      lcid      sidr       sfa       sfo      offa      offo    dattyp
         4         0    1.0000  1.000000       273     0.000         0
0,54
  ....
1400,27.3
*DEFINE_CURVE_TITLE
Steel SPECIFIC HEAT (HCLC), temperature in K
$#      lcid      sidr       sfa       sfo      offa      offo    dattyp
         3         0    1.0000  1.000000       273     0.000         0
0,4.25E+08
....
1400,6.50E+08
*MAT_ADD_THERMAL_EXPANSION
1,100,1
*DEFINE_CURVE_TITLE
Steel THERMAL EXPANSION, temperature in K
$#      lcid      sidr       sfa       sfo      offa      offo    dattyp
       100         0    1.0000  1.000000       273     0.000         0
0,1.20E-05
....
1400,2.00E-05
```

11.3.2 Aluminium

Various thin-walled aluminium structures under crash behaviour, i.e. large deformations including rupture, have been analysed experimentally and numerically in the past.

Langseth et al. (1998) uses an elasto-plastic material model with isotropic plasticity following the von Mises yield criterion and associated flow rule, see Berstad et al. (1994). Strain rate effects are often neglected for aluminium alloys, such as AA6060, in the strain rate range of 10^4 to 10^3 s^{-1}, see for example Lindholm et al. (1971). As a result, Langseth et al. are able to obtain good correspondence in terms of deformed shape, and shape of the force-displacement curve.

However, if high strain rates are to be expected, then the yield stress scaling according to Cowper-Symonds may be used. Négre et al. (2004) study the crack extension in aluminium welds using the Gurson–Tvergaard–Needleman (GTN) model and obtain reasonable correspondence in terms of force versus crack mouth opening displacement (CMOD). However, the GTN model requires a vast amount of input parameters whose physical origin cannot be directly provided. Furthermore, Négre et al. use 8-node brick elements, which are not suitable for large complex structures at present. Hence, from an engineering viewpoint this model does not suffice.

Lademo et al. (2005) utilize a coupled model of elasto-plasticity and ductile damage based on Lemaitre (1992) using the critical damage as an erosion criterion. They are able to simulate aluminium tensile experiments numerically with very good agreement using co-rotational shell elements and an anisotropic yield criterion Yld96 proposed by Barlat et al. (1997).

Such advanced material models can be easily implemented into numerical codes, and further increase in yield and ultimate strength at cryogenic temperatures, i.e. -100 and -163 °C, can be considered following the results by Yoo et al. (2011) for mild aluminium. Furthermore, a strain reference length-based approach using optical measurements as proposed by Ehlers (2009a) for steel may be used to obtain a consistent material relationship. However, for most analyses a consistent determination of the global material behaviour, see Figure A4, together with a Von Mises yield criterion will suffice.

An example input card following the LS-DYNA nomenclature for a piece wise linear material (mat_24) is given in Table A4.

Table A4: Piece wise linear aluminium material model.

*MAT_PIECEWISE_LINEAR_PLASTICITY							
$# mid	ro	e	pr	sigy	etan	fail	tdel
1	2.712E-9	75499	0.3000	200	0.000	0.1063	0.000
$# c	p	lcss	lcsr	vp			
0.000	0.000						
$# eps1	eps2	eps3	eps4	eps5	eps6	eps7	eps8
4.940E-4	8.928E-4	0.002087	0.01000	0.03630	0.0796		
$# es1	es2	es3	es4	es5	es6	es7	es8
220.7480	230.8739	241.2000	253.2500	270.3999	293.2200		

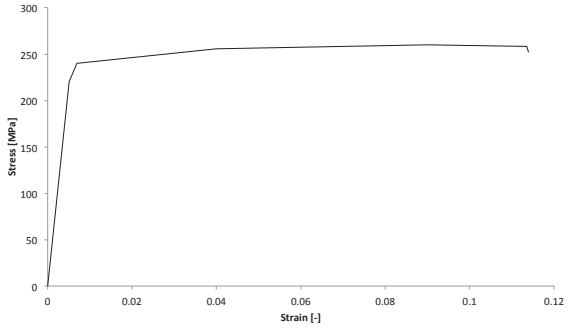

Figure A4: Example of a global strain versus stress curve from experiments.

11.3.3 Foam, Isolator, Rubber

Gielen (2008) presents an isotropic polyvinyl chloride (PVC) foam model, which exhibits elasto-damage behaviour under tension and elasto-plastic behaviour under compression. His damage model is consistent with the physical behaviour of the foam, a full-scale application and verification is however missing.

Cui et al. (2009) present a model for uniform foam based on Schraad and Harlow (2006) for disordered cellular materials under uni-axial compression. As a result, they obtain various influencing parameters affecting the energy absorption capacity under impact. Hence, functionally graded foams may be used to increase impact resistance.

In the case of rubber, a simplified rubber/foam material model (mat_181) may be used, which is defined by a single uni-axial load curve or by a family of uni-axial curves at discrete strain rates, see Figure A5. An example input card following the LS-DYNA nomenclature for such rubber material is given in Table A5.

Table A5: Simplified rubber/foam material model.

*MAT_SIMPLIFIED_RUBBER/FOAM							
$# mid	ro	k	mu	g	sigf	ref	prten
1	1.75E-9	1000	0	0	0	0	0
$# sgl	sw	st	lc/tbid	tension	eps6	avgopt	pr/beta
80	50	15	1	0	0	0	0.495

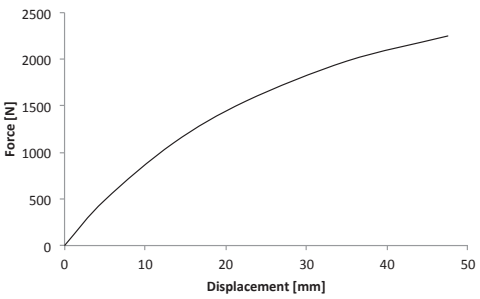

Figure A5: Exemplary force-displacement curve for rubber referenced as LC/TBID in mat_181.

11.3.4 Ice

One of the main difficulties when modelling ice is the prediction of ice failure, i.e. fracture, under loading at temperatures around the melting point of the ice. Thus the local ice-structure interaction includes transitions between the different phases. The failure process of ice begins when the edge of the moving ice hits the structure. This contact induces loads to the edge of the ice causing a stress state in the ice. When the stresses exceed the strength of ice, it fails. Ice becomes ductile with visco-elastic deformations during low loading rates and brittle during high loading rates.

Polojärvi and Tuhkuri (2009) developed specialized simulations tools utilizing the boundary element method, whereas Forsberg et al. (2010) utilizes the cohesive element method (CEM) to model ice failure. The latter is however of highly stochastic, or even random, nature and eventually results in reasonable agreement if experimental validation data becomes available.

However, Liu et al. (2011) treat the ice in a coupled dynamic ship – ice berg collision as an isotropic material, see Riska (1987), using the well-known Tsai-Wu strength criterion, see Tsai (1971). As a result, the obtained numerical results give an indication of the structural damage of the ship structure. However, their model erodes the ice at failure in an unphysical fashion resulting in purely numerical pressure fluctuation in the contact surface.

Therefore, the underlying material models and ice properties are in need to be defined consistently to account for the possible scatter and thereby to result in reliable design methods for ships and offshore structures. Hence, unless material model data is not available explicitly for tension and compression including an appropriate failure criterion for brittle ice failure based on micro-crack growth, a simple elastic model may be employed. The latter is however only valid to some extent, if, e.g. the flexural strength of an ice sheet is of interest.

Therefore, as a first attempt, ice may be modelled as a volumetric body following non-iterative plasticity with a simple plastic strain failure model (mat_13). However, therein the yield- and failure stress is note rate or pressure dependent and the temperature is assumed constant. An example input card following the LS-DYNA nomenclature for Baltic Sea ice is given in Table A6.

Table A6: Simplified ice material model.

```
*MAT_ISOTROPIC_ELASTIC_FAILURE
$#     mid        ro         g      sigy      etan      bulk
         1 916.96000 3.0800E+9 7.6000E+5 6.8900E+9 8.0300E+9
$#     epf       prf       rem      trem
  0.010800 -3.080E+5     0.000     0.000
```

11.3.5 Air

For numerical simulations of structures subjected to underwater explosions, where the target is air-backed, the air needs to be modelled. The main material parameters are the mass density and the equation of state (EOS). The latter can be expressed as a linear polynomial defining the pressure in the gas as a linear relationship with the internal energy per initial volume. The ideal gas EOS is an alternative approach to the linear polynomial EOS with a slightly improved energy accounting algorithm. In most cases, the mass density is the only parameter defined for the air. The same material properties were used in Trevino (2000) and Webster (2007).

An example input card for air following the LS-DYNA nomenclature is given in Table A7 according to Webster (2007).

Table A7: Air material model.

```
*MAT_NULL (m, kg)
$#     mid        ro        pc        mu     terod     cerod        ym        pr
         1     1.280     0.000     0.000     0.000     0.000     0.000     0.000
```

The EOS example input following the LS_DYNA nomenclature is given in Table A8 according to Webster (2007) in the most common form, which defines the parameters such that it is an ideal gas behaviour.

Table A8: Linear polynomial equation of state for air.

```
*EOS_LINEAR_POLYNOMIAL (cm, g)
$#   eosid        c0        c1        c2        c3        c4        c5        c6
         1     0.000   1.0e-02     0.000     0.000     0.400     0.400     0.000
$#      e0        v0
     0.000     0.000
```

Do (2009) describes the calculation process of e0, which can be used to define an initial pressure within the air. Additionally, an example input card for the ideal gas EOS following the LS-DYNA nomenclature is given in Table A9 according to Marc Ltd. (2007).

Table A9. Ideal gas equation of state for air.

```
*EOS_IDEAL_GAS
$#   eosid       cv0       cp0        cl        cq        t0        v0
         1  718.0000  1005.000     0.000     0.000    270.00     1.000
```

The ideal gas EOS is the equivalent of the linear polynomial with the C4 and C5 constants set to a value of (– 1).

11.3.6 Water

When conducting simulations of structures subjected to underwater explosions, water models are required.

The primary mechanical property to be defined is the mass density and in some cases the pressure cut-off and dynamic viscosity coefficient is needed. The cut-off pressure is defined to allow the material to numerically cavitate when under tensile loading. This is usually defined as a very small negative number, which allows the material to cavitate once the pressure goes below this value.

Additionally, the equation of state (EOS) needs to be defined, most commonly as a Gruneisen EOS with cubic shock-velocity-particle velocity defining the pressure for compressed materials. The constants in the Gruneisen EOS are found from the shock wave velocity versus particle velocity curve. Two example input cards following the LS-DYNA nomenclature for water (mat_009) are given according to Trevino (2000) and Webster (2007) in Table A10 and Table A11, respectively.

Table A10: Material model for water (Trevino, 2000).

```
*MAT_NULL (cm, g)
$#     mid        ro        pc        mu     terod     cerod        ym        pr
         1  1.000000     0.000     0.000     0.000     0.000     0.000     0.000
```

Table A 11: Material model for water (Webster, 2007).

```
*MAT_NULL (m, kg)
$#     mid        ro        pc        mu     terod     cerod        ym        pr
         1  1025.000  -1.0e-20   1.13e-3     0.000     0.000     0.000     0.000
```

Additionally, Gruneisen EOS is the most commonly used EOS for defining the water behaviour with underwater explosion events. An example input card following the LS-DYNA nomenclature is given in Table A12 according to Webster (2007).

Table A12: Equation of state for water.

```
*EOS_GRUNEISEN
$#   eosid         c        s1        s2        s3     gamao         a        e0
         1  2417.000  1.410000     0.000     1.000     0.000     0.000     0.000
$#      v0
     1.000
```

11.3.7 Explosives

An explosive material requires two keywords to define the behaviour of the material. These include the material keyword and the equation of state (EOS). The mechanical properties to be considered are the mass density, the detonation velocity in the explosive and the Chapman-Jouguet pressure. Furthermore, the bulk modulus, shear modulus and yield stress may be required depending on the model.

For the EOS, there are three possibilities to define the pressure for the detonation products. All of these EOS define the pressure as a function of the relative volume and the internal energy per initial volume. The most commonly used EOS for explosive behaviour is the standard Jones-Wilkins-Lee (JWL). This EOS was modified by Baker (1997) and has the added feature of better describing the high-pressure region above the Chapman-Jouguet state.

In addition to the material and EOS definitions in LS-DYNA, the INITIAL_DETONATION keyword is required to define the position and time of the initiation of the detonation process. This is the point at which the detonation initiates and the time for the remaining explosive to detonate is determined by the distance to the centre of the element divided by the detonation velocity. In the material definition for MAT_HIGH_EXPLOSIVE_BURN (mat_008) the value of BETA determines the type of detonation. If beta burn is used, any compression of the explosive material will cause detonation. For programmed burn, the explosive material can act as an elastic perfectly plastic material through the definition of the bulk modulus; shear modulus, and the yield stress. In this case, the explosive must be detonated with the INITIAL_DETONATION keyword.

An example input card following the LS-DYNA nomenclature for TNT (mat_008) is given in Table A13 according to Webster (2007).

Table A13: Explosive material model.

*MAT_HIGH_EXPLOSIVE_BURN							
$#	mid	ro	d	pcj	beta	k	g	sigy
	1	1630.000	6930.00	2.1e10	2.000	0.500	0.000	0.000

Furthermore, the most commonly used Jones-Wilkens-Lee EOS is given in Table A14 according to the LS-DYNA nomenclature (Webster, 2007).

Table A14. Equation of state for the explosive material model.

*EOS_JWL							
$#	eosid	a	b	r1	r2	omeg	e0	vo
	1	3.71e11	3.23e9	4.15	0.950	0.300	7.0e9	1.000

Keywords *LOAD_BLAST and *LOAD_BLAST_ENHANCED allow indirect modelling of the explosive and the propagation of blast wave without the need of actual discretization of the explosive or the air mesh around it. These keywords allow to define an airblast function for the application of pressure loads due to explosives described via equivalent mass of TNT. While *LOAD_BLAST only models the incident wave, the *LOAD_BLAST_ENHANCED includes enchancements for treating reflected waves, moving warheads and multiple blast surces. The loads are applied to facets defined with the keyword *LOAD_BLAST_SEGMENT. Example of indirect modelling is given in Table A15.

Table A15: Indiret modelling of explosive loading.

*LOAD_BLAST_ENHANCED								
$#	bid	m	xbo	ybo	zbo	tbo	unit	blast
	1	30	–250000	0	6850	–0.53	5	2
$#	cfm	cfl	cft	cfp	nidbo	death	negphs	
	2.205E3	3.28E–3	1E+3	145			0	

11.3.8 Risers, Umbilical or Power Cable

What all these structures have in common is the fact that they are typically very long, therefore slender. Their global mechanical properties to be defined are the bending-, torsional- and axial stiffness. Furthermore, the main aspect to be covered when modelling such structures is their stiffness dependency with respect to tension, torsion and curvature, i.e. stick-slip effects.

Therefore, experimental measurements of the global and local behaviour as well as a local analysis of the cross-section are needed. Typical numerical implementations would utilize elasto-plastic and visco-elastic material models considering friction, contact formulation (lift-off) as well as torsion/rolling effects on pipes.

Sævik (2011) studied the local behaviour of stresses in flexible pipes with a detailed model considering the cross-section build-up. However, for global analysis of an offshore structure, where the support effect of the slender structure is of interest, a simpler discretisation using beam elements with local stiffness properties can be used, see Rustad et al. (2008).

For a typical 8" flexible riser the following global parameters can be found: EI=200 kNm^2, EA = 7.7 10^8 N, GI_t = 5.9 10^6 Nm^2.

An example input card following the LS-DYNA nomenclature for a visco-elastic material (mat_117) is given in Table A16.

Table A16: Visco-elastic riser material model.

```
*MAT_VISCOELASTIC
$#     mid        ro      bulk        g0        gi      beta
         1  8650.000   2.06e11    0.8e11    0.1e11     0.200
```

11.3.9 Composites

Composite materials can be of various types, such as classical fibre-reinforced plastics or various stacks of materials, i.e. sandwich like structures. Therefore, their material parameters are very specific to the exact type of composite found in the offshore structure.

Menna et al. (2011) simulate impact tests of GFRP composite laminates using shells and provide the material parameters for a Mat Composite Failure Option Model (mat_059) of LS-DYNA. Feraboli et al. (2011) present an enhanced composite material with damage (mat_054) for orthotropic composite tape laminates together with a series of material parameters.

Most orthotropic elastic materials can be described until failure according to:

$$\lfloor \boldsymbol{C} \rfloor \{\sigma\} = \{\varepsilon\}$$

where $\boldsymbol{C}$ is the compliance matrix besides the six stress and strain components. Hence, the compliance matric can be composed of the extensional stiffness coefficients, the extensional-bending stiffness coefficients and the bending stiffness coefficients.

An example input card following the LS-DYNA nomenclature for a composite matrix material (mat_117) using such compliance matrix formulation is given in Table A17 for an equivalent stiffened plate.

Table A17: Composite material model.

```
*MAT_COMPOSITE_MATRIX
$#     mid        ro
         2 7850.0000
$#     c11        c12        c22        c13        c23        c33        c14        c24
 2.8409E+9 3.3956E+8 1.1319E+9      0.000      0.000 3.9615E+8 7.4958E+7 2.3769E+7
$#     c34        c44        c15        c25        c35        c45        c55        c16
     0.000 8.3506E+6 2.3769E+7 7.9231E+7      0.000 1.6645E+6 5.5485E+6      0.000
$#     c26        c36        c46        c56        c66       aopt
     0.000 2.7731E+7      0.000      0.000 1.9420E+6      0.000
$#      xp         yp         zp         a1         a2         a3
     0.000      0.000      0.000      0.000      0.000      0.000
$#      v1         v2         v3         d1         d2         d3       beta
     0.000      0.000      0.000      0.000      0.000      0.000      0.000
```

11.3.10 Concrete

Concrete material requires two keywords to define the behaviour of the material. These include the material keyword and the equation of state (EOS). The mechanical properties to be considered are the mass density, the shear modulus and an appropriate measure of the damage, respectively softening. The EOS describes the relation between the hydrostatic pressure and volume in the loading and unloading process of the concrete uncoupled from the deviatoric response. These parameters are typically obtained by experimental testing of the concrete under different loading directions and rates. Thus, the damage includes strain-rate effects.

Markovich et al. (2011) present a calibration model for a concrete damage model using EOS for tabulated compaction and a concrete damage, release 3, model (mat_72r3) and provide the required input parameters. Tai and Tang (2006) studied the dynamic behaviour of reinforced plates under normal impact using the Johnson–Holmquist Concrete equivalent strength model with damage and an EOS, which requires less input parameters and allows for easier implementation with good accuracy.

An example input card following the LS-DYNA nomenclature for concrete material (mat_111) is given in Table A18 according to Tai and Tang (2006).

Table A18: Concrete material model.

*MAT_JOHNSON_HOLMQUIST_CONCRETE							
$#	mid	ro	g	a	b	c	n	fc
	1	2240.000	13.467e11	0.750	1.650	0.007	0.760	48.00
$#	t	eps0	efmin	sfmax	pc	uc	pl	ul
	0.000	1.000	0.010	11.700	13.60	0.00058	1.050	0.100
$#	d1	d2	k1	k2	k3	fs		
	0.030	1.000	17.40	38.80	29.80	0.000		

11.3.11 Soil

For some simulations of hazard the seabed has to be included. However, the material parameters for seabed, respectively soil, are fairly location dependent and may vary significantly within close proximities. Therefore, it is of utmost importance to obtain experimental data for the site in question.

Typically those experiments should identify the soil stiffness in different directions, the friction, the break out resistance and a cycling behaviour (trenching). Henke (2011) presents numerical and experimental results for Niederfelder sand and uses a hypoplastic constitutive model, assuming cohesionless linear elastic behaviour, to achieve good correspondence. Vermeer and Jassmin (2011) use a SPH approach with an elastic-plastic Mohr-Coulomb model to simulate drop anchors and present the utilized material parameters. Furthermore, solid elements can be used to represent sandy soils or granular materials following the Mohr-Coulomb behaviour.

An example input card following the LS-DYNA nomenclature for a Mohr-Coulomb material (mat_173) is given in Table A19 according to the material parameters from Vermeer and Jassmin (2011).

Table A19: Soil material model.

*MAT_MOHR_COULOMB								
$#	mid	ro	gmod	rnu		phi	cval	psi
	1	1834.862	5.0e06	0.300	0	0.523	5.0e03	0.000
$#		nplanes		lccpdr	lccpt	lccjdr	lccjt	lcsfac
	0	0	0	0	0	0	0	0
$#	gmoddp	gmodgr	lcgmep	lcphiep	lcpsiep	lcgmst	cvalgr	aniso
	0.000	0.000	0.000	0.000	0.000	0.000	0.000	1.000000
$#	dip	dipang	cplane	frplane	tplane	shrmax	local	
	0.000	0.000	0.000	0.000	0.000	1.00E+20	0.000	

Another alternative for soil modelling is an isotropic material with damage that is available for solid elements. The model has a modified Mohr-Coulomb surface to determine the pressure dependent peak shear strength. It was developed for applications involving roadbase soils by Lewis (1999) for the Federal Highway Administratoin (FHWA), who extended the work of Abbo and Sloan (1995) to include excess pore water effects. Table A20 presents an example of FHWA soil model for compressed sand with the material properties obtained from Wang (2001) and FHWA (2004).

Table A20: Isotropic soil material model with damage.

*MAT_FHWA_SOIL								
$#	mid	ro	nplot	spgrav	rhowat	vn	gammar	intrmx
	2	2.35e-9	1	2.65	1e-9	1.1	0	4
$#	k	g	phimax	ahyp	coh	eccen	an	et
	19	11	0.524	5.37e-4	6.2e-3	0.7	0	0
$#	mcont	pwd1	pwksk	pwd2	phires	dint	vdfm	damlev
	0.034	0	0	0	1e-3	0.00001	6e-5	0.99
$#	epsmax							
	2							

Offshore structures exposed to hazards as defined above may undergo highly non-linear structural deformations, including rupture. Therefore, finite element analyses of these events require the input of appropriate material relations including failure representing the local material behaviour. Depending on the hazard to be analysed and the materials found on the offshore structures a selection of recommended material models can be made, see Table A21. The physical origin of these material models will be briefly presented, followed by numerical implementation possibilities as well as comments, hints and shortcomings arising from the use of those models as well as concerns of guidelines and standards. However, hazard simulations utilizing the recommended material models and input parameters can be used for basic physical checks, but they may not be applicable in general.

Table A21: Recommended material models and associated hazards.

Hazard \ Material	Steel	Aluminium	Foam, Isolator, Rubber	Ice	Air	Water	Explosives	Risers, umbilical or power cables	Composite	Concrete	Seabed
Hydrocarbon explosions	■	■	■					■	■	■	
Hydrocarbon fires	■	■	■					■	■	■	
Underwater explosions	■	■	◆		■	■	■		◆	◆	◆
Wave Impact	■	■	■			■		◆	■		
Water-In-Deck	■	■	■			■			■		
Dropped Objects	■	■	■			◆		◆	■	■	■
Ship Impact	■	■	■	■				◆	■	■	◆
Earthquakes	■	■	■			◆		■	■	■	■
Ice, Iceberg	■	■		■		■		■	■	■	
Flooding	■	■	■		■	■			■		

■ - recommended, ◆ - recommended where applicable

The material modelling represents a crucial part of all numerical simulations, because it predefines how the material is assumed to behave during the simulations. Hence, the ability of the material model to represent the physical behaviour accurately directly influences the accuracy of the simulation results and their reliability. Furthermore, the correct physical behaviour may be represented well by the underlying assumptions of the material model, because it can correspond well to the physical experiment done to obtain the properties of the material in question. However, whether or not this experiment or the correspondence represents the true material behaviour remains often a question, e.g. a classical tensile experiment is a material test by agreement even though a structural test is carried out. Hence, the utilization of such experimentally based material models using small structural tests can lead to inconsistent results when applied to general structures. Furthermore, it remains often questionable whether

the obtained material model corresponds to the discrete mathematical model, i.e. the finite element mesh, of the structure to be analysed. Hence, a material model should be unique and usable for any mesh size or conditions and should therefore not affect the results with a change in discretization of the simulation domain. In the past, often the term 'true' material model was utilized, which is however misleading as it implies that it is 'true' by all means and could be universally applied. In fact, all material measures are 'true' with respect to their determination scale, i.e. the engineering measure obtained by a tensile experiment is true with respect to the specimens' gauge length.

Hence, this chapter seeks to provide appropriate guidance to identify the material model to be used with the associated hazard according to Table A1 in such a way that it is consistent with the discretized, respectively meshed, simulation domain. Furthermore, engineering based best practices are provided as well as the associated shortcomings. The nomenclature of the numerical implementation used in the material input cards can be found in Hallquist (2007). The effects the material models account for, e.g. strain rate, temperature or damage criteria, will be provided alongside a selection of references relevant to the given material. Thereby, this database of material models will clarify common questions and uncertainties associated with the use of material models.

11.4 Guidelines and standards

ISO 19902 Ed 1 requires that the expected non-linear effects, including material yielding, buckling of structural components and pile failures, should be adequately modelled and captured. Strain rate effects should be considered as well as temperature dependency. NORSOK standard N-003 and DNV Recommended Practices DNV-RP-C204 suggest the use of the temperature dependent stress-strain relationships given in NS-ENV 1993 1-1, Part 1.2, Section 3.2. To account for the effect of residual stresses and lateral distortions compressive members should be modelled with an initial, sinusoidal imperfection with given amplitudes for elastic-perfectly plastic material and elasto-plastic material models. General class rules or CSR commonly state that an appropriate material model should be used; possibly in the form of a standard power law based material relation for large deformation analysis of steel structures. Additionally, some specify critical strain values to be used independent of the mesh size, which should, however, be sufficient, may be specified.

Hence, these guidelines and standards fail to provide a clear guidance for the analyst and may easily lead to diverse results simply by choosing different, yet not necessarily physically correct, material parameters.

11.5 Material model database

11.5.1 Steel

Commonly, the nonlinear material behaviour is selected in the form of a power law; see, for example, Alsos et al. 2009 and Ehlers et al. (2008). The power law parameters can be obtained from standard tensile experiments; see Paik (2007). However, with this approach agreement between the numerical simulation and the tensile experiment can only be achieved by an iterative procedure for a selected element size chosen a priori. Hence, the procedure needs to be repeated if the element size is changed.

Furthermore, the determination of the material relation alone does not necessarily suffice, as the failure strain, i.e. the end point of the stress versus strain curve, depends in turn on the material relation. However, a significant amount of research has been conducted to describe criteria to determine the failure strain, for example by Törnqvist (2003), Scharrer et al. (2002), Alsos et al. (2008), and to present their applicability (e.g. Tabri et al. 2007 or Alsos et al. 2009). However, all of these papers use a standard or modified power law to describe the material behaviour, and none of these papers identifies a clear relation between the local strain and stress relation and the element length.

Relations to obtain an element length-dependent failure strain value are given by Peschmann (2001), Scharrer et al. (2002), Törnqvist (2003), Alsos et al. (2008) and Hogström et al. (2009). These curve-fitting relations, known as Barba's relations, are obtained on the basis of experimental measurements. However, they define only the end point of the standard or

modified power law. Hence, Ehlers et al. (2008) conclude that the choice of an element length-dependent failure strain does not suffice in its present form.

Therefore, Ehlers and Varsta (2009) and Ehlers (2009a) presented a procedure to obtain the strain and stress relation of the materials, including failure with respect to the choice of element size using optical measurements. They introduced the strain reference length, which is a function of the discrete pixel recordings from the optical measurements and corresponds to the finite element length. As a result, they present an element length dependent material relation for NVA grade steel including failure, see Figure A1.

Moreover, Ehlers et al. (2010) identified that a constant strain failure criterion suffices for crashworthiness simulations of ship structures and that the strain rate sensitivity of the failure strain and ultimate tensile force is less than three per cent, see Figure A2. Hence, for moderate displacement speeds the strain rate influence is negligible.

An example input card following the LS-DYNA nomenclature for a piece wise linear material (mat_24) is given in Table A22.

Table A22: Piecewise linear steel material model.

*MAT_PIECEWISE_LINEAR_PLASTICITY								
$#	mid	ro	e	pr	sigy	etan	fail	tdel
	1	7850.00	2.06E+11	0.3000	3.423E+8	0.000	0.661000	0.000
$#	c	p	lcss	lcsr	vp			
	0.000	0.000						
$#	eps1	eps2	eps3	eps4	eps5	eps6	eps7	eps8
	0.006	0.02612	0.04019	0.06865	0.15071	0.345	0.64477	0.74
$#	es1	es2	es3	es4	es5	es6	es7	es8
	3.423E+8	3.530E+8	3.731E+8	4.219E+8	4.901E+8	5.827E+8	6.621E+8	6.737E+8

However, the material behaviour, that is the change in the yield stress, at higher strain rates, $\dot{\varepsilon}$, can be calculated according to the Cowper-Symonds relation

$$1 + \left(\frac{\dot{\varepsilon}}{C}\right)^{1/p}$$

where C, p are the strain rate parameters and may be chosen as 40.4/sec and 5 for mild steel, respectively. Additionally, effects on elevated temperatures may be accounted for by scaling the global yield stress as a function of the temperature, see Figure A3. The increase in yield- and ultimate strength at cryogenic temperatures, i.e. –100 and –163°C, is presented by Yoo et al. (2011) for mild stainless steel.

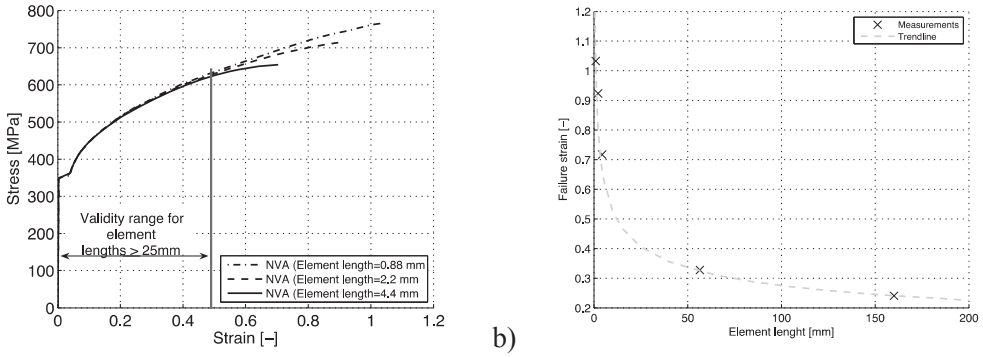

a) b)

Figure A1: NVA grade steel: measured local strain and stress relation (a) and failure strain (b) (Ehlers 2009b).

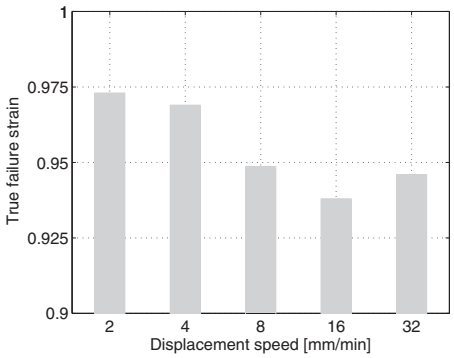

Figure A2. Influence of the displacement speed on the failure strain (Ehlers et al. 2010).

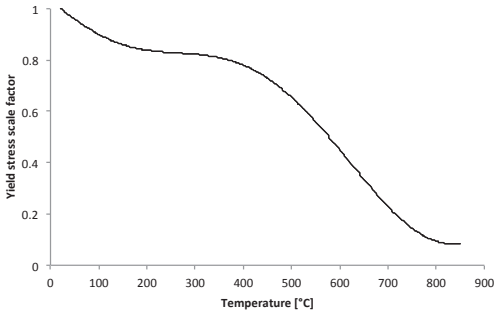

Figure A3. Global yield stress scale factor versus temperature for mild steel.

Definitial of thermal properties of materials requires additional keycards compared to the definition of basic material properties. A working example is presented in Table A3. *PART keyword should include the definitions for the basic material properties (marked with 355 in Table A3) and additional thermal material definition (marked with 2 in Table A3). Basic material definition is via *MAT_ELASTIC_PLASTIC_THERMAL, that defines gives the mechanical properties such as steel density and temperature dependent Young's moduli, Poisson's ratio, coefficients of thermal expansion, yield stresses and plastic hardening moduli. A maximum of eight temperatures with the corresponding data can be defined with a minimum of two points is needed. Keyword *MAT_THERMAL_ISOTROPIC_TD_LC allows additional isotropic thermal properties such as steel conductivity (tclc) and steel specific heat (hclc) to be specified by load curves. Finally, keyword *MAT_ADD_THERMAL_EXPANSION is used to apply the thermal expansion to a certain part according to a specified curve (curve no. 100 applied to the part no. 1 in Table A23). It should be noted that the latter overwrites the thermal expansion coefficients defined in *MAT_ELASTIC_PLASTIC_THERMAL keyword.

Table A23: Definition of thermal properties for steel (temperature in K).

*PART
Part 1 (Section 1, MAT 355, thermal material 2)

$#	pid	secid	mid	eosid	hgid	grav	adpopt	tmid
	1	1	355	0	0	0	0	2

*MAT_ELASTIC_PLASTIC_THERMAL

$#	mid	ro						
	355	7.8500e-9						
$#	t1	t2	t3	t4	t5	t6	t7	t8
	273	293	373	673	773	973	1073	1473
$#	e1	e2	e3	e4	e5	e6	e7	e8
	2.1e5	2.1e5	2.1e5	1.47e5	1.26e5	2.73e5	1.89e5	201
$#	pr1	pr2	pr3	pr4	pr5	pr6	pr7	pr8
	0.3	0.3	0.3	0.3	0.3	0.3	0.3	0.3
$#	alpha1	alpha2	alpha3	alpha4	alpha5	alpha6	alpha7	alpha8
	0	0	0	0	0	0	0	0
$#	sigy1	sigy2	sigy3	sigy4	sigy5	sigy6	sigy7	sigy8
	355	355	355	355	277	82	39	1
$#	etan1	etan2	etan3	etan4	etan5	etan6	etan7	etan8
	200	200	200	200	200	200	200	200

*MAT_THERMAL_ISOTROPIC_TD_LC

$#	mid	tro	tgrlc	tgmult
	2	7.8500E-9		
	hclc	tcl		
	3	4		

```
*DEFINE_CURVE_TITLE
Steel CONDUCTIVITY (TCLC), temperature in K
$#      lcid      sidr       sfa       sfo      offa      offo     dattyp
         4         0    1.0000  1.000000       273     0.000         0
0,54
  ....
1400,27.3
*DEFINE_CURVE_TITLE
Steel SPECIFIC HEAT (HCLC), temperature in K
$#      lcid      sidr       sfa       sfo      offa      offo     dattyp
         3         0    1.0000  1.000000       273     0.000         0
0,4.25E+08
....
1400,6.50E+08
*MAT_ADD_THERMAL_EXPANSION
1,100,1
*DEFINE_CURVE_TITLE
Steel THERMAL EXPANSION, temperature in K
$#      lcid      sidr       sfa       sfo      offa      offo     dattyp
       100         0    1.0000  1.000000       273     0.000         0
0,1.20E-05
....
1400,2.00E-05
```

11.5.2 Aluminium

Various thin-walled aluminium structures under crash behaviour, i.e. large deformations including rupture, have been analysed experimentally and numerically in the past.

Langseth et al. (1998) uses an elasto-plastic material model with isotropic plasticity following the von Mises yield criterion and associated flow rule, see Berstad et al. (1994). Strain rate effects are often neglected for aluminium alloys, such as AA6060, in the strain rate range of 10^4 to 10^3 s^{-1}, see for example Lindholm et al. (1971). As a result, Langseth et al. are able to obtain good correspondence in terms of deformed shape, and shape of the force-displacement curve.

However, if high strain rates are to be expected, then the yield stress scaling according to Cowper-Symonds may be used. Négre et al. (2004) study the crack extension in aluminium welds using the Gurson–Tvergaard–Needleman (GTN) model and obtain reasonable correspondence in terms of force versus crack mouth opening displacement (CMOD). However, the GTN model requires a vast amount of input parameters whose physical origin cannot be directly provided. Furthermore, Négre et al. use 8-node brick elements, which are not suitable for large complex structures at present. Hence, from an engineering viewpoint this model does not suffice.

Lademo et al. (2005) utilize a coupled model of elasto-plasticity and ductile damage based on Lemaitre (1992) using the critical damage as an erosion criterion. They are able to simulate aluminium tensile experiments numerically with very good agreement using co-rotational shell elements and an anisotropic yield criterion Yld96 proposed by Barlat et al. (1997).

Such advanced material models can be easily implemented into numerical codes, and further increase in yield and ultimate strength at cryogenic temperatures, i.e. -100 and -163 °C, can be considered following the results by Yoo et al. (2011) for mild aluminium. Furthermore, a strain reference length-based approach using optical measurements as proposed by Ehlers (2009a) for steel may be used to obtain a consistent material relationship. However, for most analyses a consistent determination of the global material behaviour, see Figure A4, together with a Von Mises yield criterion will suffice.

An example input card following the LS-DYNA nomenclature for a piece wise linear material (mat_24) is given in Table A24.

Table A24. Piece wise linear aluminium material model.

*MAT_PIECEWISE_LINEAR_PLASTICITY							
$# mid	ro	e	pr	sigy	etan	fail	tdel
1	2.712E-9	75499	0.3000	200	0.000	0.1063	0.000
$# c	p	lcss	lcsr	vp			
0.000	0.000						
$# eps1	eps2	eps3	eps4	eps5	eps6	eps7	eps8
4.940E-4	8.928E-4	0.002087	0.01000	0.03630	0.0796		
$# es1	es2	es3	es4	es5	es6	es7	es8
220.7480	230.8739	241.2000	253.2500	270.3999	293.2200		

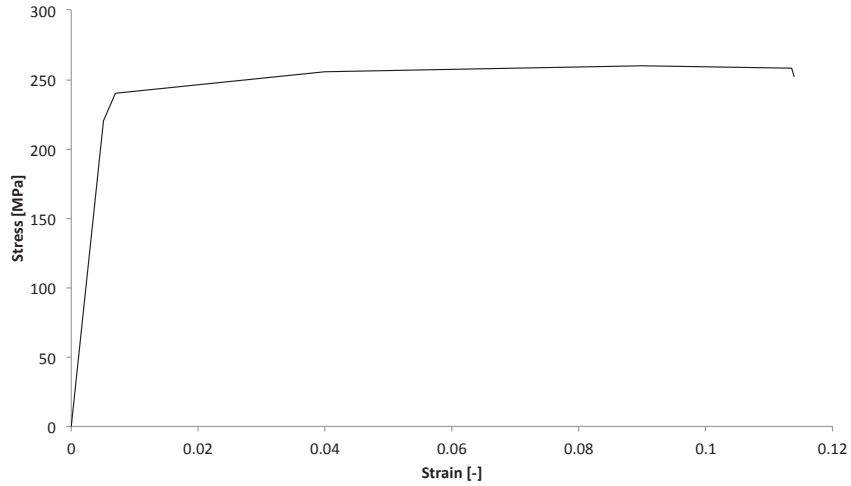

Figure A4: Example of a global strain versus stress curve from experiments.

11.5.3 Foam, Isolator, Rubber

Gielen (2008) presents an isotropic polyvinyl chloride (PVC) foam model, which exhibits elasto-damage behaviour under tension and elasto-plastic behaviour under compression. His damage model is consistent with the physical behaviour of the foam, a full-scale application and verification is however missing.

Cui et al. (2009) present a model for uniform foam based on Schraad and Harlow (2006) for disordered cellular materials under uni-axial compression. As a result, they obtain various influencing parameters affecting the energy absorption capacity under impact. Hence, functionally graded foams may be used to increase impact resistance.

In the case of rubber, a simplified rubber/foam material model (mat_181) may be used, which is defined by a single uni-axial load curve or by a family of uni-axial curves at discrete strain rates, see Figure A5. An example input card following the LS-DYNA nomenclature for such rubber material is given in Table A25.

Table A25: Simplified rubber/foam material model.

*MAT_SIMPLIFIED_RUBBER/FOAM							
$# mid	ro	k	mu	g	sigf	ref	prten
1	1.75E-9	1000	0	0	0	0	0
$# sgl	sw	st	lc/tbid	tension	eps6	avgopt	pr/beta
80	50	15	1	0	0	0	0.495

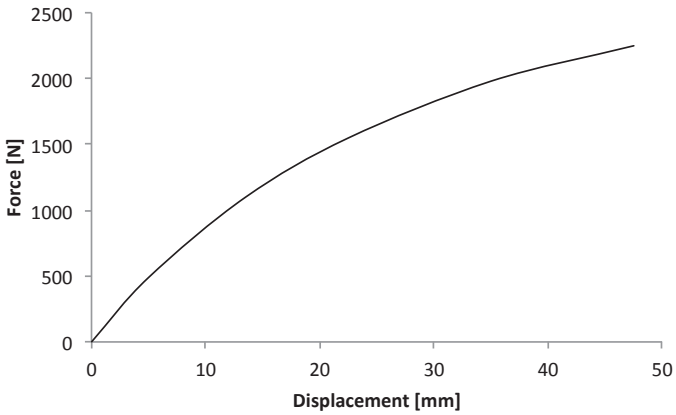

Figure A5. Exemplary force-displacement curve for rubber referenced as LC/TBID in mat_181.

11.5.4 Ice

One of the main difficulties when modelling ice is the prediction of ice failure, i.e. fracture, under loading at temperatures around the melting point of the ice. Thus the local ice-structure interaction includes transitions between the different phases. The failure process of ice begins when the edge of the moving ice hits the structure. This contact induces loads to the edge of the ice causing a stress state in the ice. When the stresses exceed the strength of ice, it fails. Ice becomes ductile with visco-elastic deformations during low loading rates and brittle during high loading rates.

Polojärvi and Tuhkuri (2009) developed specialized simulations tools utilizing the boundary element method, whereas Forsberg et al. (2010) utilizes the cohesive element method (CEM) to model ice failure. The latter is however of highly stochastic, or even random, nature and eventually results in reasonable agreement if experimental validation data becomes available.

However, Liu et al. (2011) treat the ice in a coupled dynamic ship – ice berg collision as an isotropic material, see Riska (1987), using the well-known Tsai-Wu strength criterion, see Tsai (1971). As a result, the obtained numerical results give an indication of the structural damage of the ship structure. However, their model erodes the ice at failure in an unphysical fashion resulting in purely numerical pressure fluctuation in the contact surface.

Therefore, the underlying material models and ice properties are in need to be defined consistently to account for the possible scatter and thereby to result in reliable design methods for ships and offshore structures. Hence, unless material model data is not available explicitly for tension and compression including an appropriate failure criterion for brittle ice failure based on micro-crack growth, a simple elastic model may be employed. The latter is however only valid to some extent, if, e.g. the flexural strength of an ice sheet is of interest.

Therefore, as a first attempt, ice may be modelled as a volumetric body following non-iterative plasticity with a simple plastic strain failure model (mat_13). However, therein the yield- and failure stress is note rate or pressure dependent and the temperature is assumed constant. An example input card following the LS-DYNA nomenclature for Baltic Sea ice is given in Table A26.

Table A26: Simplified ice material model.

```
*MAT_ISOTROPIC_ELASTIC_FAILURE
$#     mid        ro         g      sigy      etan      bulk
         1 916.96000 3.0800E+9 7.6000E+5 6.8900E+9 8.0300E+9
$#     epf       prf       rem      trem
  0.010800 -3.080E+5     0.000     0.000
```

11.5.5 Air

For numerical simulations of structures subjected to underwater explosions, where the target is air-backed, the air needs to be modelled. The main material parameters are the mass density and the equation of state (EOS). The latter can be expressed as a linear polynomial defining the pressure in the gas as a linear relationship with the internal energy per initial volume. The ideal gas EOS is an alternative approach to the linear polynomial EOS with a slightly improved energy accounting algorithm. In most cases, the mass density is the only parameter defined for the air. The same material properties were used in Trevino (2000) and Webster (2007).

An example input card for air following the LS-DYNA nomenclature is given in Table A27 according to Webster (2007).

Table A27: Air material model.

```
*MAT_NULL (m, kg)
$#     mid        ro        pc        mu     terod     cerod        ym        pr
         1     1.280     0.000     0.000     0.000     0.000     0.000     0.000
```

The EOS example input following the LS_DYNA nomenclature is given in Table A28 according to Webster (2007) in the most common form, which defines the parameters such that it is an ideal gas behaviour.

Table A28: Linear polynomial equation of state for air.

```
*EOS_LINEAR_POLYNOMIAL (cm, g)
$#   eosid        c0        c1        c2        c3        c4        c5        c6
         1     0.000   1.0e-02     0.000     0.000     0.400     0.400     0.000
$#      e0        v0
     0.000     0.000
```

Do (2009) describes the calculation process of e0, which can be used to define an initial pressure within the air. Additionally, an example input card for the ideal gas EOS following the LS-DYNA nomenclature is given in Table A29 according to Marc Ltd. (2007).

Table A29: Ideal gas equation of state for air.

```
*EOS_IDEAL_GAS
$#   eosid       cv0       cp0        cl        cq        t0        v0
         1  718.0000  1005.000     0.000     0.000    270.00     1.000
```

The ideal gas EOS is the equivalent of the linear polynomial with the C4 and C5 constants set to a value of ($\gamma - 1$).

11.5.6 Water

When conducting simulations of structures subjected to underwater explosions, water models are required.

The primary mechanical property to be defined is the mass density and in some cases the pressure cut-off and dynamic viscosity coefficient is needed. The cut-off pressure is defined to allow the material to numerically cavitate when under tensile loading. This is usually defined as a very small negative number, which allows the material to cavitate once the pressure goes below this value.

Additionally, the equation of state (EOS) needs to be defined, most commonly as a Gruneisen EOS with cubic shock-velocity-particle velocity defining the pressure for compressed materials. The constants in the Gruneisen EOS are found from the shock wave velocity versus particle velocity curve. Two example input cards following the LS-DYNA nomenclature for water (mat_009) are given according to Trevino (2000) and Webster (2007) in Table A30 and Table A31, respectively.

Table A30: Material model for water (Trevino, 2000).

```
*MAT_NULL (cm, g)
$#     mid        ro        pc        mu      terod      cerod        ym        pr
         1  1.000000     0.000     0.000     0.000     0.000     0.000     0.000
```

Table A 31: Material model for water (Webster, 2007).

```
*MAT_NULL (m, kg)
$#     mid        ro        pc        mu      terod      cerod        ym        pr
         1  1025.000  -1.0e-20   1.13e-3     0.000     0.000     0.000     0.000
```

Additionally, Gruneisen EOS is the most commonly used EOS for defining the water behaviour with underwater explosion events. An example input card following the LS-DYNA nomenclature is given in Table A32 according to Webster (2007).

Table A32: Equation of state for water.

```
*EOS_GRUNEISEN
$#   eosid         c        s1        s2        s3     gamao         a        e0
         1  2417.000  1.410000     0.000     1.000     0.000     0.000     0.000
$#      v0
     1.000
```

11.5.7 Explosives

An explosive material requires two keywords to define the behaviour of the material. These include the material keyword and the equation of state (EOS). The mechanical properties to be considered are the mass density, the detonation velocity in the explosive and the Chapman-Jouguet pressure. Furthermore, the bulk modulus, shear modulus and yield stress may be required depending on the model.

For the EOS, there are three possibilities to define the pressure for the detonation products. All of these EOS define the pressure as a function of the relative volume and the internal energy per initial volume. The most commonly used EOS for explosive behaviour is the standard Jones-Wilkins-Lee (JWL). This EOS was modified by Baker (1997) and has the added feature of better describing the high-pressure region above the Chapman-Jouguet state.

In addition to the material and EOS definitions in LS-DYNA, the INITIAL_DETONATION keyword is required to define the position and time of the initiation of the detonation process. This is the point at which the detonation initiates and the time for the remaining explosive to detonate is determined by the distance to the centre of the element divided by the detonation velocity. In the material definition for MAT_HIGH_EXPLOSIVE_BURN (mat_008) the value of BETA determines the type of detonation. If beta burn is used, any compression of the explosive material will cause detonation. For programmed burn, the explosive material can act as an elastic perfectly plastic material through the definition of the bulk modulus; shear modulus, and the yield stress. In this case, the explosive must be detonated with the INITIAL_DETONATION keyword.

An example input card following the LS-DYNA nomenclature for TNT (mat_008) is given in Table A33 according to Webster (2007).

Table A33: Explosive material model.

```
*MAT_HIGH_EXPLOSIVE_BURN
$#     mid        ro         d       pcj      beta         k         g      sigy
         1  1630.000   6930.00    2.1e10     2.000     0.500     0.000     0.000
```

Furthermore, the most commonly used Jones-Wilkens-Lee EOS is given in Table A34 according to the LS-DYNA nomenclature (Webster, 2007).

Table A34: Equation of state for the explosive material model.

```
*EOS_JWL
$#   eosid         a         b        r1        r2      omeg        e0        vo
         1   3.71e11    3.23e9      4.15     0.950     0.300     7.0e9     1.000
```

Keywords *LOAD_BLAST and *LOAD_BLAST_ENHANCED allow indirect modelling of the explosive and the propagation of blast wave without the need of actual discretization of the explosive or the air mesh around it. These keywords allow to define an airblast function for the application of pressure loads due to explosives described via equivalent mass of TNT. While *LOAD_BLAST only models the incident wave, the *LOAD_BLAST_ENHANCED includes enchancements for treating reflected waves, moving warheads and multiple blast surces. The loads are applied to facets defined with the keyword *LOAD_BLAST_SEGMENT. Example of indirect modelling is given in Table A35.

Table A35: Indiret modelling of explosive loading.

*LOAD_BLAST_ENHANCED								
$#	bid	m	xbo	ybo	zbo	tbo	unit	blast
	1	30	-250000	0	6850	-0.53	5	2
$#	cfm	cfl	cft	cfp	nidbo	death	negphs	
	2.205e3	3.28E-3	1e+3	145			0	

11.5.8 Risers, Umbilical or Power Cable

What all these structures have in common is the fact that they are typically very long, therefore slender. Their global mechanical properties to be defined are the bending-, torsional- and axial stiffness. Furthermore, the main aspect to be covered when modelling such structures is their stiffness dependency with respect to tension, torsion and curvature, i.e. stick-slip effects.

Therefore, experimental measurements of the global and local behaviour as well as a local analysis of the cross-section are needed. Typical numerical implementations would utilize elasto-plastic and visco-elastic material models considering friction, contact formulation (lift-off) as well as torsion/rolling effects on pipes.

Sævik (2011) studied the local behaviour of stresses in flexible pipes with a detailed model considering the cross-section build-up. However, for global analysis of an offshore structure, where the support effect of the slender structure is of interest, a simpler discretisation using beam elements with local stiffness properties can be used, see Rustad et al. (2008).

For a typical 8" flexible riser the following global parameters can be found: EI = 200 kNm^2, EA = 7.7 10^8 N, GI_t = 5.9 10^6 Nm^2.

An example input card following the LS-DYNA nomenclature for a visco-elastic material (mat_117) is given in Table A36.

Table A36: Visco-elastic riser material model.

```
*MAT_VISCOELASTIC
$#     mid        ro      bulk        g0        gi      beta
         1  8650.000   2.06e11    0.8e11    0.1e11     0.200
```

11.5.9 Composites

Composite materials can be of various types, such as classical fibre-reinforced plastics or various stacks of materials, i.e. sandwich like structures. Therefore, their material parameters are very specific to the exact type of composite found in the offshore structure.

Menna et al. (2011) simulate impact tests of GFRP composite laminates using shells and provide the material parameters for a Mat Composite Failure Option Model (mat_059) of LS-DYNA. Feraboli et al. (2011) present an enhanced composite material with damage (mat_054) for orthotropic composite tape laminates together with a series of material parameters.

Most orthotropic elastic materials can be described until failure according to:

$$\lfloor C \rfloor \{\sigma\} = \{\varepsilon\}$$

where $\boldsymbol{C}$ is the compliance matrix besides the six stress and strain components. Hence, the compliance matric can be composed of the extensional stiffness coefficients, the extensional-bending stiffness coefficients and the bending stiffness coefficients.

An example input card following the LS-DYNA nomenclature for a composite matrix material (mat_117) using such compliance matrix formulation is given in Table A37 for an equivalent stiffened plate.

Table A37: Composite material model.

```
*MAT_COMPOSITE_MATRIX
$#     mid        ro
         2 7850.0000
$#     c11       c12       c22       c13       c23       c33       c14       c24
 2.8409E+9 3.3956E+8 1.1319E+9     0.000     0.000 3.9615E+8 7.4958E+7 2.3769E+7
$#     c34       c44       c15       c25       c35       c45       c55       c16
     0.000 8.3506E+6 2.3769E+7 7.9231E+7     0.000 1.6645E+6 5.5485E+6     0.000
$#     c26       c36       c46       c56       c66      aopt
     0.000 2.7731E+7     0.000     0.000 1.9420E+6     0.000
$#      xp        yp        zp        a1        a2        a3
     0.000     0.000     0.000     0.000     0.000     0.000
$#      v1        v2        v3        d1        d2        d3      beta
     0.000     0.000     0.000     0.000     0.000     0.000     0.000
```

11.5.10 Concrete

Concrete material requires two keywords to define the behaviour of the material. These include the material keyword and the equation of state (EOS). The mechanical properties to be considered are the mass density, the shear modulus and an appropriate measure of the damage, respectively softening. The EOS describes the relation between the hydrostatic pressure and volume in the loading and unloading process of the concrete uncoupled from the deviatoric response. These parameters are typically obtained by experimental testing of the concrete under different loading directions and rates. Thus, the damage includes strain-rate effects.

Markovich et al. (2011) present a calibration model for a concrete damage model using EOS for tabulated compaction and a concrete damage, release 3, model (mat_72r3) and provide the required input parameters. Tai and Tang (2006) studied the dynamic behaviour of reinforced plates under normal impact using the Johnson–Holmquist Concrete equivalent strength model with damage and an EOS, which requires less input parameters and allows for easier implementation with good accuracy.

An example input card following the LS-DYNA nomenclature for concrete material (mat_111) is given in Table A38 according to Tai and Tang (2006).

Table A38: Concrete material model.

```
*MAT_JOHNSON_HOLMQUIST_CONCRETE
$#     mid        ro         g         a         b         c         n        fc
         1  2240.000 13.467e11     0.750     1.650     0.007     0.760     48.00
$#       t      eps0     efmin     sfmax        pc        uc        pl        ul
     0.000     1.000     0.010    11.700    13.60   0.00058     1.050     0.100
$#      d1        d2        k1        k2        k3        fs
     0.030     1.000     17.40     38.80     29.80     0.000
```

11.5.11 Soil

For some simulations of hazard the seabed has to be included. However, the material parameters for seabed, respectively soil, are fairly location dependent and may vary

significantly within close proximities. Therefore, it is of utmost importance to obtain experimental data for the site in question.

Typically those experiments should identify the soil stiffness in different directions, the friction, the break out resistance and a cycling behaviour (trenching). Henke (2011) presents numerical and experimental results for Niederfelder sand and uses a hypoplastic constitutive model, assuming cohesionless linear elastic behaviour, to achieve good correspondence. Vermeer and Jassmin (2011) use a SPH approach with an elastic-plastic Mohr-Coulomb model to simulate drop anchors and present the utilized material parameters. Furthermore, solid elements can be used to represent sandy soils or granular materials following the Mohr-Coulomb behaviour.

An example input card following the LS-DYNA nomenclature for a Mohr-Coulomb material (mat_173) is given in Table A39 according to the material parameters from Vermeer and Jassmin (2011).

Table A39: Soil material model.

*MAT_MOHR_COULOMB								
$#	mid	ro	gmod	rnu		phi	cval	psi
	1	1834.862	5.0e06	0.300	0	0.523	5.0e03	0.000
$#		nplanes		lccpdr	lccpt	lccjdr	lccjt	lcsfac
	0	0	0	0	0	0	0	0
$#	gmoddp	gmodgr	lcgmep	lcphiep	lcpsiep	lcgmst	cvalgr	aniso
	0.000	0.000	0.000	0.000	0.000	0.000	0.000	1.000000
$#	dip	dipang	cplane	frplane	tplane	shrmax	local	
	0.000	0.000	0.000	0.000	0.000	1.00E+20	0.000	

Another alternative for soil modelling is an isotropic material with damage that is available for solid elements. The model has a modified Mohr-Coulomb surface to determine the pressure dependent peak shear strength. It was developed for applications involving roadbase soils by Lewis (1999) for the Federal Highway Administratoin (FHWA), who extended the work of Abbo and Sloan (1995) to include excess pore water effects. Table A20 presents an example of FHWA soil model for compressed sand with the material properties obtained from Wang (2001) and FHWA (2004).

Table A40: Isotropic soil material model with damage.

*MAT_FHWA_SOIL								
$#	mid	ro	nplot	spgrav	rhowat	vn	gammar	intrmx
	2	2.35e-9	1	2.65	1e-9	1.1	0	4
$#	k	g	phimax	ahyp	coh	eccen	an	et
	19	11	0.524	5.37e-4	6.2e-3	0.7	0	0
$#	mcont	pwd1	pwksk	pwd2	phires	dint	vdfm	damlev
	0.034	0	0	0	1e-3	0.00001	6e-5	0.99
$#	epsmax							
	2							

11.6 Reference

Abbo, A. & Sloan, S. 1995. A smooth hyperbolic approximation to the Mohr-Coulomb yield criterion. *Computers & structures,* 54, 427-441.

Alsos, H. S., Amdahl, J. & Hopperstad, O. S. 2009. On the resistance to penetration of stiffened plates, Part II: Numerical analysis. *International Journal of Impact Engineering,* 36, 875-887.

Alsos, H. S., Hopperstad, O. S., Törnqvist, R. & Amdahl, J. 2008. Analytical and numerical analysis of sheet metal instability using a stress based criterion. *International Journal of Solids and Structures,* 45, 2042-2055.

Baker, E. L. & Stiel, L. I. Improved Quantitative Explosive Performance Prediction Using Jaguar. 1997 Insensitive Munitions and Energetic Materials Technology Symposium, Tampa, FL, 1997.

Barlat, F., Maeda, Y., Chung, K., Yanagawa, M., Brem, J. C., Hayashida, Y., Lege, D. J., Matsui, K., Murtha, S. J. & Hattori, S. 1997. Yield function development for aluminum alloy sheets. *Journal of the Mechanics and Physics of Solids,* 45, 1727-1763.

Berstad, T., Langseth, M. & Hopperstad, O. S. Elasto-viscoplastic constitutive models in the explicit finite element code LS-DYNA3D. Second International LS-DYNA3D conference, San Francisco, 1994.

Cui, L., Kiernan, S. & Gilchrist, M. D. 2009. Designing the energy absorption capacity of functionally graded foam materials. *Materials Science and Engineering: A,* 507, 215-225.

Do, I. H. P. 2009. *LS-DYNA ALE Addvanced Application Course Notes,* Livermore, CA.

Ehlers, S. 2010a. A procedure to optimize ship side structures for crashworthiness. *Proceedings of the Institution of Mechanical Engineers, Part M: Journal of Engineering for the Maritime Environment,* 224, 1-11.

Ehlers, S. 2010b. Strain and stress relation until fracture for finite element simulations of a thin circular plate. *Thin-Walled Structures,* 48, 1-8.

Ehlers, S., Broekhuijsen, J., Alsos, H. S., Biehl, F. & Tabri, K. 2008. Simulating the collision response of ship side structures: a failure criteria benchmark study. *International Shipbuilding Progress,* 55, 127-144.

Ehlers, S., Tabri, K., Romanoff, J. & Varsta, P. 2012. Numerical and experimental investigation on the collision resistance of the X-core structure. *Ships and offshore structures,* 7, 21-29.

Ehlers, S. & Varsta, P. 2009. Strain and stress relation for non-linear finite element simulations. *Thin-Walled Structures,* 47, 1203-1217.

Feraboli, P., Wade, B., Deleo, F., Rassaian, M., Higgins, M. & Byar, A. 2011. LS-DYNA MAT54 modeling of the axial crushing of a composite tape sinusoidal specimen. *Composites Part A: Applied Science and Manufacturing,* 42, 1809-1825.

Forsberg, J., Hilding, D. & Gürtner, A. 2010. A homogenized cohesive element ice model for simulation of ice action a first approach. *In:* Ehlers, S. & Romanoff, J. (eds.) *5th International Conference on Collision and Grounding of Ships.* Espoo, Finland.

Gielen, A. W. J. 2008. A PVC-foam material model based on a thermodynamically elasto-plastic-damage framework exhibiting failure and crushing. *International Journal of Solids and Structures,* 45, 1896-1917.

Hallquist, J. O. 2007. *LS-DYNA keyword user's manual, Version 971,* California, Livermore software technology cooperation.

Henke, S. Numerical and experimental investigations of soil plugging in open-ended piles. Proceedings of the Workshop Ports for Container Ships of Future Generations, J. Grabe, ed, 2011. 97-122.

Hogström, P., Ringsberg, J. W. & Johnson, E. 2009. An experimental and numerical study of the effects of length scale and strain state on the necking and fracture behaviours in sheet metals. *International Journal of Impact Engineering,* 36, 1194-1203.

Lademo, O. G., Hopperstad, O. S., Berstad, T. & Langseth, M. 2005. Prediction of plastic instability in extruded aluminium alloys using shell analysis and a coupled model of elasto-plasticity and damage. *Journal of materials processing technology,* 166, 247-255.

Langseth, M., Hopperstad, O. S. & Hanssen, A. G. 1998. Crash behaviour of thin-walled aluminium members. *Thin-walled structures,* 32, 127-150.

Lemaitre, J. & Lippmann, H. 1996. *A course on damage mechanics*, Springer Berlin.

Lindholm, U. S., Bessey, R. L. & Smith, G. V. 1971. Effect of strain rate on yield strength, tensile strength and elongation of three aluminum alloys. *J MATER,* 6, 119-133.

Liu, Z., Amdahl, J. & Løset, S. 2011. Plasticity based material modelling of ice and its application to ship–iceberg impacts. *Cold regions science and technology,* 65, 326-334.

Markovich, N., Kochavi, E. & Ben-Dor, G. 2011. An improved calibration of the concrete damage model. *Finite Elements in Analysis and Design,* 47, 1280-1290.

Martec-Limited 2007. Numerical Study of Soil Modelling Approaches using LS-DYNA. Unclassifed: Defence R&D Canada Valcartier.

Menna, C., Asprone, D., Caprino, G., Lopresto, V. & Prota, A. 2011. Numerical simulation of impact tests on GFRP composite laminates. *International Journal of Impact Engineering,* 38, 677-685.

Nègre, P., Steglich, D. & Brocks, W. 2004. Crack extension in aluminium welds: a numerical approach using the Gurson–Tvergaard–Needleman model. *Engineering Fracture Mechanics,* 71, 2365-2383.

Paik, J. K. 2007. Practical techniques for finite element modeling to simulate structural crashworthiness in ship collisions and grounding (Part I: Theory). *Ships and Offshore Structures,* 2, 69-80.

Peschmann, J. 2001. *Energy absorption computations of ship steel structures under collision and grounding (translated from German).* Doctoral Dissertation. Technical University of Hamburg.
Polojärvi, A. & Tuhkuri, J. 2009. 3D discrete numerical modelling of ridge keel punch through tests. *Cold Regions Science and Technology,* 56, 18-29.
Riska, K. 1987. Modelling ice load during penetration into ice. Joint report of the technical research center of Finland and the National Research Council of Canada.
Rustad, A. M., Larsen, C. M. & Sørensen, A. J. 2008. FEM modelling and automatic control for collision prevention of top tensioned risers. *Marine Structures,* 21, 80-112.
Sævik, S. 2011. Theoretical and experimental studies of stresses in flexible pipes. *Computers & Structures,* 89, 2273-2291.
Scharrer, M., Zhang, L. & Egge, E. D. 2002. Collision calculations in naval design systems. *Report Nr. ESS.*
Schraad, M. W. & Harlow, F. H. 2006. A stochastic constitutive model for disordered cellular materials: Finite-strain uni-axial compression. *International Journal of Solids and Structures,* 43, 3542-3568.
Tabri, K., Maattanen, J. & Ranta, J. 2007. Model-scale experiments of symmetric ship collisions. *Journal Marine Science and Technology,* 13, 71-84.
Tai, Y. S. & Tang, C. C. 2006. Numerical simulation: The dynamic behavior of reinforced concrete plates under normal impact. *Theoretical and Applied Fracture Mechanics,* 45, 117-127.
Törnqvist, R. 2003. *Design of crashworthy ship structures.* Technical University of Denmark Kgns Lyngby, Denmark.
Trevino, T. 2000. Applications of arbitrary lagrangian eulerian (ALE) analysis approach to underwater and air explosion problems. DTIC Document.
Tsai, S. W. & Wu, E. M. 1971. A general theory of strength for anisotropic materials. *Journal of composite materials,* 5, 58-80.
Vermeer, P. & Jassim, I. 2011. On the dynamic elastoplastic material point method. *Ports for container ships of future generations workshop.* Hamburg.
Webster, K. G. 2007. Investigation of close proximity underwater explosion effects on a ship-like structure using the multi-material arbitrary Lagrangian Eulerian finite element method.
Yoo, C. H., Kim, K. S., Choung, J., Shim, C. S., Kang, J. K., Kim, D. H., Suh, Y. S., Shim, Y. L., Urm, H. S., Kim, M. S. & An, G. B. 2011. An experimental study on mechanical, fatigue and crack propagation properties of IMO type B CCS materials at room and cryogenic temperatures. *In:* Soares, C. G. & Fricke, W. (eds.) *Advances in Marine Structures.* London, UK: Taylor & Francis Group.